AD-A170 642 AFRRI (ARMED FORCES RADIOBIOLOGY RESEARCH INSTITUTE) 1/2
REPORTS APRIL - JUNE 1986(U) ARMED FORCES RADIOBIOLOGY
RESEARCH INST BETHESDA MD 1986

UNCLASSIFIED F/G 6/18 NL

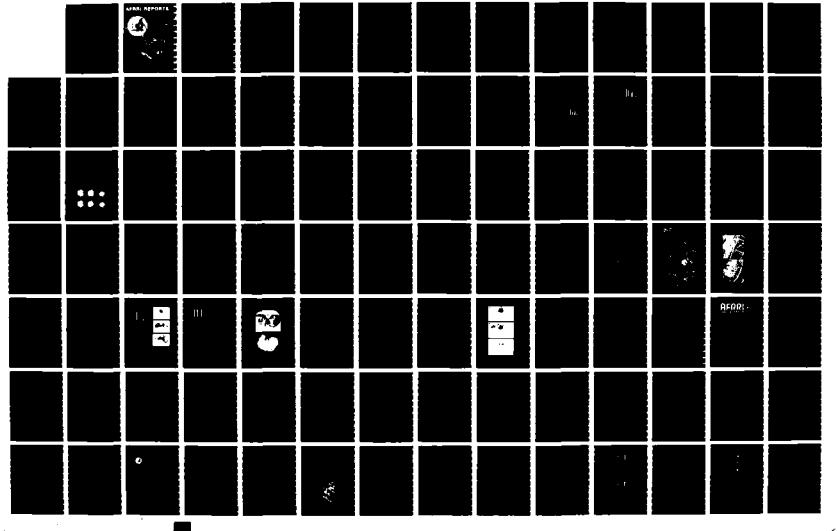

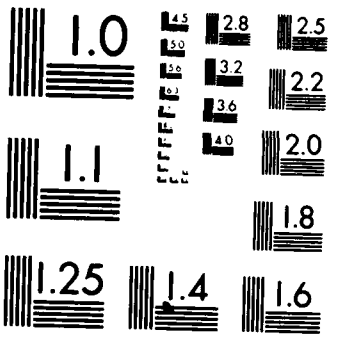

MICROCOPY RESOLUTION TEST CHART
NATIONAL BUREAU OF STANDARDS 1963-A

AFRRI REPORTS

April
May
June
1986

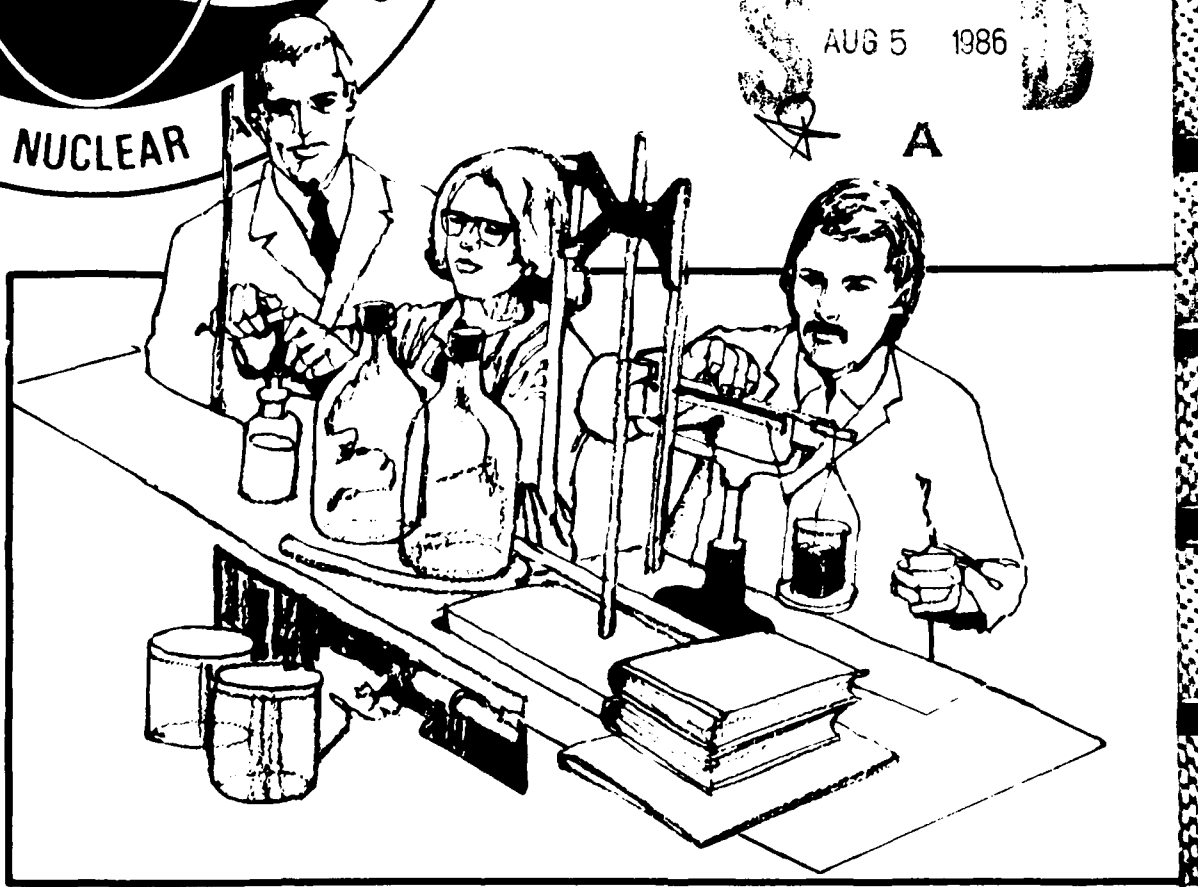

Defense Nuclear Agency

Armed Forces Radiobiology Research Institute

Bethesda, Md 20814-5145

UNCLASSIFIED

SECURITY CLASSIFICATION OF THIS PAGE

REPORT DOCUMENTATION PAGE

1a. REPORT SECURITY CLASSIFICATION UNCLASSIFIED	1b. RESTRICTIVE MARKINGS
2a. SECURITY CLASSIFICATION AUTHORITY	3. DISTRIBUTION/AVAILABILITY OF REPORT Approved for public release; distribution unlimited.
2b. DECLASSIFICATION/DOWNGRADING SCHEDULE	
4. PERFORMING ORGANIZATION REPORT NUMBER(S) SR86-14 through SR86-22, SP86-2, and TR86-1	5. MONITORING ORGANIZATION REPORT NUMBER(S)
6a. NAME OF PERFORMING ORGANIZATION Armed Forces Radiobiology Research Institute 6b. OFFICE SYMBOL (If applicable) AFRRI	7a. NAME OF MONITORING ORGANIZATION
6c. ADDRESS (City, State and ZIP Code) Defense Nuclear Agency Bethesda, Maryland 20814-5145	7b. ADDRESS (City, State and ZIP Code)
8a. NAME OF FUNDING/SPONSORING ORGANIZATION Defense Nuclear Agency 8b. OFFICE SYMBOL (If applicable) DNA	9. PROCUREMENT INSTRUMENT IDENTIFICATION NUMBER
8c. ADDRESS (City, State and ZIP Code) Washington, DC 20305	10. SOURCE OF FUNDING NOS. PROGRAM ELEMENT NO. / PROJECT NO. / TASK NO. / WORK UNIT NO.
11. TITLE (Include Security Classification) AFRRI Reports, Apr-Jun 1986	
12. PERSONAL AUTHOR(S)	
13a. TYPE OF REPORT Reprints/Technical 13b. TIME COVERED FROM _____ TO _____	14. DATE OF REPORT (Yr., Mo., Day) 15. PAGE COUNT 114
16. SUPPLEMENTARY NOTATION	
17. COSATI CODES FIELD / GROUP / SUB GR	18. SUBJECT TERMS (Continue on reverse if necessary and identify by block number) N/A

19. ABSTRACT (Continue on reverse if necessary and identify by block number)

This volume contains AFRRI Scientific Reports SR86-14 through SR86-22, Special Report SP86-2, and Technical Report TR86-1 for Apr-Jun 1986.

20. DISTRIBUTION/AVAILABILITY OF ABSTRACT UNCLASSIFIED/UNLIMITED ☒ SAME AS RPT ☐ DTIC USERS ☐	21. ABSTRACT SECURITY CLASSIFICATION UNCLASSIFIED
22a. NAME OF RESPONSIBLE INDIVIDUAL Junith A. Van Deusen	22b. TELEPHONE NUMBER (Include Area Code) (301) 295-2017 22c. OFFICE SYMBOL ISD

DD FORM 1473, 83 APR EDITION OF 1 JAN 73 IS OBSOLETE

UNCLASSIFIED

SECURITY CLASSIFICATION OF THIS PAGE

CONTENTS

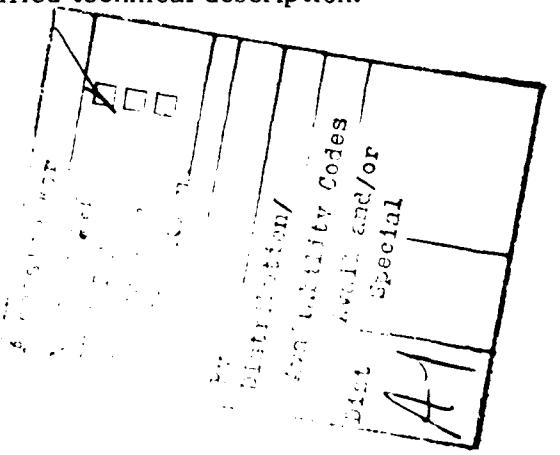

DISODIUM CROMOGLYCATE, A MAST-CELL STABILIZER, ALTERS POSTRADIATION REGIONAL CEREBRAL BLOOD FLOW IN PRIMATES

L. G. Cockerham, T. F. Doyle, E. L. Pautler, J. D. Hampton

Physiology Department, Armed Forces Radiobiology Research Institute, Bethesda, Maryland

Early transient incapacitation (ETI) is the complete cessation of performance during the first 30 min after radiation exposure, and performance decrement (PD) is a reduction in performance at the same time. Supralethal doses of radiation have been shown to produce a marked decrease in regional cerebral blood flow in primates concurrent with systemic hypotension and a dramatic release of mast-cell histamine. In an attempt to elucidate mechanisms underlying the radiation-induced ETI/PD phenomena and the postradiation decrease in cerebral blood flow, primates were given the mast-cell stabilizers disodium cromoglycate (DSCG) or BRL 22321 (Beecham Pharmaceuticals, Research Division) before exposure to 100 Gy whole-body gamma radiation. Hypothalamic and cortical blood flows were measured by hydrogen clearance, before and after radiation exposure. Systemic blood pressures were determined simultaneously. The data indicated that DSCG was successful in diminishing postradiation decrease in cerebral blood flow. Irradiated animals pretreated with DSCG, showed only a 10% decrease in hypothalamic blood flow 60 min postradiation, while untreated, irradiated animals showed a 57% decrease. The cortical blood flow of DSCG treated, irradiated animals showed a triphasic response, with a decrease of 38% at 10 min postradiation, then a rise to 1% below baseline at 20 min, followed by a fall to 42% below baseline by 50 min postradiation. In contrast, the untreated, irradiated animals showed a steady decrease in cortical blood flow to 79% below baseline by 50 min postradiation. There was no significant difference in blood-pressure response between the treated and untreated, irradiated animals. Systemic blood pressure showed a 60% decrease at 10 min postradiation, falling to a 71% decrease by 60 min. The effects of BRL 22321 in altering postradiation blood flow in the cerebral cortex and hypothalamus were intermediate between the irradiated controls and those pretreated with DSCG, but were not considered to be significant at the concentration employed. The overall results of this study indicate that the postradiation decrease in regional cerebral blood flow may be partially alleviated by treatment with a mast-cell stabilizer.

INTRODUCTION

Early transient incapacitation (ETI) is the complete cessation of motor performance, occuring transiently and within the first 30 min

This study was supported by Armed Forces Radiobiology Research Institute, Defense Nuclear Agency, under Research Work Unit MJ 00053. The views presented in this paper are those of the authors; no endorsement by the Defense Nuclear Agency has been given or should be inferred.

The authors would like to thank M. H. Owens for preparation of the manuscript.

Requests for reprints should be sent to Lorris G. Cockerham, Physiology Department, Armed Forces Radiobiology Research Institute, Bethesda, Maryland 20814-5145.

Journal of Toxicology and Environmental Health, 18:91–101, 1986

following exposure to supralethal doses of ionizing radiation (Kimeldorf and Hunt, 1965), and performance decrement (PD) is a reduction in performance at the same time. Since supralethal exposure to ionizing radiation such as gamma photons results in postradiation hypotension (Cockerham et al., 1984a) with the arterial blood pressure often decreasing to less than 50% of normal (Doyle et al., 1974), this is a possible explanation for ETI. In one investigation (Bruner et al., 1975) the PD was closely correlated with postradiation hypotension, the decrement following usually within a few minutes of the initial fall in blood pressure.

Postradiation hypotension produces a decrease in cerebral blood flow (CBF) even though the central nervous system (CNS) can otherwise maintain CBF under conditions of severe hypotension through the mechanism of autoregulation. One study (Chapman and Young 1968) demonstrated a dramatic fall of CBF immediately following a single 25-Gy ^{60}Co exposure, and another study (Cockerham et al., 1984c) reported a precipitous drop in regional blood flow in the visual cortex of primates exposed to 100 Gy ^{60}Co radiation. It is, therefore, conceivable that the ETI/PD phenomena following postradiation systemic hypotension may result substantially from a secondarily decreased cerebral blood flow.

There are reported elevations of circulating blood histamines in humans undergoing radiation therapy (Lasser and Stenstrom, 1954). Decreases in tissue histamine levels in rats (Eisen and Wilson, 1957), as well as increases in canine plasma histamine levels (Cockerham et al., 1984b, 1985) and primate plasma histamine levels (Alter et al., 1983; Cockerham et al., 1986; Doyle and Strike, 1977), following radiation exposure have also been reported. Histamine, stored in mast cells throughout the body (Metcalfe et al., 1981), is released under the stimulus of ionizing radiation and is implicated in radiation-induced hypotension. One study (Doyle et al., 1974) even reported the prevention or modification of radiation-induced performance changes and hypotension by the preradiation administration of an antihistamine. This study was designed to determine if the radiation-induced systemic hypotension and decreased cerebral blood flow could be mitigated by the preradiation administration of either disodium cromoglycate (DSCG) (Fisons Corporation, Bedford, Mass.) or BRL 22321 (Beecham Pharmaceuticals, Research Division), two mast-cell stabilizers (Spicer et al., 1983).

Two contrasting regions of the brain were selected for this study. The supraoptic nucleus of the hypothalamus was selected as the first region of interest, because mast cells are particularly numerous in the hypothalamus (Edvinsson et al., 1977) and the hypothalamus contains the highest histamine concentrations in the brain (Gross, 1982; Taylor et al., 1972). In contrast, the second region of interest, the postcentral

gyrus, is an area with little histamine (Taylor et al., 1972) and few mast cells (Edvinsson et al., 1977).

MATERIALS AND METHODS

Twenty-five rhesus monkeys (*Macaca mulatta*), weighing between 2.4 and 4.6 kg (3.3 ± 0.13 SEM), were used in this study. The animals were divided randomly into three groups of six animals each and one group of seven. The animals were grouped as follows: group I, 6 sham-radiated monkeys; group II, 7 radiated monkeys; group III, 6 monkeys given the mast-cell stabilizer disodium cromoglycate (DSCG) by iv infusion (100 mg/kg) 60 min before radiation; and group IV, 6 monkeys given the mast-cell stabilizer BRL 22321 iv (0.1 mg/kg) 5 min before radiation. These dosages were selected to approximate the levels reported by Spicer et al. (1983) for maximum effectiveness in rats.

Research was conducted according to the principles enunciated in the Guide for the Care and Use of Laboratory Animals prepared by the Institute of Laboratory Animal Resources, National Research Council. The monkeys were initially anesthetized in their cages with an im injection of 60 mg of ketamine hydrochloride with 0.04 mg atropine sulfate and were then moved to the surgery, where the remainder of the experiment was conducted.

Approximately 3 h before radiation or sham radiation, the animals were intubated with a cuffed endotracheal tube and ventilated using a forced-volume respirator to maintain a stable blood pH and oxygen tension. After insertion of the endotracheal tube, each animal was placed on a circulating water blanket to maintain body temperature between 36 and 38°C. A rectal probe was inserted to monitor body temperature. A femoral arterial catheter was used to withdraw blood for blood gas determinations and to measure systemic arterial blood pressure using a Statham P23 Db pressure transducer. A systemic venous catheter was used to administer the DSCG, BRL 22321, physiological saline, and maintenance doses of anesthetic (α - chloralose, as needed, for a total dose of 100 mg/kg).

The animal's head was positioned on the headholder of a stereotaxic instrument (David Kopf Instruments, Tujunga, Calif.) and the scalp was shaved and incised, allowing access to the skull. Using the stereotaxic micromanipulator, the skull was marked for insertion of four electrodes, and small burr holes were drilled through the skull at these marks. Again, using the micromanipulator, one electrode was placed in the left and one in the right supraoptic nucleus of the hypothalamus (Snider and Lee, 1961). In the same manner, one electrode was placed in the left and one in the right posterior central gyrus of the parietal cortex, 4 mm each side of the longitudinal fissure. The latter two electrodes were placed so that the tips were 2 mm below the sur-

face to insure that measurements would be taken from the cortical grey matter. The electrodes were Teflon-coated, platinum–iridium wire of 0.178 mm diameter, encased in, but insulated from, rigid stainless-steel tubing (22-gauge spinal needle) with exposed tips of approximately 2 mm. The exposed dura was covered with moistened pledgets, and the electrodes were sealed and secured to the skull with dental acrylic. A stainless-steel reference electrode was placed in neck tissue.

Regional cerebral blood flow was measured by the hydrogen clearance technique for 30 min before radiation or sham radiation and for 60 min after (Aukland et al., 1964; Young, 1980). This technique is essentially an amperometric method, which measures the current induced in a platinum electrode by the reduction of hydrogen. The current produced has a linear relationship with the concentration of hydrogen in the tissue (Hyman, 1961). Hydrogen was introduced into the blood via inhalation through the endotracheal tube at a rate of approximately 5% of the normal respiratory intake for 1–2 min for each flow measurement. Blood flow was measured by each of the four electrodes every 5–10 min. The electrodes were maintained electrically at +600 mV in respect to the reference electrode to reduce possible oxygen and ascorbate interference. This method has been successfully employed in several similar studies (Cockerham et al., 1986).

Measurement of currents from each electrode were fed through the polarographic amplifier (Triangle Research and Development Corporation, Research Triangle Park, N.C.) and then to a recorder, which produced curves depicting the clearance of hydrogen from the tissues. The clearance curves were then analyzed by a PDP 11/70 computer equipped with a VT55 terminal and a Versatex plotter (Digital Equipment Corporation, Maynard, Mass.). The first 60 s after the peak of the curves was neglected to obviate contamination by arterial recirculation (Martins et al., 1974). Data points were measured every second for 60 s. The flow was calculated between every two points, and a linear regression was performed over the 60-s period.

After 30 min of baseline recording, the animals were disconnected from the respirator and recording apparatus to facilitate radiation in a separate room. After radiation, or sham radiation for controls, the animals were reconnected to the respirator and recording apparatus at 4 min postradiation, and measurements were continued for a minimum of 60 min. At 30 and 10 min before radiation or sham radiation, and at 6, 15, 30, 45, and 60 min after radiation or sham radiation, blood samples were taken via the arterial catheter to monitor stability of blood pH and oxygen tension, and respiration was adjusted to maintain preradiation levels. Body temperature was monitored and maintained with the water blanket. Mean systemic arterial blood pressure was determined via the arterial catheter for the duration of the experiment. After termi-

nation of the measurements, the location of the electrodes was examined visually for verification of placement.

Irradiation was accomplished with a bilateral, whole-body exposure to gamma-ray photons from a cobalt-60 source located at the Armed Forces Radiobiology Research Institute (AFRRI). Exposure was limited to a mean of 1.38 min at 74 Gy/min steady state, free-in-air. Dose-rate measurements at depth were made with an ionization chamber placed in a tissue-equivalent model. The measured midline tissue dose rate was 69 Gy/min, producing a calculated total dose of 100 Gy, taking into account the rise and fall of the radiation source.

Blood pressure and blood flow data were grouped into 10-min intervals, measured in relation to midtime of radiation, and plotted at the middle of the interval. The Wilcoxon rank sum test was used to analyze statistically the blood pressure and blood flow data. A 95% level of confidence was employed to determine significance. Since all the animals were treated identically before radiation or sham radiation, and since the preradiation data for the control and test animals showed no significant differences, the preradiation data for the irradiated and sham-irradiated animals were combined.

RESULTS

As seen in Fig. 1, the mean systemic arterial blood pressure (MABP) of untreated, irradiated animals decreased to 46% of the preradiation

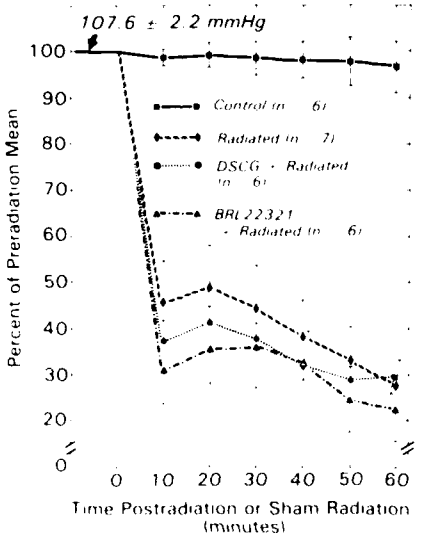

FIGURE 1. Mean ± SEM arterial blood pressure after exposure to 100 Gy whole-body gamma radiation presented as percent of preradiation level. Treated groups received either 100 mg/kg DSCG at 60 min preradiation or 0.1 mg/kg BRL 22321 at 5 min preradiation.

mean of 107.6 ± 2.2 mmHg within 10 min postradiation. A slight, non-significant rise was seen at 20 min postradiation, followed by a steady decline to a 60-min postradiation level that was 28% of the preradiation values. After sham radiation there was no significant change in MABP for the six control monkeys. The 12 treated, irradiated monkeys (groups II and III) displayed a decreased MABP that was not different statistically from the 7 untreated, irradiated monkeys. The MABP values for the irradiated groups, although not different statistically from each other, are different statistically from the sham-irradiated control group. The respiration of each subject was maintained at preradiation levels and, although not presented, the blood gas data revealed a general stability of blood pH and oxygen tension throughout the experimental period.

Figure 2 displays a preradiation mean blood flow of 64.9 ± 5.3 ml/100 g tissue • min in the supraoptic nucleus of the hypothalamus. The postradiation blood flow values for the sham-irradiated, control monkeys showed only a slight, insignificant increase during the 60 min after sham radiation. However, the postradiation values for the untreated, irradiated animals showed a rapid, significant decline to 66% of the preradiation levels at 10 min postradiation. At 60 min postradiation the blood flow had decreased to 43% of the preradiation or baseline level. There was a significant difference ($p = 0.05$) between the control

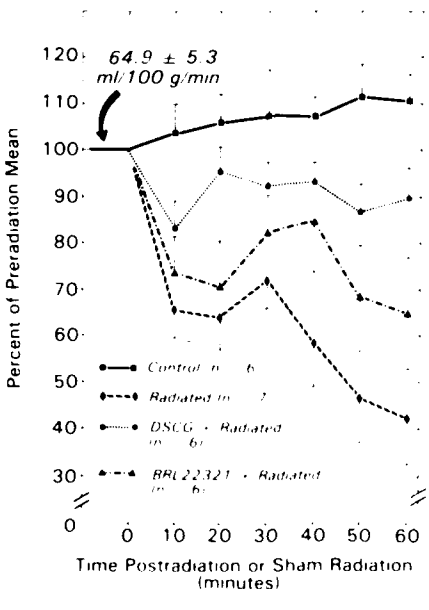

FIGURE 2. Mean (± SEM) hypothalamic blood flow after exposure to 100 Gy whole-body gamma radiation, presented as percent of preradiation level. Treated groups received either 10 mg/kg DSCG at 60 min preradiation or 0.1 mg/kg BRL 22321 at 5 min preradiation.

and untreated, radiated groups at all postradiation times of measurement. In contrast, the hypothalamic blood flow in the DSCG-treated, irradiated monkeys fell only slightly, to about 84% by 10 min postradiation, and averaged about 90% of the preradiation baseline for the remainder of the 60 min. At the 10-min postradiation observation there was no significant difference between this group and the other two radiated groups; however, a statistically significant difference did exist between the DSCG-treated, irradiated group and the untreated, irradiated group from 20 min postradiation through the remainder of the measurements. There was no significant difference between the DSCG-treated, irradiated group and the sham-irradiated group from 20 to 60 min postradiation. Monkeys given the mast-cell stabilizer BRL 22321 (group IV) exhibited a supraoptic nucleus postradiation blood flow that decreased to 73% by 10 min postradiation and was significantly different from that of the control animals at the 10, 20, 50, and 60 min postradiation times. At no time postradiation did the BRL 22321-treated monkeys significantly differ in hypothalamic blood from the untreated, irradiated group (II) of animals or from the DSCG-treated, irradiated group (III) of animals.

The preradiation cortical blood flow, as shown in Fig. 3, was 45.0 ± 3.6 ml/100 g tissue • min. The postradiation flow for the sham-irradiated group of monkeys showed no significant changes for the 60-min observation period. The postradiation blood flow values for the untreated, radiated monkeys showed a steady decline to 21% of the preradiation levels by 50 min postradiation. These levels became significantly different ($p = 0.05$) from those of the control group at 10 min postradiation and remained that way for the remainder of the observations.

In the cortex, as in the hypothalamus, blood flow in DSCG-treated, irradiated monkeys did not follow the same pattern as in the untreated, irradiated animals. The cortical blood flow in the DSCG-treated group dropped to approximately 60% in 10 min and then increased to baseline levels at 20 min postradiation, followed by a steady decline to 58% of baseline by 50 min postradiation. The cortical blood flow values for the DSCG-treated group were significantly different ($p = 0.05$) from the control group at 10 min postradiation, but not from the untreated, irradiated group. However, at 20 and 30 min postradiation this group was significantly different from the untreated, irradiated group, but not from the control group. This relationship between the DSCG-treated group and the other two groups reversed again for the remainder of the observations, with the treated group now again significantly different from the control group, but not from the untreated, irradiated group.

The postradiation cortical blood flow for the BRL 22321-treated monkeys followed a pattern similar to the one for the DSCG-treated group, decreasing to 60% in 10 min and then increasing to 79% of the

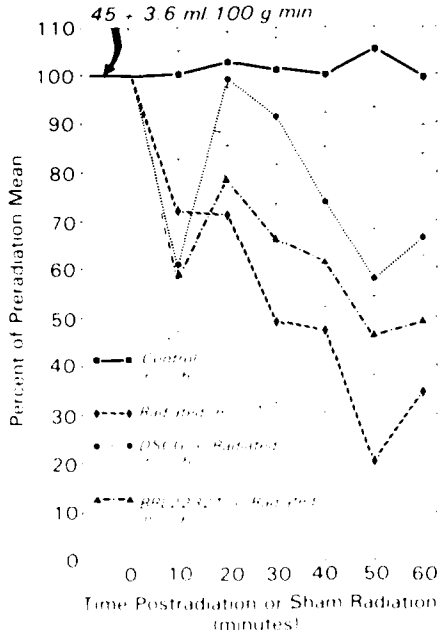

FIGURE 3. Mean (+ SEM) cortical blood flow after exposure to 100 Gy whole-body gamma radiation, presented as percent of preradiation level. Treated groups received either 100 mg kg DSCG at 60 min preradiation or 0.1 mg kg BRL 22321 at 5 min preradiation.

preradiation level at 20 min postradiation. This increase was followed by a steady decrease to 46% of preradiation values by 50 min postradiation. At 20 min postradiation this group was not significantly different from the other three groups, but did differ from the control group at all other times. At no time postradiation did the BRL 22321-treated monkeys significantly differ from the untreated, irradiated group (II) or the DSCG-treated, irradiated group (III) in cortical blood flow.

DISCUSSION

Postradiation hypotension has been well documented in the rhesus monkey, and a critical postradiation mean arterial blood pressure (MABP) of 50–60% of the preradiation MABP must be maintained for adequate autoregulation of cerebral circulation (Chapman and Young, 1968; Doyle et al., 1974; Farrar et al., 1981). The initial precipitous decline in MABP to 46% of the preradiation levels may then be associated with the similar immediate decrease in blood flow seen in both the hypothalamus and the cerebral cortex of the untreated, irradiated animals. A similar decrease in cerebral blood flow accompanied by symptoms and signs of cerebral ischemia has been reported in

humans (Finnerty et al., 1957). On the basis of the diminished cerebral blood flow reported in these animals, one might expect a severe functional impairment of the CNS in monkeys following radiation. In fact, postradiation early transient incapacitation (ETI) has been reported in monkeys starting as early as 2 min postradiation, lasting for 10–30 min and often accompanied by severe systemic hypotension during which MABP decreased to less than 50% of normal (Bruner, 1977; Doyle et al., 1971). The decline in MABP and cerebral blood flow (CBF) reported here corresponds closely in time with the observed occurrence of ETI (Bruner, 1977; Curran et al., 1973; Doyle et al., 1974) and suggests a causal relationship between the depressed MABP, CBF, and the appearance of ETI.

However, the maintenance of a normal MABP in postradiated monkeys administered norepinephrine did not improve postradiation performance significantly above those injected with saline (Turns et al., 1971). Conversely, the antihistamine chlorpheniramine maleate was effective in reducing ETI and postradiation performance decrement, while at the same time reducing postradiation hypotension in monkeys (Doyle et al., 1974). This study, however, using the mast-cell stabilizers disodium cromoglycate (DSCG) or BRL 22321, was not able to prevent postradiation hypotension in monkeys, but was able to alter postradiation cerebral blood flow (to a significant extent in the case of DSCG).

Autoregulation of cerebral blood flow to the hypothalamus appeared to be intact in animals pretreated with DSCG, even though the postradiation MABP fell to approximately 30% of the preradiation level. Based on the high concentration of mast cells in the hypothalamus (Edvinsson et al., 1977) and the ability of DSCG to stabilize mast cells, it seems that the degranulation of mast cells may be responsible, in part, for the radiation-induced loss of autoregulation of blood flow in the hypothalamus and, therefore, partially responsible for the radiation-induced performance decrement. This contention is supported by investigators who have reported radiation-induced release of histamine from mast cells (Doyle and Strike, 1977) and the reduction of ETI by the administration of antihistamines (Doyle et al., 1974). Further, the difference in the magnitude of the protective effect of DSCG between the cortex and the hypothalamus, seen in the latter time periods, implicates a local histamine release as a mediator of the response.

The measurements of cortical blood flow in the postcentral gyrus of radiated monkeys pretreated with mast-cell stabilizers, when plotted at postradiation times (Fig. 3), present a graph strikingly similar to the performance graph of monkeys exposed to 89 Gy of mixed gamma–neutron radiation (Curran et al., 1973), with the same temporal relationship. This triphasic response in monkeys pretreated with mast-cell stabilizers indicates that the degranulation of mast cells is involved

with, but may not be able to completely account for, the loss of autoregulation of blood flow to the postcentral gyrus.

Even though a temporal relationship does seem to exist between cortical blood flow and ETI, the presence of other factors must not be excluded. Some other chemical factor(s) could be released by radiation, cause the release of histamine from mast cells, and produce ETI by acting as a neurotransmitter or neuromodulator in the central nervous system. Before a temporal relationship, and definitely a causal relationship, can be established, postradiation measurements of blood chemistry, cerebral blood flow, and behavioral effects must be accomplished on the same animal subject.

While the effects of BRL 22321 in altering postradiation blood flow in the cerebral cortex and hypothalamus were found to be intermediate between the irradiated controls and those pretreated with DSCG, revealing a similar trend, these results were not considered to be significant at the concentration employed. As previously mentioned, the dosages were calculated to approximate the levels reported to be maximally effective in rats (Spicer et al., 1983). Although it is difficult to compare the two studies, since different species and different perturbations were employed, the results suggest that a larger dosage of BRL 22321 may yet (as has DSCG) prove to be effective in maintaining postradiation cerebral blood flow.

REFERENCES

Alter, W. A., III, Hawkins, R. N., Catravas, G. N., Doyle, T. F., and Takenaga, J. K. 1983. Possible role of histamine in radiation induced hypotension in the rhesus monkey. *Radiat. Res.* 94:654.

Aukland, K., Bower, B. B., and Berliner, R. W. 1964. Measurement of local blood flow with hydrogen gas. *Circ. Res.* 14:164–287.

Bruner, A. 1977. Immediate dose-rate effects of ^{60}Co on performance and blood pressure in monkeys. *Radiat. Res.* 70:378–390.

Bruner, A., Bogo, V., and Henderson, E. A. 1975. Dose-rate effects of ^{60}Co irradiation on performance and physiology in monkeys. Lovelace Foundation for Medical Education and Research, Albuquerque, N. Mex., Topical Report DNA 3660T.

Chapman, P. H., and Young, R. J. 1968. Effect of cobalt-60 gamma irradiation on blood pressure and cerebral blood flow in the *Macaca mulatta*. *Radiat. Res* 35:78–85.

Cockerham, L. G., Doyle, T. F., Trumbo, R. B., and Nold, J. B. 1984a. Acute postradiation canine intestinal blood flow. *Int. J. Radiat. Biol.* 45:65–72.

Cockerham, L. G., Doyle, T. F., Donlon, M. A., and Helgeson, E. A. 1984b. Canine postradiation histamine levels and subsequent response to Compound 48/80. *Aviat. Space Environ. Med.* 55:1041–1045.

Cockerham, L. G., Pautler, E. L., and Hampton, J. D. 1984c. Postradiation blood flow in the visual cortex of primates. *Toxicologist* 5:82.

Cockerham L. G., Doyle, T. F., Donlon, M. A., and Gossett-Hagerman, C. J. 1985. Antihistamines block radiation-induced increased intestinal blood flow in canines. *Fundam. Appl. Toxicol.* 5:597–604.

Cockerham, L. G., Cerveny, T. J., and Hampton, J. D. 1986. Postradiation regional cerebral blood flow in primates. *Aviat. Space Environ. Med.*, in press.

Curran, C. R., Young, R. W., and Davis, W. F. 1973. The performance of primates following exposure to pulsed whole-body gamma-neutron radiation. Armed Forces Radiobiology Research Institute, Bethesda, Md., AFRRI Scientific Report SR73-1.

Doyle, T. F., and Strike, T. A. 1977. Radiation-released histamine in the rhesus monkey as modified by mast-cell depletion and antihistamine. *Experientia* 33:1047–1048.

Doyle, T. F., Turns, J. E., and Strike, T. A. 1971. Effect of an antihistamine on early transient incapacitation of monkeys subjected to 4000 rads of mixed gamma–neutron radiation. *Aerospace Med.* 42:400–403.

Doyle, T. F., Curran, C. R., and Turns, J. E. 1974. The prevention of radiation-induced, early transient incapacitation of monkeys by an antihistamine. *Proc. Soc. Exp. Biol. Med.* 145:1018–1024.

Edvinsson, L., Cervos-Navarro, J., Larsson L.-I., Owman, C. H., and Ronnberg, A.-L. 1977. Regional distribution of mast cells containing histamine, dopamine, or 5-hydroxytryptamine in the mammalian brain. *Neurology* 27:878–883.

Eisen, V. D., and Wilson, C. W. M. 1957. The effect of β-irradiation on skin histamine and vascular responses in the rat. *J. Physiol.* 136:122–130.

Farrar, J. K., Gamache, F. W., Jr., Ferguson, G. G., Barker, J., Varkey, G. P., and Drake, C. G. 1981. Effects of profound hypotension on cerebral blood flow during surgery for intracranial aneurysms. *J. Neurosurg.* 55:857–864.

Finnerty, F. A., Jr., Guillaudeu, R. L., and Fazekas, J. F. 1957. Cardiac and cerebral hemodynamics in drug induced postural collapse. *Circ. Res.* 5:34–39.

Gross, P. M. 1982. Cerebral histamine: Indications for neuronal and vascular regulation. *J. Cereb. Blood Flow Metabol.* 2:3–23.

Hyman, E. S. 1961. Linear system for quantitating hydrogen at a platinum electrode. *Circ. Res.* 9:1093–1097.

Kimeldorf, D. J., and Hunt, E. L. 1965. Neurophysiological effects of ionizing radiation. In *Ionizing Radiation: Neural Function and Behavior*, eds. D. J. Kimeldorf and E. L. Hunt, pp. 59–108. New York: Academic.

Lasser, E. C., and Stenstrom, K. W. 1954. Elevation of circulating blood histamine in patients undergoing deep roentgen therapy. *Am. J. Roentgenology* 72:985–988.

Martins, A. N., Kobrine, A. I., Doyle, T. F., and Ramirez, A. 1974. Total cerebral blood flow in the monkey measured by hydrogen clearance. *Stroke* 5:512–517.

Metcalfe, D. D., Kaliner, M., and Donlon, M. A. 1981. The mast cell. In *CRC Critical Reviews in Immunology*, ed. M. Z. Atassi, pp. 23–74. Boca Raton, Fla.: CRC.

Snider, R. S., and Lee, J. C. 1961. *A Sterotaxic Atlas of the Monkey Brain* (Macaca mulatta). Chicago: University of Chicago Press.

Spicer, B. A., Ross, J. W., Clarke, G. D., Harling, E. J., Hassall, P. A., Smith, H., and Taylor, J. F. 1983. BRL 22321, a compound that has mast cell stabilizing activity similar to that of disodium cromoglycate and in addition has smooth muscle relaxing activity. *Agents Actions* 13:301–309.

Taylor, K. M., Gfeller, E., and Snyder, S. H. 1972. Regional localization of histamine and histidine in the brain of the rhesus monkey. *Brain Res.* 41:171–179.

Turns, J. E., Doyle, T. F., and Curran, C. R. 1971. Norepinephrine effects on early postirradiation performance decrement in the monkeys. Armed Forces Radiobiology Research Institute, Bethesda, Md., AFRRI Scientific Report SR71-16.

Young, W. 1980. H2 clearance measurement of blood flow: A review of technique and polarographic principles. *Stroke* 11:552–564.

Received June 28, 1985
Revised September 23, 1985
Accepted December 1, 1985

Brain Research, 368 (1986) 366–370
Elsevier

BRE 21426

Intracellular recordings from pineal cells in tissue culture: membrane properties and response to norepinephrine

JOSEPH E. FRESCHI and ANDREW G. PARFITT

Physiology Department, Armed Forces Radiobiology Research Institute, Bethesda, MD 20814 (U.S.A.)

(Accepted November 12th, 1985)

Key words: pineal — electrophysiology — intracellular recording — patch-clamp — voltage-clamp — noradrenaline

Membrane properties and responsiveness to norepinephrine were studied in pinealocytes in tissue culture using both conventional and whole-cell patch-clamp techniques. Action potentials could be recorded in normal and tetrodotoxin-containing saline. Both outward and inward rectification were prominent. Under voltage-clamp, depolarizing voltage steps evoked time-dependent outward currents showing no inactivation over time. Hyperpolarizing steps evoked slowly developing inward currents which did not inactivate. If the holding potential was sufficiently negative, depolarizing steps also elicited a transient outward current. Iontophoresis of norepinephrine produced a hyperpolarization in 30% of cells tested.

The interaction between sympathetic nerve terminals and pinealocytes has been among the most thoroughly studied neurotransmitter–effector relationships in the nervous system. It was one of the earliest, and still remains one of the few, systems wherein the link between agonist–receptor binding and subsequent functional biochemical changes were thoroughly characterized. Surprisingly, there have been few studies of the intracellular electrophysiological correlates to the well characterized biochemical effects of pineal β-adrenoreceptor activation[9,14]. Furthermore, nothing is known about the intrinsic membrane properties of pinealocytes. Proper interpretation of neurotransmitter effects requires that the underlying membrane conductances be known[6].

In this study we used intracellular electrophysiological techniques to investigate membrane properties of pinealocytes in culture and their responsiveness to norepinephrine. Tissue culture methods and conventional electrophysiological techniques have been fully described elsewhere[5,10]. Pineal glands were removed from 2-day-old rats, dissociated and plated onto 35-mm plastic culture dishes. Cultures were maintained for up to a month using modified Ham's F_{12} growth medium supplemented with 5% (v/v) fetal bovine serum and fresh glutamine and ascorbic acid. Under these conditions it has been shown previously that pinealocytes differentiate in culture, acquiring β-adrenoreceptors and the metabolic mechanisms for melatonin production[10,13].

Recording electrodes were filled with 4 M potassium acetate and had resistances of 100–200 MΩ. For iontophoresis, (−)-norepinephrine hydrochloride (Sigma) was dissolved in distilled water, immediately before use, at a concentration of 0.1 or 1.0 M, pH 4–5. Norepinephrine was ejected by passing positive current pulses by means of a constant-current microiontophoretic programmer (WP Instruments Model 160). A negative braking current, 1–3 nA, was maintained, and the drug pipette was moved away from the pinealocyte between drug applications. Current pulses of opposite polarity were applied in order to detect possible current artifacts. Positive current pulses from pipettes containing HCl, pH 3, caused either no response or a small, rapid (less than 2 mV) depolarizing response in 5 consecutively studied pinealocytes.

Whole-cell clamping was done as described by

Correspondence J.E. Freschi. Present address: Department of Neurology, 401 Woodruff Memorial Research Building, Emory University School of Medicine, Atlanta, GA 30322, U.S.A.

Hamill et al.[7]. Suction was applied to a fire-polished micropipette pressed against the pinealocyte membrane until a membrane–electrode seal exceeding 10 GΩ in resistance was attained. The membrane patch under the electrode was then ruptured by increasing the suction applied to the pipette. Several solutions were used to fill the patch pipette in these experiments. The standard internal solution contained (in mM): NaCl 10, KCl 145, $MgCl_2$ 1.0, $CaCl_2$ 1.0, EGTA 1.5, HEPES 10 (pH 7.2 with KOH). Because pinealocytes rather quickly deteriorated after internal perfusion, potassium aspartate was substituted for KCl, but with little notable improvement in pinealocyte survival. Other variations in internal solutions are noted in figure legends. Experiments were done both in HEPES-buffered tissue culture medium or in HEPES-buffered Hank's saline. All norepinephrine iontophoresis experiments were done at 37 °C because of earlier reports that the response to norepinephrine may depend on temperature-sensitive mechanisms[9]. Investigations of voltage- and time-dependent membrane conductances were done at room temperature. Tetraethylammonium chloride (TEA), up to 50 mM, was substituted for equimolar quantitites of NaCl in some experiments. Tetrodotoxin (TTX), 3 μM, was used in some experiments to block the voltage-dependent sodium current in order to uncover smaller inward currents.

More than 60 cells were studied using either conventional or patch-clamp technique. Twenty-five

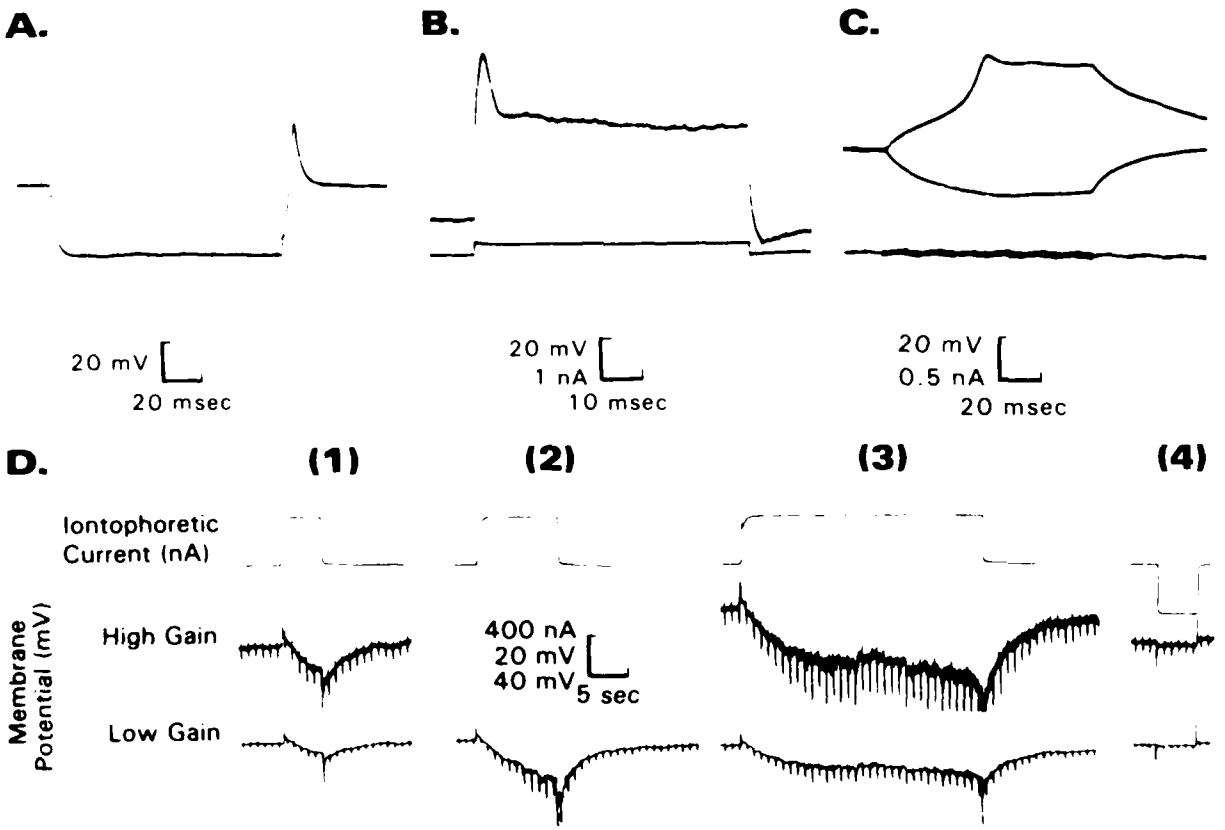

Fig. 1. Top panel (A–C): action potentials in pinealocytes in culture. Upper trace, voltage; lower trace, current. A and B (different cells) show intracellular recordings with potassium acetate microelectrodes. A: anodal break spike. Resting membrane potential −38 mV. B: spike evoked by depolarizing current pulse; resting potential −40 mV. C: slow regenerative response measured with whole-cell patch technique. Input resistance, measured as voltage displacement at end of hyperpolarizing step divided by the applied current, was 1 GΩ; resting potential −70 mV. D: hyperpolarizing response of pinealocyte to norepinephrine. D_{1-3}: response increased in amplitude as iontophoretic pulse increased in duration. Response showed no decline during prolonged pulse. D_4: Pulse of opposite polarity had no effect on membrane potential. Downward deflections on voltage traces are responses to small hyperpolarizing current pulses (not seen at low gain on current trace) used to assess membrane input resistance and status of amplifier bridge balance. Vertical calibration bar represents 400 nA for the top (current) traces, 20 mV for the middle (high voltage gain) traces and 40 mV for the lower (low voltage gain) traces.

cells were studied using conventional intracellular pipettes. Of these, in 13 consecutively examined cells, resting membrane properties were determined. Norepinephrine was applied to 30 cells, 25 of which were studied with conventional electrodes and 5 with patch-clamp electrodes.

When pinealocytes were penetrated with conventional potassium acetate electrodes, there was usually a rapid and progressive decline in membrane potential and input resistance. These cells were not further studied. In those cells where stable membrane potentials were recorded, there was usually an initial rapid fall in potential before a steady-state potential was reached. In such cells the mean membrane potential was 32 ± 3.2 mV (mean ± S.E.M., n = 13). In some of these cells, small anodal break spikes were seen (Fig. 1A), and in some, if the membrane potential was made more negative by passing steady inward current via the amplifier bridge circuit, a small spike could be evoked by depolarizing current pulses (Fig. 1B). In most cells, even when steady resting membrane potentials were attained, spike electrogenesis rapidly disappeared.

We had hoped that we could achieve more stable long-term recordings by using the whole-cell patch-clamp technique. This method has permitted accurate recording from some types of small cells. We found that, despite varying intracellular solutions, we still could not record from pinealocytes for more than about 5 min. In some respects, however, the gigaohm seal did offer some notable refinements over conventional techniques. Because of the very high membrane–electrode seal resistance, the pinealocyte input resistances were not shunted by the patch technique as they were by conventional microelectrodes. With the standard intracellular solution, resting potentials were in the range of −50 to −70 mV, and input resistances commonly exceeded 1 GΩ (Fig. 1C). This is in accord with results obtained in other small secretory cells (see discussion below).

Using the whole-cell patch technique in the current clamp mode, overshooting action potentials, which declined in several seconds, were frequently seen. Over the next several minutes small active responses and anodal break spikes could still be evoked in most cells (Figs. 1C, 2A). Frequently, pinealocytes exhibited prolonged undershooting active responses (Fig. 1C). Active responses were seen both in the presence

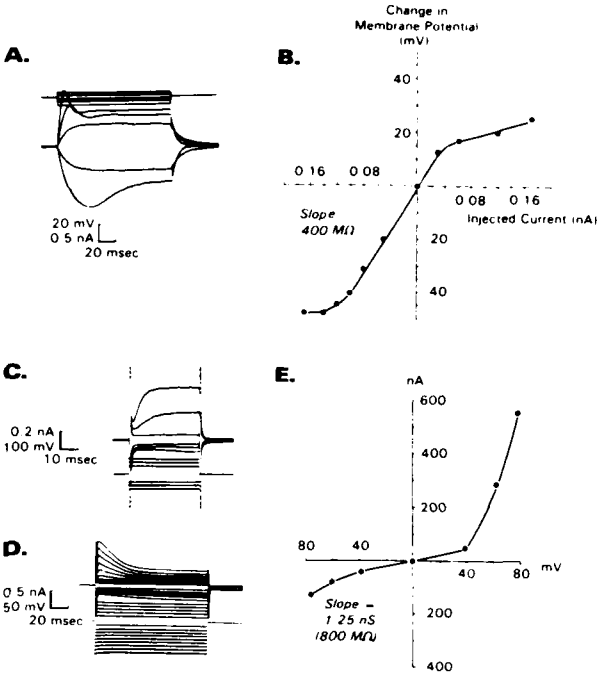

Fig. 2. Inward and outward rectification in pinealocytes; whole-cell patch-clamp recordings. Modifications in standard (see text) solutions: TEA, 10 mM, present in external bath solution; EGTA, 1 mM, and no added calcium in pipette solution. A–D from different cells; C and E from same cell. A: responses to constant current steps. Upper trace, current; lower trace, voltage. Depolarization caused slow, overshooting active response followed by delayed (outward) rectification. Resting potential was −40 mV. B: voltage–current plot of data from another cell which showed no overshooting action potentials. Line drawn by eye. Resting potential was −58 mV. C–E: voltage- and time-dependent membrane currents in voltage-clamped pinealocytes. In C and D, upper series of traces is current; lower series of traces is voltage. C: inward and outward rectification; V_H −46 mV. D: transient outward currents and inward rectification; V_H −83 mV. E: current–voltage relationship plotted from data shown in C; line drawn by eye; slope measured from linear portion of plot.

and absence of 3 μM TTX. Because of the fragile nature of these cells, the mechanical vibrations caused by perfusion prohibited us from examining the spike before and after TTX washout. Therefore, we could not determine to what extent TTX-sensitive sodium channels (vs calcium channels or other types of sodium channels) contribute to spike electrogenesis.

The most persistent and striking finding was the prominent inward and outward rectification present in these cells (Fig. 2). Outward rectification developed within about 20 ms. Inward rectification was a much slower process, usually requiring more than 100 ms for its full activation. In the presence of up to

50 mM TEA, both the inward and outward rectification were still present with little evidence of inhibition (Fig. 2). As a consequence, TEA did not substantially enhance the amplitude or duration of the action potentials.

Under voltage-clamp, depolarizing steps from holding potentials (V_H) equal to the resting potential gave rise to labile, slow net inward currents that declined within seconds. Corresponding to the rectification seen in the current clamp mode, the membrane currents that persisted in time were the slow outward currents elicited by depolarizing voltage steps and the slow inward currents following hyperpolarizing voltage steps (Fig. 2C–E). When V_H was shifted to more negative values, depolarizing steps evoked a transient outward current (Fig. 2D), which peaked within 10–20 ms and decayed over about 50 ms.

In about 30% of the pinealocytes tested, norepinephrine caused a change in membrane potential. In every case, this response was a hyperpolarization. As shown in Fig. 1D, the response was dose-dependent, increasing in amplitude as the iontophoretic current was increased in amplitude or duration. During prolonged application of iontophoretic current, the hyperpolarization persisted, showing no sign of desensitization. When the iontophoretic current was reversed in polarity, there was no resultant alteration in pinealocyte membrane potential. By passing constant current steps across the pinealocyte membrane, we attempted to monitor the membrane input resistance during the norepinephrine-induced hyperpolarization. In most cased there appeared to be an increase in input resistance, as judged by the larger voltage responses to the constant-current steps during the norepinephrine response (Fig. 1D).

In this study was have used intracellular electrophysiological techniques to examine membrane properties of rat pinealocytes in tissue culture. The values of resting membrane potential are similar to those found by Parfitt et al. (see ref. 9) in acutely removed pineal glands in vitro. The results obtained with the patch technique; however, suggest that this value may be low and may reflect considerable shunting through the membrane–pipette seal, a problem commonly encountered when recording from small cells having high input resistances. On the other hand, although the more negative potentials obtained with the patch technique may more accurately represent the cells' resting potentials, it must be realized that the cytoplasm is completely perfused with the intrapipette solution[4]. Therefore, the recorded potential reflects the ratio of the intrapipette ions to the ions bathing the outside of the cell, and this ratio may be far from physiological.

We found that only 30% of the pinealocytes tested showed a response to norepinephrine and that all of these responding cells were hyperpolarized by the drug. This agrees with the finding by Semm and Vollrath[16] that the frequency of spontaneous spikes in 38% of tested single units recorded in anesthetized guinea pigs were inhibited by norepinephrine. The hyperpolarization recorded in these pinealocytes in culture was like that found by Parfitt et al.[9] in rat pineal glands in vitro. We were unable to determine the ionic mechanism of this response because the fragility of the cells and short recording periods did not allow perfusion of solutions containing various ion concentrations or channel blockers.

Pinealocyte membranes show strong rectification to both inward and outward currents. Functionally, these properties may serve to hold the membrane potential 'clamped' within a narrow range. Of a practical nature is the effect that this rectification has on interpretation of the resistance changes caused by norepinephrine. Together with the difficulty of balancing the bridge circuit with high-resistance electrodes, such membrane rectification does not allow one to accurately determine the effect of norepinephrine on membrane resistance. Such an analysis will require determination of complete current–voltage relationships before and after norepinephrine.

The transient outward current seen in these cells is similar to that described by Neher[8] and by Connor and Stevens[1]. It has since been found in many different types of excitable cells (where it is usually termed the A-current). Functionally, it is believed that this current serves to limit the speed at which the membrane potential can reach the spike threshold; therefore, it controls the frequency of repetitive spiking[2].

There has been uncertainty as to whether pinealocytes may generate action potentials. Our studies, in agreement with Ronnekleiv et al.[12] show that pinealocytes are capable of spike electrogenesis. As in many secretory cells, it seems likely that a part of the spike potential is due to calcium current because action potentials could be recorded in the presence of TTX.

This would in part explain the rapid loss of spike electrogenesis during both conventional and whole-cell recording, for calcium currents are particularly sensitive to cell injury and to intracellular perfusion[3,15]. Our consistent finding that norepinephrine caused membrane hyperpolarization (also reported by Sakai and Marks[14]) would suggest that sympathetic stimulation should decrease the frequency of pinealocyte spiking. How this membrane hyperpolarization may be linked to subsequent biochemical events and the eventual secretion of melatonin is not known. A clue to the nature of such a link would come from knowledge of the ionic and biochemical mechanisms of the hyperpolarization.

It is interesting to compare pinealocytes to the phylogenetically related photoreceptors. The normal resting potential of rod cells is between −10 and −30 mV (ref. 17). Light flashes hyperpolarize the cell by closing sodium or calcium channels that are open at rest[11]. The hyperpolarization is not inhibitory to the neural network, but rather it facilitates transfer of information through the system. By analogy, the resting potential of −30 to −40 mV that we and others have recorded in pinealocytes may be normal, and the hyperpolarization caused by norepinephrine may not be an inhibitory mechanism.

Supported by Armed Forces Radiobiology Research Institute, Defense Nuclear Agency, under Research Work Unit MJ00013. The views presented in this paper are those of the authors; no endorsement by the Defense Nuclear Agency has been given or should be inferred.

1 Connor, J.A. and Stevens, C.F., Voltage-clamp studies of a transient outward membrane current in gastropod neural somata, *J. Physiol. (London)*, 213 (1971) 21–30.
2 Connor, J.A. and Stevens, C.F., Prediction of repetitive firing behavior from voltage clamp data on an isolated neurone soma, *J. Physiol. (London)*, 213 (1971) 31–53.
3 Fedulova, S.A., Kostuyk, P.G. and Tsyndrenko, A.Y., Calcium channels in the somatic membrane of the rat dorsal root ganglion neurons. Effect of cAMP, *Brain Research*, 214 (1978) 210–214.
4 Fenwick, E.M., Marty, A. and Neher, E., A patch-clamp study of bovine chromaffin cells and of their sensitivity to acetylcholine, *J. Physiol. (London)*, 331 (1982) 577–597.
5 Freschi, J.E., Parfitt, A.G. and Shain, W.G., Electrophysiology and pharmacology of striated muscle fibres cultured from dissociated neonatal rat pineal glands, *J. Physiol. (London)*, 293 (1979) 1–10.
6 Ginsborg, B.L., Ion movements in junctional transmission, *Pharmacol. Rev.*, 19 (1967) 289–316.
7 Hamill, O.P., Marty, A., Neher, E., Sakmann, B. and Sigworth, F.J., Improved patch-clamp techniques for high-resolution current recording from cells and cell-free membrane patches, *Pflugers Arch.*, 391 (1981) 85–100.
8 Neher, E., Two fast transient current components during voltage clamp on snail neurons, *J. Gen. Physiol.*, 58 (1971) 36–53.
9 Parfitt, A., Weller, J.L., Klein, D.C., Sakai, K.K. and Marks, B.H., Blockade by ouabain or elevated potassium ion concentration of the adrenergic and adenosine cyclic 3′,5′-monophosphate-induced stimulation of pineal serotonin N-acetyltransferase activity, *Mol. Pharmacol.*, 11 (1975) 241–255.
10 Parfitt, A., Freschi, J.E., Shain, W.G., Schmechel, D.E., Auerbach, D.A. and Turner, J.N., Pineal cells: culture and co-culture with neurons from the superior cervical ganglia. In D.C. Klein (Ed.), *Melatonin Rhythm Generating System*, Karger, Basel, 1982, pp. 62–83.
11 Penn, R.D. and Hagins, W.A., Kinetics of the photocurrent of retinal rods, *Biophys. J.*, 12 (1972) 1073–1094.
12 Ronnekleiv, O.K., Kelly, M.J. and Wuttke, W., Single unit recordings in the rat pineal gland: evidence for habenula-pineal neural connections, *Exp. Brain Res.*, 39 (1980) 187–192.
13 Rowe, V., Neale, E.A., Avins, L., Guroff, G. and Schrier, B.K., Pineal gland cells in culture, *Exp. Cell Res.*, 104 (1977) 345–356.
14 Sakai, K.K. and Marks, B.H., Adrenergic effects on pineal cell membrane potential, *Life Sci.*, 11 (1972) 285–291.
15 Schwindt, P. and Crill, W., Role of a persistent inward current in motoneuron bursting during spinal seizures, *J. Neurophysiol.*, 43 (1980) 1296–1318.
16 Semm, P. and Vollrath, L., Electrophysiology of the guinea-pig pineal organ: sympathetically influenced cells responding differently to light and darkness, *Neurosci. Lett.*, 12 (1979) 93–96.
17 Werblin, F.S. and Dowling, J.E., Organization of the retina of the mudpuppy, *Necturus maculosus*. II. Intracellular recording, *J. Neurophysiol.*, 32 (1969) 355–399.

Gamma radiation affects active electrolyte transport by rabbit ileum: basal Na and Cl transport

PAMELA J. GUNTER-SMITH
Physiology Department, Armed Forces Radiobiology Research Institute, Bethesda, Maryland 20814-5145

GUNTER-SMITH, PAMELA J. *Gamma radiation affects active electrolyte transport by rabbit ileum: basal Na and Cl transport.* Am. J. Physiol. 250 (Gastrointest. Liver Physiol. 13): G540–G545, 1986.—The effect of whole-body gamma radiation (5–12 Gy) on electrolyte transport by rabbit ileum in vitro was assessed for 1–96 h postirradiation using the short-circuit technique and radioisotopic fluxes. Although there was no effect of radiation on short-circuit current (I_{sc}), transepithelial potential, or resistance 1 h after exposure, by 24 h the basal parameters of ileal segments isolated from irradiated animals were significantly greater than those of sham-irradiated controls. The I_{sc} increased in a dose-dependent fashion and was greatest 24 h postexposure. Isotope flux experiments revealed that the increased I_{sc} following irradiation resulted in part from a stimulation of active serosal-to-mucosal net Cl flux. There was no observable change in net Na transport. The results demonstrate that radiation exposure alters cellular transport processes, which may contribute to the fluid and electrolyte imbalance observed following radiation exposure.

electrolyte transport; radiation; chloride secretion

IONIZING RADIATION has pronounced effects on both the morphology and the physiology of the gastrointestinal tract. Collectively, these effects are termed the gastrointestinal syndrome (20), which is characterized by progressive fluid and electrolyte imbalance and bacteremia. This syndrome is a major determinant of lethality at doses of X- and gamma radiation of 10–100 Gy. The time course of the development of the pathophysiology is predictable, with death of the animal generally corresponding to the time for denudation of the intestinal mucosa. In spite of the well-documented effects of radiation on gastrointestinal physiology, very little is known concerning the mechanism by which radiation produces these effects. In particular, it has yet to be determined whether the fluid and electrolyte loss associated with the gastrointestinal syndrome results from alterations in transepithelial transport processes or is a consequence of other factors, such as the loss of functional cells due to denudation. Indeed, few studies exist concerning the effect of radiation on electrolyte transport processes of epithelial cells.

In the present study, I report on the effect of ^{60}Co radiation on intestinal ion transport by rabbit ileal mucosa. The results demonstrate a radiation-related change in transepithelial ion transport, as indicated by changes in short-circuit current and ion fluxes at times >24 h postirradiation. In particular, the basal short-circuit current is significantly higher in irradiated animals, due in part to a stimulation of net Cl secretion across the ileal mucosa.

METHODS

Animals and solutions. New Zealand White male rabbits (Hazelton Dutchland, Denver, PA, and Hilltop Lab Animals, Scottdale, PA) weighing 2–3 kg were used in these experiments. The animals were fed standard rabbit chow ad libitum, except for "fasted" rabbits, from which food was removed. Rabbits were irradiated in the Armed Forces Radiobiology Research Institute's ^{60}Co facility in Plexiglas restraining cages. Whole-body doses of 5, 7.5, 10, and 12 Gy were administered. These doses were selected to bracket the range of doses associated with the gastrointestinal syndrome. The dose rate was a constant fraction (1/10) of the total dose, maintaining the exposure time at 10 min. Sham-irradiated animals served as controls.

At the appropriate time (1, 24, 48, 72, or 96 h postirradiation), control and irradiated or fasted animals were killed by pentobarbital sodium (Nembutal) injection and the terminal ileum of each was removed. The tissue was opened lengthwise along its mesenteric border and stripped of its underlying musculature using blunt dissection. Tissue isolated from sham-irradiated, irradiated, and fasted animals are termed control, irradiated, and fasted tissues, respectively.

The intestinal segments were mounted in Plexiglas Ussing chambers (E. W. Wright, Guilford, CT), exposing 1.12 cm^2 of tissue, and bathed with a Ringer solution containing (in mM): 140 Na, 119 Cl, 21 HCO_3, 1.2 Ca, 1.2 Mg, 0.5 PO_4, and 5.4 K; pH 7.4. The solutions were circulated and oxygenated by a gas-lift system in reservoirs using 95% O_2-5% CO_2. All experiments were performed at 37°C.

Electrical measurements. The transepithelial potential difference (PD, mV) with respect to the mucosal bathing solution was measured with a digital voltmeter in contact with both bathing solutions via 3 M KCl-agar bridges and calomel half cells. Current was passed by means of a battery in series with resistors and in contact with both bathing solutions by means of Ringer-agar bridges and Ag-AgCl electrodes. Current was passed periodically to drive the transepithelial PD to zero. This current, the short-circuit current (I_{sc}, $\mu A \cdot cm^{-2}$), represents the sum

of all "active" ion movements across the tissue (23). The I_{sc} was corrected for the potential drop across the fluid resistance. In some experiments an automatic voltage clamp device (Physiologic Instruments, Houston, TX) was used to measure PD and I_{sc}, eliminating the need for this correction. The transepithelial resistance (R_t, $\Omega \cdot cm^2$) was calculated from the deflection in PD produced by 20-μA bipolar current pulses.

In preliminary experiments, considerable animal-to-animal variation in the absolute magnitude of the transepithelial electrical parameters was observed. To minimize the possible influence of different "batches" of animals, the electrical parameters of tissue isolated from irradiated or fasted animals were compared with that of a control animal from the same shipment. Four segments of tissue were isolated from each animal, with the mean tissue value determined from those segments having a resistance within 25% of the mean value. In some cases, the results are expressed as the difference between values obtained from irradiated or fasted and control animals within an experiment.

Na and Cl fluxes. The radioisotopic fluxes of Na and Cl were determined simultaneously in tissues isolated from irradiated animals and their sham-irradiated controls. The ileal segments were incubated in normal Ringer solution for 80 min to allow for the establishment of a stable base line. Irradiated or control segments were then paired according to resistance (within 25%), and short-circuited and tracer amounts of ^{22}Na and ^{36}Cl were added to either mucosal or serosal solutions. After a 40 min equilibration period, the unidirectional fluxes of Na and Cl from mucosal-to-serosal ($J_{m \to s}$) and serosal-to-mucosal ($J_{s \to m}$) were determined from five samples taken at 15-min intervals. The difference in unidirectional fluxes of an ion is the net flux (J_{net}). The residual ion flux (J^R) represents the inequality of *a*) the sum of net Na flux (J^{Na}_{net}) and net Cl flux (J^{Cl}_{net}) and *b*) the I_{sc}. All fluxes are expressed in $\mu eq \cdot h^{-1} \cdot cm^{-2}$ and are compared with I_{sc} expressed in similar units.

Statistics. The significance of differences was determined by either a Student's *t* test or an analysis of variance and the Newman-Keuls test for multiple comparisons. A value of $P < 0.05$ was taken as statistically significant.

RESULTS

The basal I_{sc} of ileal segments isolated from four irradiated animals (10 Gy) 1 and 24 h postexposure is compared with that of four sham-irradiated controls in Fig. 1. Values of I_{sc} of control tissues were similar to those reported previously (9). At 1 h, there was no apparent effect of radiation exposure on I_{sc} by this or any of the doses studied. Likewise, no difference in either PD or R_t was observed.

In contrast, by 24 h (Fig. 1), prior exposure to radiation elicited dramatic changes in ileal electrolyte transport. Figure 2 shows the difference in steady-state basal I_{sc} of ileal segments isolated from irradiated rabbits compared with that of their matched controls for 5, 7.5, 10, and 12 Gy with respect to time postexposure.[1] The basal I_{sc} of irradiated tissues exceeded that of controls for doses greater than 5 Gy. Although the magnitude of this increase clearly declined with respect to time postexposure, the I_{sc} remained elevated for up to 72 h for 7.5 Gy and 96 h for 10 Gy. The magnitude of the increase in I_{sc} was also dose dependent. For example, the increase 24 h following 12 Gy ($\Delta I_{sc} = 93.2 \pm 12.3$ $\mu A \cdot cm^{-2}$) is significantly greater than that observed following 7.5 Gy ($\Delta I_{sc} = 43.7 \pm 7.7$ $\mu A \cdot cm^{-2}$) for the same time point.

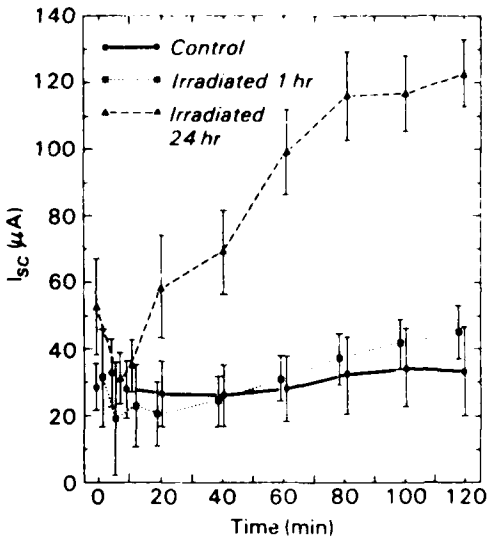

FIG. 1. Short-circuit current of control (*filled circles*) and irradiated segments (10 Gy) 1 h (*filled squares*) and 24 h (*filled triangles*) postexposure; $n = 4$.

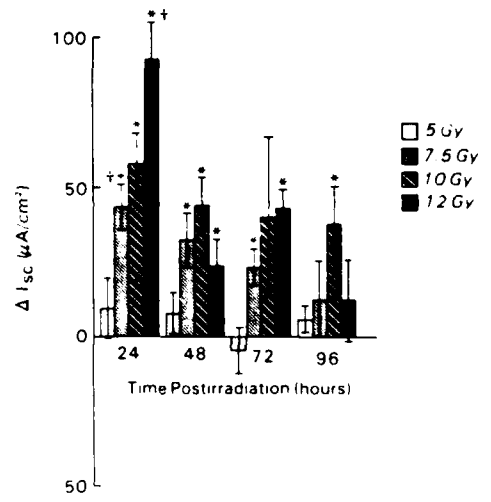

FIG. 2. Difference in basal steady state short-circuit current (I_{sc}) of tissues isolated from irradiated animals compared with their matched controls. Each *bar* is mean difference of 4 irradiated animals from their "matched" controls. * Significant difference from zero; † significant difference between groups.

[1] In many but not all cases, the I_{sc} of irradiated segments gradually increases with time to a stable value. Mechanisms underlying this slow equilibration period are presently not known. It most likely reflects reestablishment of ion gradients, etc., in the tissue. Values of I_{sc} were stable generally within 60 min after mounting. The steady state I_{sc} was taken as the value of I_{sc} 120 min after mounting.

TABLE 1. *Effect of radiation on basal PD and R_t*

	24 h	48 h	72 h	96 h
5 Gy				
PD	0.7±0.5	−2.0±0.6	0.1±0.2	0.3±0.2
R_t	−0.3±5.3	1.6±2.3	−8.2±3.2	1.0±2.3
7.5 Gy				
PD	2.0±0.4*	1.7±0.8*	0.4±0.2	0.5±0.4
R_t	6.4±1.8*	5.0±4.3	3.4±5.7	1.3±2.1
10 Gy				
PD	2.7±0.8*	1.9±0.6*	0.8±0.8	2.8±0.5*
R_t	10.1±6.0	6.5±2.9	−3.2±2.9	22.1±10.3
12 Gy				
PD	4.0±0.4*	1.4±0.5*	2.0±1.2*	0.8±0.5
R_t	5.8±3.1	4.7±4.7	−0.8±4.0	−0.3±2.4

Values are means ± SE. PD, potential difference; R_t, transepithelial resistance. Difference in PD (mV) and R_t ($\Omega \cdot cm^2$) of irradiated tissues compared with controls. * Significantly different from zero; $n = 4$.

TABLE 2. *Comparison of fasting and radiation effects on basal I_{sc}*

	24 h	48 h	72 h	96 h
Fasting	22.5±5.1*	30.6±7.3*	9.1±17.5	26.6±6.8*
7.5 Gy	43.7±7.7*	32.8±9.1*	23.4±6.3*	NS
10 Gy	58.0±10.4*†	44.0±9.7*	NS	38.0±12.6*
12 Gy	93.2±12.3*†	23.9±9.0*	43.3±6.3*	NS

Values means ± SE expressed as difference between fasting or irradiated and control. * Significantly different from zero; † significantly different from fasting; $n = 4$.

In addition to changes in I_{sc}, radiation also altered the PD and R_t (Table 1). The PD of segments isolated from animals irradiated with greater than 5 Gy exceeded the control value of 1.3 ± 0.6 mV. The transepithelial resistance (R_t) of irradiated tissues isolated 24 h after 7.5 Gy was also greater, exceeding the control value of 24.5 ± 0.32 by 6.4 ± 1.8 $\Omega \cdot cm^2$. While there appears to be no significant difference in mean R_t for other doses and times postexposure, of those irradiated tissues whose basal I_{sc} exceeded controls, R_t of 80% of them exceeded that of matched controls.

Effect of fasting of basal I_{sc}. Food intake of irradiated animals was found to be depressed immediately following exposure. Thus it was important to evaluate the potential contribution of reduced food intake on the changes observed above. The response of ileal segments isolated from rabbits from which food was withdrawn ("fasted" animals[2]) was compared with that of nonirradiated control animals for periods of time corresponding to those used in the radiation experiments above. As shown in Table 2, in some cases fasting produced changes in electrolyte transport similar to those observed in irradiated animals. There was a small increase in the base-line I_{sc} 24 h following fasting, which remained elevated during the time periods studied.

However, a comparison of radiation-related changes with fasting-related changes in Table 2 reveals a significant effect of radiation beyond that which could be attributed to fasting. The increase in base-line I_{sc} noted at 24 h postirradiation with 10 and 12 Gy is significantly greater ($P < 0.05$) than that observed for the same time point with fasting. A distinction between radiation and fasting effects on basal I_{sc} at later time points is not as evident, but as will be discussed below, it is less likely that fasting contributes to these later changes.

[2] Since rabbits are coprophagous, animals from which food has been removed cannot be considered totally fasted. Irradiated animals are also not completely fasted. They continue to feed, although at a reduced rate that increases toward normal with time postirradiation. Thus the effect of food withdrawal on I_{sc} most likely overestimates the influence of fasting on the radiation results.

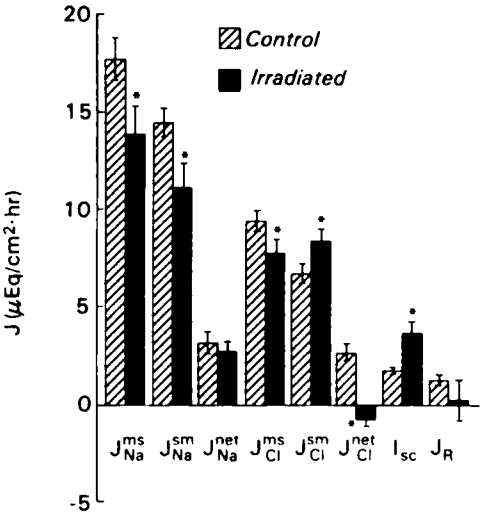

FIG. 3. Unidirectional fluxes ($J^{Na}_{m\to s}$, $J^{Na}_{s\to m}$, $J^{Cl}_{m\to s}$, and $J^{Cl}_{s\to m}$) and net fluxes (J^{Na}_{net}, J^{Cl}_{net}) of Na and Cl, short-circuit current (I_{sc}) and residual flux (J^R) of control (*hatched bars*) and irradiated tissues (*filled bars*) determined 24 h following 10 Gy. Each *bar* is mean of 5 animals. * Significant difference between irradiated and control values.

Flux measurements. To determine the ionic basis of the increase in I_{sc} observed following radiation exposure, the radioisotopic fluxes of Na and Cl were determined in ileal segments from animals irradiated with 10 Gy and compared with that of their sham-irradiated controls.[3] As shown in Fig. 3, radiation exposure resulted in significant changes in both unidirectional and net fluxes. Both $J_{m\to s}$ and $J_{s\to m}$ of Na (13.9 ± 1.4 and 11.5 ± 1.3 $\mu eq \cdot h^{-1} \cdot cm^{-2}$, respectively) of irradiated tissues were significantly reduced compared with controls (17.7 ± 1.1 and 14.5 ± 0.8 $\mu eq \cdot h^{-1} \cdot cm^{-2}$). A difference in J_{net}, however, was not apparent. The $J_{m\to s}$ of Cl of the irradiated animal was also decreased (7.8 ± 0.8 vs. 9.5 ± 0.6 $\mu eq \cdot h^{-1} \cdot cm^{-2}$). However, the $J_{s\to m}$ was increased (8.5 ± 0.6 vs. 6.8 ± 0.5 $\mu eq \cdot h^{-1} \cdot cm^{-2}$), resulting in change of net Cl transport from absorption (2.7 ± 0.4 of controls) to secretion (−0.7 ± 0.4 $\mu eq \cdot h^{-1} \cdot cm^{-2}$). This difference in J^{Cl}_{net} exceeded the difference in I_{sc} observed for irradiated and control tissues, suggesting that some other ion may be involved in the response. Related to this, J^R of irradiated segments appeared smaller but was not significantly different from that of controls.

DISCUSSION

Effect of radiation exposure on electrolyte transport. The present study was undertaken to determine whether

[3] This dose and time point were selected to maximize the difference in ion transport observed postirradiation. Twenty-four hours is the time point at which the peak difference in I_{sc} is observed. Although the increase in I_{sc} at 12 Gy exceeds that observed for 10 Gy, survival of the animals was more consistent at the lower dose.

radiation-related fluid and electrolyte loss results from changes in active cellular transport mechanisms, as has been described for other diarrheal states, or rather simply from leakage of these substances across a "leaky" intestinal mucosa. The results clearly demonstrate, for the first time, that whole-body gamma exposure elicits changes in active basal electrolyte transport. This was evidenced by the dose- and time-dependent increase in I_{sc} and changes in Na and Cl fluxes observed in irradiated animals. There was no apparent change in net Na absorption, although both unidirectional fluxes of this ion were reduced. Since R_t of irradiated tissues often exceeds that of controls, the decrease in net mucosal-to-serosal ($J^{Na}_{m\rightarrow s}$) and serosal-to-mucosal ($J^{Na}_{s\rightarrow m}$) flux of Na may reflect decreased Na movement through a paracellular pathway. By contrast, net Cl transport following irradiation was secretory rather than absorptive as in control animals. The change in Cl transport resulted from a decrease in $J_{m\rightarrow s}$ and an increase in $J_{s\rightarrow m}$ of this ion. It is presently unclear whether changes in Cl transport entirely account for the difference in I_{sc} observed between irradiated and control animals. A small but insignificant decrease in residual ion flux was noted that may implicate a role for some other ion in this response.

In many respects the changes in ion transport observed following irradiation are similar to those observed previously for various secretagogues that elevate intracellular cAMP and Ca. These agents increase I_{sc} by a stimulation of active blood to lumen Cl and (in some cases) Na secretion (8, 17). In addition, these agents also increase transepithelial PD and R_t. The increases in I_{sc}, R_t, and PD observed following irradiation are strikingly similar to those changes mentioned above for secretagogues. Thus changes in cell transport processes previously proposed to underlying the response of rabbit ileum to secretagogues may be elicited by radiation exposure. The magnitude of the response to irradiation declined with time postexposure. The reasons for this decline are presently unknown. However, interestingly, a similar decline in the response of irradiated segments to the secretagogue theophylline has also been observed (unpublished observations).

Relation to radiation pathophysiology. The results of this study clearly indicate that radiation exposure elicits changes in electrolyte transport. As such, they dispute some of the previously conceived notions concerning the mechanisms underlying radiation-induced fluid and electrolyte loss. Morphological studies of intestinal mucosa isolated from irradiated mice by Porvazn[illegible]19) revealed a decrease in the integrity of the tight junctional complexes between adjacent absorptive and goblet cells. It was suggested that the compromised tight junction may serve as a low-resistance pathway for the entry of bacterial toxins leading to bacteremia. Such breaks in the strands of the tight junctional complex could also serve as a route for fluid and electrolyte loss. Comparable morphological studies are not available for rabbit ileum. However, the increase in I_{sc}, decrease in unidirectional Na fluxes, and lack of a decrease in R_t observed in this study suggest that possible damage to tight junctions by radiation exposure is at least initially of little consequence to postirradiation electrolyte transport. More importantly, the results dispel the notion that radiation-induced fluid and electrolyte loss result only from simple denudation of the intestinal mucosa.

Previous in vivo studies have been consistent with changes in transcellular transport following irradiation. These earlier studies concentrated primarily on radiation-related changes in Na absorption. Forkey et al. (10) suggested that decreased ileal Na absorption resulted in Na loss via the bile in irradiated rats. They and others (13, 14, 23, 26) further suggested that the resulting electrolyte imbalance contributed significantly to lethality of the gastrointestinal syndrome. Indeed, Curran et al. (5) observed decreased ileal Na absorption in vivo by rats as early as 13 h following 25–30 Gy abdominal X-irradiation and net Na secretion 67 h after exposure. Although they are suggestive of changes in cellular transport processes, these observations were far from conclusive.

A stimulation of active Na secretion was not observed in the present study. It is not yet clear whether a change in net Na transport following irradiation is a species-dependent phenomena or is evident only at times greater than 24 h. A major finding of this study is a stimulation of active Cl secretion. To my knowledge, previous studies have not investigated changes in the transport of this ion following irradiation.

The results of this study raise two pertinent questions. First, can the changes in net Cl secretion observed in this study account for fluid and electrolyte loss observed in vivo postirradiation? Stimulation of Cl secretion may be responsible for both. Stimulation of anion secretion would promote a passive osmotic water flux as observed for other secretagogues such as cholera toxin. Thus Cl secretion would promote the fluid loss and diarrhea associated with the gastrointestinal syndrome. In support of this, diarrhea, while not a consistent finding perhaps due to colonic reabsorption, was observed in ~80% of the irradiated animals in this study (unpublished observations).

The stimulation of Cl secretion may also be responsible for Na loss observed previously. In vivo, the ileum is essentially in the open-circuit state. Thus anion secretion would create an electrical driving force (lumen-negative PD) for the secretion of a cation such as Na. Na secretion would not be apparent in this study, since fluxes were measured under short-circuit conditions in which this electrical driving force is dissipated. Thus the results point to the stimulation of Cl secretion as the primary event responsible in radiation-induced fluid and electrolyte loss.

Second, is the stimulation of Cl secretion a direct effect of radiation on cell membrane transport or a consequence of other factors? Although this question cannot be answered definitively by this study, the time course of the changes suggests that secondary effects of irradiation stimulate Cl secretion. Alterations in basal electrolyte transport were not apparent until 24 h postirradiation. Similar delays were observed by Curran et al. (5) for the onset of Na transport changes in X-irradiated rats. Thus it is likely that events occurring subsequent to irradiation, such as decreased food intake, intestinal vascular

changes, or radiation-released agents initiated the changes in electrolyte transport observed. The possible role of one of these, decreased food intake, was investigated in this study. Although the I_{sc} of fasted animals was greater than controls, the increase in I_{sc} following irradiation exceeded that observed in fasted animals. Ion fluxes were not measured in fasted animals; thus a contribution of fasting to the changes observed postirradiation cannot totally be excluded. However, since fasting overestimates the decreased food intake of irradiated animals and the response to irradiation is dose and time dependent, it is unlikely that Cl secretion postirradiation is linked to decreased food intake. Furthermore, Cl absorption rather than secretion has been reported in rabbit ileum following an overnight fast (11).[4]

Although not directly tested, other possible factors that may influence electrolyte transport postirradiation deserve comment. Both increases (3) and decreases in intestinal blood flow (15) have been reported in irradiated animals, leading to the proposal that radiation-induced fluid and electrolyte loss result from intestinal vascular changes. Evidence to date make it unlikely that such changes can directly account for the stimulation of I_{sc} observed in the present study. Studies in which ileal interstitial pressure is increased reveal that the resulting stimulation of fluid secretion arises from passive filtration-secretion phenomena rather than changes in active transport processes (22). Such increases would be predicted if, as suggested by Cockerham et al. (3), increased intestinal blood flow resulted in intestinal edema. While direct effects of changes in intestinal blood flow probably play little or no role in the stimulation of Cl secretion following irradiation, the subsequent release of agents locally may be important in the response. For example, fluid and electrolyte secretion following intestinal ischemia has been suggested to result from agents released due to necrosis (1).

A variety of agents may be released following radiation exposure that can ultimately be responsible for the changes in electrolyte transport observed in this study. These include the intestinal secretagogues, serotonin (6, 16), which may be released subsequent to radiation's mast cell degranulation (4), prostaglandins, which have been observed to increase in rat small intestine postirradiation (2, 7), and neurotransmitters released from enteric neurons (11, 12). The action of these agents present the most attractive explanation for the stimulation of Cl secretion postirradiation. Furthermore, the observation that irradiation of the exteriorized small intestine alone can elicit changes associated with the gastrointestinal syndrome (18, 21) suggests that the effective agent may be released locally as suggested above for the stimulation of secretion following ischemia. Distinguishing direct effects of radiation on cellular transport processes from possible secondary effects will require further study.

In summary, exposure to ionizing radiation alters active ileal electrolyte transport primarily by stimulating Cl secretion. In this and other respects, changes in ion transport following irradiation are similar to those elicited by secretagogues that increase intracellular cAMP and Ca. Furthermore, the stimulation of Cl secretion may represent the primary event responsible for fluid and electrolyte loss observed postirradiation.

[4] Overnight fast probably corresponds to 12–15 h. Recent unpublished observations indicate changes in I_{sc} postirradiation within this time frame.

The author thanks M. Landesman, T. Wilczynski, and B. Case for their technical expertise; M. Owens for the preparation of the manuscript; and Drs. Gallin, Livengood, and Pellmar for their critical reading of the manuscript.

This work was supported by Armed Forces Radiobiology Research Institute, Defense Nuclear Agency, under Research Work Unit MJ 00107. The views presented in this paper are those of the author; no endorsement by the Defense Nuclear Agency has been given or should be inferred.

Received 12 June 1985; accepted in final form 4 November 1985.

REFERENCES

1. BINDER, H. J. Net fluid and electrolyte secretion: The pathophysiologic basis for diarrhea. In: *Mechanisms of Intestinal Secretion*, edited by H. J. Binder. New York: Liss, 1979, p. 1–16.
2. BOROWSKA, A., S. SIERAKOWSKI, J. MACKOWAIK, AND K. WISNIEWSK. A prostaglandin like activity in the small intestine and postirradiation gastrointestinal syndrome. *Experientia* 35: 1368–1370, 1979.
3. COCKERHAM, L. G., T. F. DOYLE, R. B. TRUMBO, AND J. B. NOLD. Acute post irradiation canine intestinal blood flow. *Int. J. Radiat. Biol.* 45: 65–72, 1984.
4. CONTE, F. P., G. S. MELVILLE, JR., AND A. C. UPTON. Effect of graded doses of whole-body X-irradiation on mast cells in the rat mesentery. *Am. J. Physiol.* 187: 160–167, 1956.
5. CURRAN, P. F., E. W. WEBSTER, AND J. A. HOUSEPAIN. The effect of X irradiation on sodium and water transport in rat ileum. *Radiat. Res.* 13: 360–380, 1960.
6. DONOWITZ, M., A. N. CHARNEY, AND Y. H. TAI. A comprehensive picture of serotonin induced ileal secretion. In: *Mechanisms of Intestinal Secretion*, edited by H. J. Binder. New York: Liss, 1979, p. 217–230.
7. EISEN, V., AND D. I. WALKER. Effect of ionizing radiation on prostaglandin 15-OH-dehydrogenase (PGDH) (Abstract). *Br. J. Pharmacol.* 62: 461P, 1978.
8. FIELD, M. Intracellular mediators of secretion in the small intestine. In: *Mechanisms of Intestinal Secretion*, edited by H. J. Binder. New York: Liss, 1979, p. 83–93.
9. FIELD, M., D. FROMM, AND I. MCCOLL. Ion transport in rabbit ileal mucosa. I. Na and Cl fluxes and short circuit current. *Am. J. Physiol.* 220: 1388–1396, 1971.
10. FORKEY, D. J., K. L. JACKSON, AND G. M. CHRISTENSEN. Contribution of bile to radiation-induced sodium loss via the rat small intestine. *Int. J. Radiat. Biol.* 14: 49–57, 1967.
11. HUBEL, K. A. The effects of electrical field stimulation and tetrodotoxin on ion transport by the isolated rabbit ileum. *J. Clin. Invest.* 62: 1039–1047, 1978.
12. HUBEL, K. A. Intestinal nerves and ion transport: stimuli, reflexes, and responses. *Am. J. Physiol.* 248 (*Gastrointest. Liver Physiol.* 11): G261–271, 1985.
13. JACKSON, K. L., AND C. ENTENMAN. The role of bile secretion in the gastrointestinal radiation syndrome. *Radiat. Res.* 10: 67–79, 1959.
14. JACKSON, K. L., R. RHODES, AND C. ENTENMAN. Electrolyte excretion in the rat after severe intestinal damage by X irradiation. *Radiat. Res.* 8: 361–373, 1958.
15. KABAL, J., S. J. BAUM, AND L. J. PARKHURST. Canine intestinal vasoactivity during development of the gastrointestinal syndrome. *Radiat. Res.* 50: 528–538, 1972.
16. KISOFF, B., AND F. W. MOORE. Effect of serotonin on water and electrolyte transport in the in vivo rabbit small intestine. *Gastroenterology* 71: 1033–1038, 1976.
17. MILLER, R. J., J. F. KACHUR, M. FIELD, AND J. RIVIER. Neurohumoral control of ileal electrolyte transport. *Ann. NY Acad. Sci.* 372: 571–593, 1981.
18. MUHIUDDIN, M., K. TAMURA, AND P. DEMARIE. Changes in ab

sorption of glucose and proline following irradiation to the exteriorized ileum. *Radiat. Res.* 74: 186–190, 1978.

19. PORVAZNIK, M. Tight junction disruption and recovery after sublethal γ-irradiation. *Radiat. Res.* 78: 233–250, 1979.
20. QUASTLER, H. The nature of intestinal radiation death. *Radiat. Res.* 4: 303–320, 1956.
21. SULLIVAN, M. F., S. MARKS, P. L. HACKETT, AND R. C. THOMPSON. X-irradiation of the exteriorized or in situ intestine of the rat. *Radiat. Res.* 11: 653–666, 1959.
22. SWABB, E. A., R. A. HYNES, W. G. MARNANE, J. S. MCNIEL, R. A. DECKER, Y.-H. TAI, AND M. DONOWITZ. Intestinal filtration-secretion due to increased intraluminal pressure in rabbits. *Am. J. Physiol.* 242 (*Gastrointest. Liver Physiol.* 5): G65–G75, 1982.
23. SWIFT, M. N., AND S. T. TAKETA. Effect of circulating blood volume of partial shielding of rat intestine during X-irradiation. *Radiat. Res.* 8: 516–525, 1958.
24. TAKETA, S. T. Water-electrolyte and antibiotic therapy against acute (3-to-5 day) intestinal radiation death in the rat. *Radiat. Res.* 16: 312–326, 1965.
25. USSING, H. H., AND K. ZEHARN. Active transport of sodium as the source of electrical current in the short-circuited isolated frog skin. *Acta Physiol. Scand.* 19: 43–56, 1951.
26. ZSEBOK, Z., AND G. PETRANYI. Changes in electrolyte balance in the gastorintestinal syndrome. *Acta Radiol. Ther. Phys. Biol.* 2: 377–383, 1964.

Behavioral Neuroscience
1986, Vol. 100, No. 1, 79-84

Histamine H_2 Receptors Mediate Morphine-Induced Locomotor Hyperactivity of the C57BL/6J Mouse

G. Andrew Mickley
Behavioral Sciences Department
Armed Forces Radiobiology Research Institute, Bethesda, Maryland

Morphine-induced locomotor hyperactivity of the C57BL/6J mouse was challenged with intracranial injections of antihistamines or the opiate antagonist naloxone. When cimetidine (H_2 receptor blocker) was injected into the nucleus accumbens/stria terminalis, it significantly reduced opiate-stimulated locomotion. However, ventricular injections of cimetidine did not significantly alter either morphine or amphetamine hyperactivity, nor did cimetidine depress spontaneous locomotion. Although naloxone eliminated morphine-induced locomotion when injected into either the nucleus accumbens or the ventricles, chlorpheniramine (H_1 receptor blocker) failed to reduce this behavior. These data suggest that opiate-stimulated locomotion of the C57BL/6J mouse may be partially mediated by histamine H_2 receptors of the nucleus accumbens or closely adjacent structures.

In most species a large dose of morphine produces catatonia and akinesia (Brown, Derrington, & Segal, 1979). However, morphine causes a dose-dependent stereotypic locomotor hyperactivity in the C57BL/6J mouse (Oliverio & Castellano, 1974; Teitelbaum, Giammatteo, & Mickley 1979). A similar behavior is observed after an intracranial injection of enkephalin (Puglisi-Allegra, Castellano, Filibeck, Oliverio, & Melchiorri, 1982). This behavioral response is mediated, at least in part, by neurons of the nucleus accumbens, bed nucleus of the stria terminalis, and portions of the striatum. Lesions of these brain areas significantly reduce, but do not abolish, morphine-stimulated locomotion (Siegfried, Filibeck, Gozzo, & Castellano, 1982; Teitelbaum et al., 1979).

Although the opioid-induced locomotor hyperactivity of the mouse has been well described and some of the neuronal systems subserving this response have been identified, the neurochemical mediators that produce the behavior have yet to be fully elucidated. The present experiments addressed the possibility that histamine receptors play a role in morphine-stimulated locomotion. Endorphins, enkephalins, their receptors, histaminergic neurons, and histamine receptors are all prominent in the brain areas responsible for morphine-induced hyperactivity (Akil et al., 1984; Burkard, 1978; Garbarg et al., 1980; Palacios, Wamsley, & Kuhar, 1981; Sazara, 1982; Snyder & Childers, 1979; Watanabe et al., 1984). In mice, the blockade of H_2 receptors inhibits the development of morphine tolerance (Wong & Roberts, 1975). Others have reported that brain histamine levels are inversely proportional to morphine-induced locomotion of the mouse (Lee & Fennessy, 1976); High, locomotion-producing doses of morphine reduce levels of brain histamine in the C57BL/6J mouse (McClain, Catravas, & Teitelbaum, 1977). However, this may not be true for all strains of mice (Hough et al., 1984).

The present study was conducted to further clarify the role of brain histamine in the production of morphine-induced locomotion. This was accompanied by challenging the opiate-stimulated locomotion of the C57BL/6J mouse with injections of antihistamines into the nucleus accumbens/stria terminalis or lateral ventricles.

Method

Subjects

Forty-three male C57BL/6J mice between 60 and 120 days of age were used in this study. Throughout the experiment the mice were fed on an ad-lib food and water schedule in a room maintained on a 12:12 hr light/dark cycle (lights on at 0600). They were housed and tested at a room temperature of approximately 70 °F (21.1 °C).

Surgical Procedure

With the mice under sodium pentobarbital (75 mg/kg, ip) and supplemental Methoxy-flurane anesthesia, they were implanted with chronic bilateral 22-ga. cannulas in the posterior n. accumbens/stria terminalis (ACCUM+STRIA) or lateral ventricles (VENT). Prior to anesthetization, a dose of 0.4 mg/kg atropine sulfate was administered ip. The stereotaxic coordinates used for the placement of the ACCUM+STRIA cannula were 0.8 mm anterior to bregma, ±0.8 mm lateral to midline zero, and 4.0 mm ventral to the skull surface. The coordinates for the ventricle implants were identical except that the

This work was supported by the Armed Forces Radiobiology Research Institute, Defense Nuclear Agency (DNA) under Research Work Unit 4332-00125. Views presented in this article are those of the author. No endorsement by DNA has been given or should be inferred. Portions of these data were presented at the meeting of the Society for Neuroscience, October 1984. Animals were cared for according to the principles enumerated in the "Guide for Care and Use of Laboratory Animals" prepared by the Institute of Laboratory Animal Resources, National Research Council.

The author acknowledges the excellent technical assistance of Paul Brenner, Diane Pickle, Bernard Dennison, Gerald Kessel, Marta Hean, Karen Stevens, and Kathryn Chantry. I thank Endo Laboratories for its kind gift of naloxone. W. E. Jackson offered superior statistical advice. Marion Golightly typed this manuscript.

Correspondence concerning this article should be addressed to G. Andrew Mickley, Behavioral Sciences Department, Armed Forces Radiobiology Research Institute, Bethesda, Maryland 20814-5145.

vertical reading was set at 3.0 mm ventral to the skull surface. The atlas of Slotnick and Leonard (1975) was used as a guide for the placement of the cannulas. Stainless steel stylets were used to keep the cannulas patent. Postoperative behavioral tests were initiated no sooner than 1 week after the surgery.

Procedure

Locomotor activity was measured by the Automex D system (Columbus Instruments). The mice were always tested between 0800 and 1000 in order to control for circadian variations. Testing occurred in the subject's plastic home cage (30 × 19 × 12 cm). In order to discourage high spontaneous locomotor activity counts, the mice resided in their home cage for at least 1 day before any data were collected.

Mouse locomotion, observed after an initial ip injection, was challenged by a subsequent intracranial (ic) drug injection. At the beginning of each test day, an ip injection of 4 mg/kg *d*-amphetamine sulfate, 30 mg/kg morphine sulfate, or an equal volume of saline was administered. Amphetamine-stimulated locomotion (nonopiate mediated) was used here as an active control in order to provide behavioral comparisons with morphine-injected mice. After a 5-min delay, the locomotor response to each drug was determined in a 10-min baseline test period. The morphine- and amphetamine-injected animals were required to meet a minimum criterion level of locomotor activity (80 counts/min) before proceeding to the next phase of the experiment. If they failed to meet criterion, they were not run that day.

Subsequent to successfully reaching the post-ip-injection criterion, each mouse received bilateral 1-μl ic injections in the ACCUM+STRIA or VENT of naloxone hydrochloride (2 μg), cimetidine (H_2 receptor blocker, 75 μg), chlorpheniramine (H_1 receptor blocker, 20 μg), or saline. Previously published studies (Bugajski & Zacny, 1981; Cohn, Ball, & Hirsch, 1973; Kalivas, 1982) and pilot experiments from this laboratory demonstrated that similar ic doses of chlorpheniramine and cimetidine have antihistaminergic effects in rodents. The ic injections were accomplished through the use of a 30-ga. injection cannula which was inserted into the brain 0.5 mm beyond the guide cannula. A Harvard infusion pump was used to inject the ic solutions into the brain at a rate of 0.03 μl/s for 30 s. With the injection cannula in place, an additional 30 s were allowed for full delivery of the drug. Each mouse was then returned to the locomotor activity monitors for a 30-min test period. The order of presentation of the 12 combined ip and ic drug treatments was randomly determined. Mice were tested no more frequently than every other day.

Histology

After completion of testing, animals were perfused, and brain tissue was frozen sectioned. The tissue was then stained with thionine, and cannula placements were verified. Only animals with cannula tracks just above or in the ACCUM+STRIA or VENT were retained in the experiment. Thirty minutes before the perfusion of some animals, 1 μl of Evans blue dye was injected into each cannula. Then, while the tissue was being sectioned, drawings were made of the spread of the dye in the brain. In this way the probable brain areas that came into contact with the injected drug were imaged (see Figure 1).

Because some of the subjects died without completing all 12 conditions, these procedures resulted in the following number of mice in each treatment group: ACCUM+STRIA: amphetamine/naloxone, n = 11; amphetamine/cimetidine, n = 9; amphetamine/chlorpheniramine, n = 11; amphetamine/saline, n = 13; morphine/naloxone, n

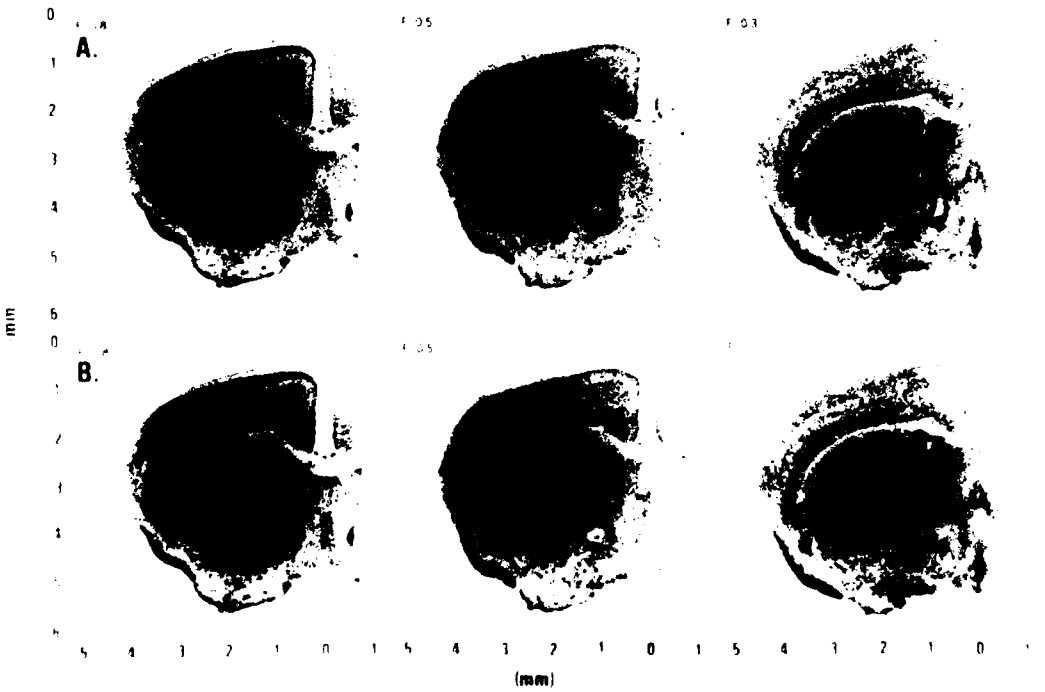

Figure 1. Coronal sections of the mouse brain showing probable intracranial injection sites (A = placement in posterior nucleus accumbens and stria terminalis; B = placement in lateral ventricles). (Refer to atlas of Slotnick and Leonard, 1975. Thionine stain. See Plate I.)

= 18; morphine/cimetidine, n = 11; morphine/chlorpheniramine, n = 12; morphine/saline, n = 13; saline/naloxone, n = 13; saline/cimetidine, n = 15; saline/chlorpheniramine, n = 15; saline/saline, n = 13; VENT: amphetamine/naloxone, n = 17; amphetamine/cimetidine, n = 13; amphetamine/chlorpheniramine, n = 15; amphetamine/saline, n = 16; morphine/naloxone, n = 16; morphine/cimetidine, n = 16; morphine/chlorpheniramine, n = 16; morphine/saline, n = 14; saline/naloxone, n = 18; saline/cimetidine, n = 17; saline/chlorpheniramine, n = 16; saline/saline, n = 18.

A preliminary analysis of the data suggested nonhomogeneity of variances between treatment groups, and therefore Kruskal-Wallis nonparametric one-way analyses of variance (ANOVAS) were computed (Siegel, 1956). Initial comparisons were made between baseline locomotor responses produced by ip drug injections. In a further analysis, I compared the locomotion of subjects (of either ACCUM+STRIA or VENT groups) that had received ip morphine and then the various ic injections. Similar comparisons were made for both amphetamine and saline groups. Four time periods were analyzed: pre-ic-drug baseline and 5–10 min, 15–20 min, and 25–30 min post-ic-drug injections. One ANOVA was computed for each time period. When statistically significant differences were identified, Dunn's test (Hollander & Wolfe, 1973; α = .05) was used to specify individual treatment groups that were reliably different from one another.

Results

Reductions in morphine-induced locomotion were observed after intra-accumbens/stria terminalis injections of naloxone or cimetidine but not chlorpheniramine. Intraventricular injections of naloxone produced a similar attenuation, but ventricularly placed antihistamines did not significantly alter the opiate-stimulated behavior of these mice. Cimetidine, when placed in the ACCUM+STRIA (but not the VENT) also produced a partial attenuation of amphetamine locomotion. Chlorpheniramine and naloxone failed to reduce the amphetamine-stimulated locomotor hyperactivity.

In an initial analysis of baseline locomotion (after ip injection), subjects from the two implant groups (ACCUM+STRIA and VENT) were combined. Both morphine and amphetamine (ip) produced a statistically significant increase in baseline locomotion, relative to saline, $\chi^2(2, N = 346) = 215.116$, $p < .001$. Baseline locomotor drug responses did not differ between morphine- and amphetamine-injected mice (Figures 2 and 3).

At all three time periods analyzed, morphine-induced locomotor hyperactivity was significantly reduced, $\chi^2(3, N = 54) = 7.873$–$12.064$, $p < .05$, by subsequent injections of either naloxone or cimetidine into the ACCUM+STRIA (compared with ic saline, see Figure 2). Chlorpheniramine had no effect on morphine-stimulated locomotion. Intra-accumbens/stria terminalis injections of cimetidine also significantly reduced amphetamine hyperactivity at all analyzed times, $\chi^2(3, N = 44) = 7.979$–$8.031$, $p < .05$. However, these decreases were not so great as those observed in morphine-treated subjects (Mann-Whitney U, $ps < .05$). Neither naloxone nor chlorpheniramine, when injected into the ACCUM+STRIA area,

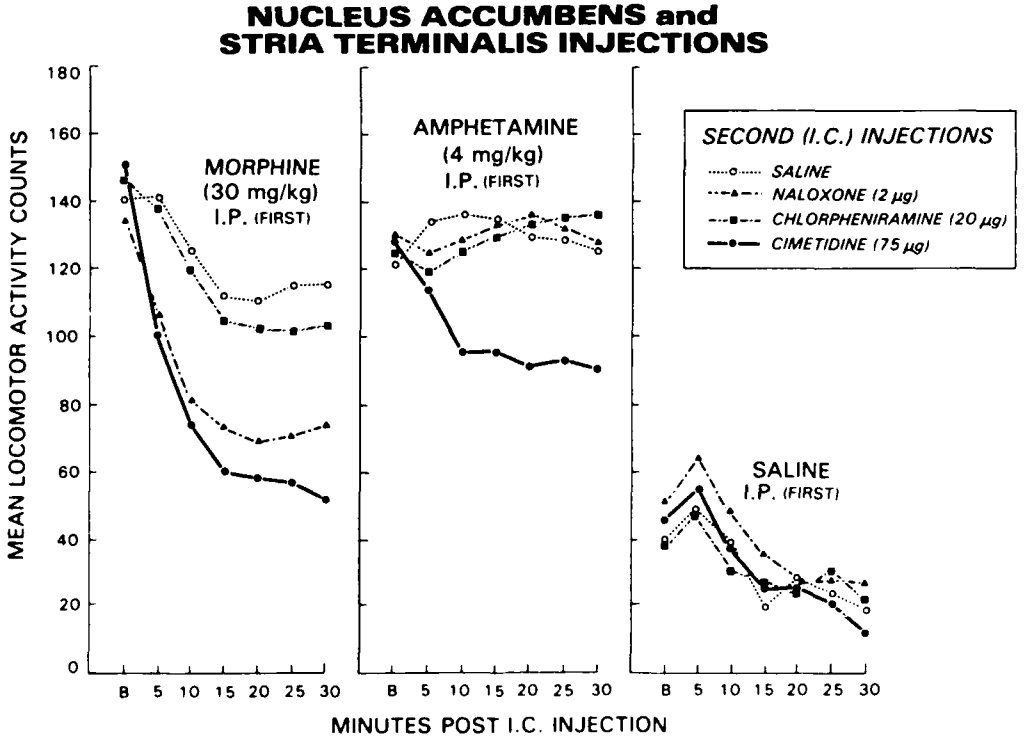

Figure 2. Mean locomotor activity counts of mice after an initial ip injection of morphine (30 mg/kg), amphetamine (4 mg/kg), or saline followed by bilateral intracranial (ic) injections of naloxone (2 µg), cimetidine (75 µg), chlorpheniramine (20 µg), or saline. (Intracranial injections were placed in the nucleus accumbens and stria terminalis [see Figure 1].)

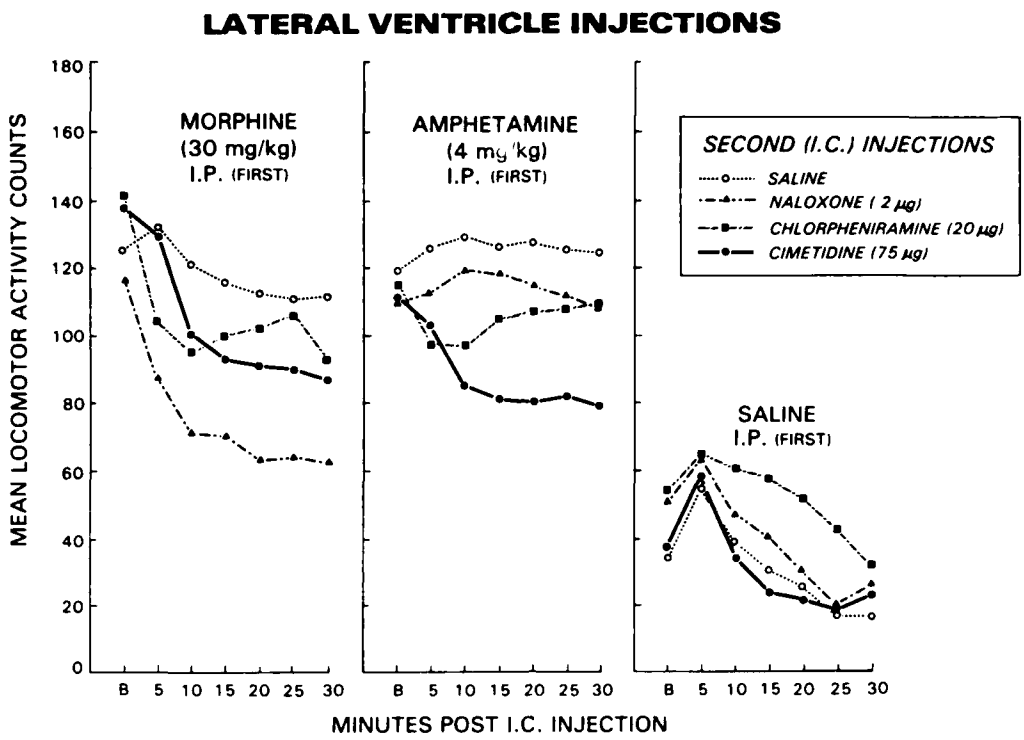

Figure 3. Mean locomotor activity counts of mice after an initial ip injection of morphine (30 mg/kg), amphetamine (4 mg/kg), or saline followed by bilateral intracranial (ic) injections of naloxone (2 μg), cimetidine (75 μg), chlorpheniramine (20 μg), or saline. (Intracranial injections were placed in the lateral ventricles [see Figure 1].)

altered amphetamine-stimulated locomotion. Apparently, intra-accumbens injections of naloxone, cimetidine, and chlorpheniramine (at the doses used here) do not cause depression of spontaneous locomotion, that is, ip-saline-injected subjects did not change their locomotor response at any time after these intracranial drug treatments, $\chi^2(3, N = 56) = 0.856$–$2.020$, $p > .05$.

Compared with saline, intraventricular naloxone significantly reduced morphine's locomotor activating effects at each of the three time periods analyzed, $\chi^2(3, N = 62) = 7.910$–$8.932$, $p < .05$. However, neither of the antihistamines altered this opiate-induced hyperactivity. Although there exists a trend toward a cimetidine-induced reduction of amphetamine hyperactivity, this trend just failed to achieve statistical significance, $\chi^2(3, N = 61) = 5.950$–$7.089$, $p > .05$. Similarly, intraventricular naloxone and chlorpheniramine failed to alter this amphetamine response. Spontaneous locomotion measured after a saline (ip) injection was unaffected by all the intracranial drug treatments except chlorpheniramine. Here, control mice exhibited a slight but consistent (statistically significant) increase, $\chi^2(3, N = 69) = 8.900$, $p < .05$, in locomotion 15–20 min after the intraventricular injection of this H_1 receptor blocker.

Discussion

Cimetidine, when injected into the nucleus accumbens/stria terminalis, countered morphine-induced locomotion, but it was not effective in altering this response when it was injected into the lateral ventricles. Intracranial injection of chlorpheniramine, at either site, did not significantly change the quantity of opiate-stimulated locomotion. These data suggest a role for H_2 receptors (but not H_1 receptors) of the ACCUM+STRIA in the production of this behavioral response. Similarly, others have reported that cimetidine antagonizes morphine analgesia (Hanig, Hui, & Sun, 1981) as well as opiate effects on the guinea pig ileum (Takayanagi, Iwayama, & Kasuya, 1978). In addition, the apparent difference in behavioral mediation of the two histamine receptor subtypes is not unprecedented; for example, Malec and Langwinski (1983) suggested that H_1 receptor blockers antagonize morphine catalepsy but that H_2 antagonists do not.

When naloxone was injected into either the ventricles or the ACCUM+STRIA, it antagonized the behavioral effects of morphine. However, cimetidine significantly attenuated opiate-induced stimulation only when it was injected into the ACCUM+STRIA. Opiate receptors that mediate this locomotor response are apparently located both within and outside the ACCUM+STRIA areas. Thus there may be at least two noncongruent opiate systems that play a role in the production of morphine-induced locomotor hyperactivity: a partially histaminergic one located in or near the nucleus accumbens and a second system, outside the accumbens, in which histaminergic neurons may not be involved. Other experiments offer

some support for this hypothesis. Hough et al. (1984) reported that neither chlorpheniramine (ip) nor cimetidine (ip or intraventricular) antagonized morphine-induced antinociception of mice. Similarly, others have found that intraventricular cimetidine did not impair the locomotor activity of morphine-treated rats (Bluhm, Zsigmond, & Winnie, 1982; Netti, Bossa, Galatulas, Sibilia, & Pecile, 1984). Likewise, the present data suggest that both chlorpheniramine and cimetidine do not (at the dose used) significantly alter opiate-stimulated locomotion when injections are intraventricular. However, inasmuch as ACCUM+STRIA injections of cimetidine reduced morphine locomotion, my data highlight a role for H_2 receptors, of this specific brain region, in the production of opiate-stimulated movement.

Because injection cannulas aimed at the nucleus accumbens pass through the lateral ventricles, there is the potential for some of the injected drug to backwash into the ventricular system. This may make interpretations concerning locus of drug action difficult. However, in the present study, the behavioral effects of accumbens- and ventricular-injected subjects were quite different (see Figures 2 and 3). These findings, along with the observations that injected dye flowed only to the brain targets, support the contention that intra-accumbens drug injections did not move into other portions of the brain.

Cimetidine (75 μg/hemisphere) injected into the nucleus accumbens produced an incomplete (although statistically significant) reduction in the hyperactivity produced by 4 mg/kg amphetamine. A similar (but less reliable) reduction was observed after intraventricular injections of this antihistamine. H_2 receptors may be partially responsible for the production of this amphetamine locomotor response.

The doses of amphetamine and morphine used in the experiment produced similar degrees of locomotor hyperactivity. However, cimetidine did not reduce amphetamine-stimulated locomotion to levels as low as those exhibited by morphine-injected mice that also received this antihistamine. Therefore, the available data suggest that histamine may be less involved in amphetamine-induced locomotion than in morphine-stimulated activity. This interpretation should be made cautiously, however, as a variety of doses of morphine and amphetamine were not administered.

Apparently this dose of cimetidine (75 μg/hemisphere) does not produce a generalized depression because intracranial injections, at either ACCUM+STRIA or VENT sites, did not alter spontaneous locomotion. In addition, cimetidine failed to significantly reduce amphetamine-induced locomotion when this antihistamine was injected into the lateral ventricles.

There is an apparent inverse relation between levels of brain histamine and locomotor activity of the morphine-treated mouse (McClain et al., 1977). Lee and Fennesy (1976) suggested that the opiate-stimulated decrease in measured histamine levels in the brains of hyperactive mice may reflect release of the amine. Because cimetidine blocks morphine-induced locomotion, the present data are in consonance with the hypothesis that stimulation of histaminergic neurons may be involved in the production of morphine-induced locomotion. Further, these data suggest specific involvement of H_2 receptors in the opiate-stimulated hyperactivity response of the C57BL/6J mouse.

References

Akil, H., Watson, S. J., Young, E., Lewis, M. E., Khachaturian, H., & Walker, M. (1984). Endogenous opioids: Biology and function. *Annual Review of Neuroscience, 7,* 223–255.

Bluhm, R., Zsigmond, E. K., & Winnie, A. P. (1982). Potentiation of opioid analgesia by H_1 and H_2 antagonists. *Life Sciences, 31,* 1229–1232.

Brown, R. G., Derrington, D. C., & Segal, C. S. (1979). Comparison of opiate and opioid-peptide-induced immobility. *Life Sciences, 24,* 933–942.

Bugajski, J., & Zacny, E. (1981). The role of central histamine H_1 and H_2-receptors in hypothermia induced by histamine in the rat. *Agents and Actions, 11,* 442–447.

Burkard, W. P. (1978). Histamine H_2-receptor binding with ^{3}H-cimetidine in brain. *European Journal of Pharmacology, 50,* 449–450.

Cohn, C. K., Ball, G. G., & Hirsch, J. (1973). Histamine: Effect on self-stimulation. *Science, 180,* 757–758.

Garbarg, M., Barbin, G., Llorens, C., Palacios, J. M., Pollard, H., & Schwartz, J. C. (1980). Recent developments in brain histamine research: Pathways and receptors. In W. B. Essman (Ed.), *Neurotransmitters, receptors and drug action* (pp. 179–202). New York: Spectrum Publications.

Hanig, J. P., Hui, F. W., & Sun, C. L. (1981). The role of H_1 and H_2 agonists and antagonists and morphine in antinociception. *Federation Proceedings, 40,* 282.

Hollander, M., & Wolfe, D. A. (1973). *Nonparametric statistical methods.* New York: Wiley.

Hough, L. B., Su, K. L., Goldschmidt, R. C., Khandelwal, J. K., Newton, M. V., & Glick, S. D. (1984). No evidence for histamine-mediated morphine analgesia. *Neuropharmacology, 23,* 705–709.

Kalivas, P. W. (1982). Histamine-induced arousal in the conscious and pentobarbital-treated rat. *Journal of Pharmacology and Experimental Therapeutics, 222,* 37–42.

Lee, J. R., & Fennessy, M. R. (1976). Effects of morphine on brain histamine, antinociception and activity in mice. *Clinical and Experimental Pharmacology and Physiology, 3,* 179–189.

Malec, D., & Langwinski, R. (1983). The effect of antihistamines on cataleptogenic actions of analgesics and haloperidol. *Polish Journal of Pharmacology and Pharmacy, 35,* 293–300.

McClain, D. E., Catravas, G. N., & Teitelbaum, H. (1977). Age and genotype dependent changes in morphine induced locomotor activity and brain histamine levels. *Society for Neuroscience Abstracts, 3,* 297.

Netti, C., Bossa, R. Galatulas, I. Sibilia, V., & Pecile, A. (1984). Antinociceptive effect of centrally administered cimetidine and dimaprit in the rat. *Pharmacology, 28,* 262–267.

Oliverio, A., & Castellano, C. (1974). Genotype-dependent sensitivity and tolerance to morphine and heroin: Dissociation between opiate-induced running and analgesia in the mouse. *Psychopharmacology, 39,* 13–22.

Palacios, J. M., Wamsley, J. K., & Kuhar, M. J. (1981). The distribution of histamine H_1 receptors in the rat brain: An autoradiographic study. *Neuroscience, 6,* 15–37.

Puglisi-Allegra, S., Castellano, C., Filibeck, U., Oliverio, A., & Melchiorri, P. (1982). Behavioral data on dermorphins in mice. *European Journal of Pharmacology, 82,* 223–272.

Sazara, S. (1982). Opiate receptors and endogenous opiates: Pano-

rama of opiate research. *Progress in Neuro-psychopharmacology and Biological Psychiatry, 6,* 3–15.

Siegel, S. (1956). *Nonparametric statistics for the behavioral sciences.* New York: McGraw-Hill.

Siegfried, B., Filibeck, U., Gozzo, S., & Castellano, C. (1982). Lack of morphine-induced hyperactivity in C57BL/6J mice following striatal kainic acid lesions. *Behavioural Brain Research, 4,* 378–399.

Slotnick, B. M., & Leonard, C. M. (1975). *A stereotaxic atlas of the albino mouse forebrain* (Publication No. [ADM]75-100). Washington, DC: Department of Health, Education, and Welfare.

Snyder, S. H., & Childers, S. R. (1979). Opiate receptors and opioid peptides. *Annual Review of Neuroscience, 2,* 35–64.

Takayanagi, I., Iwayama, Y., & Kasuya, Y. (1978). Narcotic antagonistic action of cimetidine on the guinea pig ileum. *Journal of Pharmacy and Pharmacology, 30,* 519–520.

Teitelbaum, H., Giammatteo, P., & Mickley, G. A. (1979). Differential effects of localized lesions of the n. accumbens on morphine- and amphetamine-induced locomotor hyperactivity in the C57BL/6J mouse. *Journal of Comparative and Physiological Psychology, 93,* 745–751.

Watanabe, T., Taguchi, Y. Shiosaka, S., Tanaka, J., Kubota, H., Terano, Y., Tohyama, M., & Wada, H. (1984). Distribution of the histaminergic neuron system in the central nervous system of rats: A fluorescent immunohistochemical analysis with histadine decarboxylase as a marker. *Brain Research, 295,* 13–25.

Wong, C. L., & Roberts, M. B. (1975). The possible role of brain histamine and H_1 and H_2 receptors in the development of morphine tolerance and physical dependence in mice. *Agents and Actions, 5,* 476–483.

Received December 15, 1984
Revision received March 25, 1985 ■

0022-1767/86/1367-2483$02.00/0
THE JOURNAL OF IMMUNOLOGY

Vol. 136, No. 7, April 1, 1986
Printed in U.S.A.

INTERLEUKIN 1 IS A RADIOPROTECTOR[1]

RUTH NETA,* SUSAN DOUCHES,* AND JOOST J. OPPENHEIM†

*From the *Experimental Hematology Department, Armed Forces Radiobiology Research Institute, Bethesda, MD 20814-5145, and the †Laboratory of Molecular Immunoregulation, Biological Response Modifiers Program, National Cancer Institute-FCRF, Frederick, MD 21701*

Pretreatment with recombinant interleukin 1 (IL 1) protects mice in a dose-dependent manner from lethal effects of ionizing radiation. Two thousand units of IL 1, given i.p. 20 hr before irradiation, protect 88% of C57Bl/6 mice from an $LD_{100/17}$ radiation dose (dose of radiation that kills 100% mice in 17 days), and 1000 U of IL 1 protect 100% of DBA/1 mice from an $LD_{50/30}$ dose. This finding provides the first evidence that a cytokine, IL 1, which acts as a differentiation- and maturation-inducing agent for a variety of cells, also can serve as a signal that initiates radioprotective events in vivo. Because many of the exogenous immunomodulators that have been shown to be radioprotective also induce endogenous IL 1 production, our observation suggests that IL 1 may mediate their radioprotective effects.

Exposure of mammals to ionizing radiation causes the development of a complex, dose-dependent series of potentially fatal physiologic and morphologic changes, known as acute radiation syndrome. Radiation-induced destruction of the lymphoid and hematopoietic systems is the primary cause of septicemia and death. Enhanced susceptibility to infections with opportunistic microorganisms occurs in parallel with progressive radiation-induced atrophy of lymph nodes, spleen, and bone marrow (1). Protection and/or recovery from the consequences of ionizing radiation has been investigated at different cellular and molecular levels. DNA repair mechanisms and the chemical radioprotection afforded by thiol compounds have been studied extensively (2, 3). Transplantation of as few as 10^4 bone marrow cells per kg body weight into lethally irradiated (with $LD_{100/30}$) animals or patients protects them from death. This well-documented clinical and experimental procedure provides proof that despite radiation-induced damage to many cell types and tissues, it is the more radiosensitive cells of the immune and hematopoietic systems that are crucial for defenses against lethal complications of radiation, in a dose range below induction of gastrointestinal syndrome (1).

Radioprotection has also been reported to be conferred by immunomodulatory substances. Numerous microbial components such as bacterial lipopolysaccharide (LPS), muramyl dipeptide, *Mycobacterium bovis* strain BCG, and glucan have radioprotective effects when administered before irradiation (4). It has been suggested that radioprotective activity conferred by immunomodulators can be attributed to their capacity to enhance hematopoietic and immune functions. Our understanding of the mechanisms by which these agents are radioprotective and the participation of endogenous cytokines or lymphokines that are known to be induced by immunomodulatory substances remain to be established. The availability of recombinant interleukin 1 (IL 1) (5) free of endotoxin and other cytokines and peptides permits study of the role of the cytokine in radioprotective events. We considered IL 1 to be a logical candidate for an endogenous radioprotective mediator, because exogenous immunomodulatory radioprotectors elicit its production. Furthermore, the addition of monocyte-conditioned media, containing IL 1, to cultures of irradiated human T cells has been reported to partially restore PHA-induced proliferation of these cells (6).

In this report, we will present evidence that i.p. administration of IL 1 protects mice from the lethal effects of irradiation.

MATERIALS AND METHODS

Mice. Inbred strains of female mice, C57Bl/6 and DBA/1, were obtained from The Jackson Laboratory, Bar Harbor, ME. All mice were quarantined and were acclimated for at least 2 wk to the conditions of the Veterinary Medicine Department Facility at the Armed Forces Radiobiology Research Institute. Mice were kept in cages, nine mice per cage, with filter lids. Standard lab chow and HCl-acidified water, pH 2.4, were given ad libitum. All cage-cleaning procedures were carried out in a micro-isolator.

Irradiation. Mice were placed in Plexiglass containers and were given whole body irradiation at 0.40 Gy/min by bilaterally positioned ^{60}Co elements. The total dose was 9.5 Gy (950 rad).

IL 1 and control protein. Recombinant IL 1 (Lot No. 11319-159-46) was a generous gift from Drs. W. Benjamin and P. Lomedico of Hoffman-LaRoche, Nutley, NJ. This preparation, with specific activity of 6×10^6 U/mg or 2×10^6 U/ml, was supplied in 5 M guanidine hydrochloride. As a control, a preparation of a purified protein from a bacterial extract (Lot No. 11319-177-46) containing the plasmid without IL 1 cDNA was used (Hoffman-LaRoche). This protein was extracted with 5 M guanidine HCl and was treated in the same manner as the IL 1 preparation. The molecular size of the protein was similar to that of IL 1. The LPS contamination of both substances was established at Hoffman-LaRoche by a Limulus assay to contain less than 2 U or 0.4 ng of LPS per ml in the IL 1 preparation, and less than 20 U or 4 ng per milliliter for the bacterial extract protein. The Limulus assay was performed by diluting the protein preparations to the concentration of guanidine HCl that did not interfere with the assay (Dr. Lomedico, private communication). Both substances were diluted in pyrogen-free saline so that the final

Received for publication September 24, 1985.
Accepted for publication December 16, 1985.
The costs of publication of this article were defrayed in part by the payment of page charges. This article must therefore be hereby marked *advertisement* in accordance with 18 U.S.C. Section 1734 solely to indicate this fact.

[1] This work was supported by the Armed Forces Radiobiology Research Institute, Defense Nuclear Agency, under Research Work Unit M-J00148. The views presented in this paper are those of the authors; no endorsement by the Defense Nuclear Agency has been given or should be inferred. Research was conducted according to principles enunciated in the "Guide for the Care and Use of Laboratory Animals" prepared by the Institute of Laboratory Animal Resources, National Research Council.

concentration contained less than 4 pg LPS/ml in the IL 1 inoculum and less than 40 pg/ml of LPS in the extract protein inoculum.

RESULTS AND DISCUSSION

Female C57Bl/6 mice, 2 to 4 mo old, were injected i.p. with IL 1 in 0.5 ml of pyrogen-free saline 20 hr before irradiation. The doses of IL 1 ranged from 350 to 2000 U per mouse (58 to 333 ng protein, containing less than 1 to 4 pg LPS contamination). The bacterial extract protein was used in amounts equivalent to the protein content of 1000 or 2000 U of IL 1, i.e., 166 or 333 ng protein (containing less than 20 or 40 pg LPS contamination). Administration of IL 1, but not of bacterial protein extract, protected C57Bl/6 mice from the lethal effects of radiation, as demonstrated in Figure 1.

Similar radioprotection was also demonstrated in DBA/1 mice. This strain, however, was more radioresistant than C57Bl/6. Whereas 950 rad corresponded to $LD_{50/30}$ for DBA/1 mice, the same dose killed 100% of C57Bl/6 mice within 17 days. A dose of 1000 U of IL 1 per mouse protected 100% of DBA/1 mice from radiation lethality (Fig. 2). Neither strain of mice demonstrated any obvious deleterious effects from any of the doses of IL 1 administered i.p. Figure 2 shows, however, that mice injected with bacterial protein extract had enhanced radiation mortality. This effect was observed only in one experiment and may be due to the toxicity of guanidine. Repeated experiments with this preparation did not show significantly enhanced mortality. Because the bacterial protein extract serves as a control only, this effect was not examined further. In both strains, administration of IL 1 4 hr before irradiation resulted in lower degrees of protection (reduced from 88% at 20 hr to 30% survival for C57Bl/6 mice at 4 hr). Furthermore, administration of IL 1 45 hr before irradiation resulted in 12.5% survival vs 75% survival of C57Bl/6 mice treated with IL 1 20 hr before irradiation.

This is the first report in which a preparation of a single cytokine, IL 1, free of other macrophage-derived substances, was shown to initiate considerable radioprotective effects in vivo. Previous studies which suggested a radioprotective role for interferon evaluated only partially purified preparations (7). Because IL 1 is as potent a radioprotector as many bacterial components known to induce it, IL 1 can be used instead of radioprotective bacterial components, many of which remain in the host long after irradiation and which are also known to have harmful systemic effects. The rapid clearance of IL 1 from the circulation (8) makes it unlikely that this cytokine would exert harmful long-term effects on the host after irradiation.

Much recent data on IL 1 activity (9, 10) suggest its importance in many cell functions. Originally perceived primarily as a mediator of inflammation, IL 1 lately has also been implicated as a differentiation- and maturation-inducing agent for a variety of cell types. IL 1 has been suggested to participate in wound healing and in increasing protection from infection (9, 10). In addition, enhanced levels of IL 1 detected in the placenta (11), in circulation after exercise (12), and post-ovulation (13) suggest that even though IL 1 may have some noxious effects, such as fever induction, this cytokine may play a constructive role in normal functions, in development as well as in host defenses.

Although the basis for the radioprotective effect of IL 1 remains unclear, a variety of mechanisms have been postulated to explain the radioprotective effects of immunomodulators and may account for the radioprotective activity of IL 1. Immunomodulators induce neutrophilia by mobilizing polymorphonuclear cells from the bone marrow, a function also attributed to IL 1 (9, 10). The migration of the neutrophils from the bone marrow into the circulation may render them less susceptible to enhanced radiation levels, due to secondary electrons emitted from mineral bone after photoelectric absorption (4). Another radioprotective pathway may depend on IL 1-induced procoagulant formation by endothelial cells and stimulation of increased levels of fibrinogen in circulation (14), which would promote the formation of microthrombi. The hypoxic conditions created in such a milieu would protect the cells from radiation damage. Yet another radioprotective mechanism may be related to a well-documented effect of IL 1 in enhancing oxygen metabolism in neutrophils (15). As a result, the intracellular oxygen levels of neutrophils in tissues would be depleted, making the cells more resistant to radiation. Previous work indicates that cells in the late S phase of the cell cycle are more resistant to radiation damage (16). Consequently, IL 1 induction of the production of other lymphokines, such as colony-stimulating factors and inter-

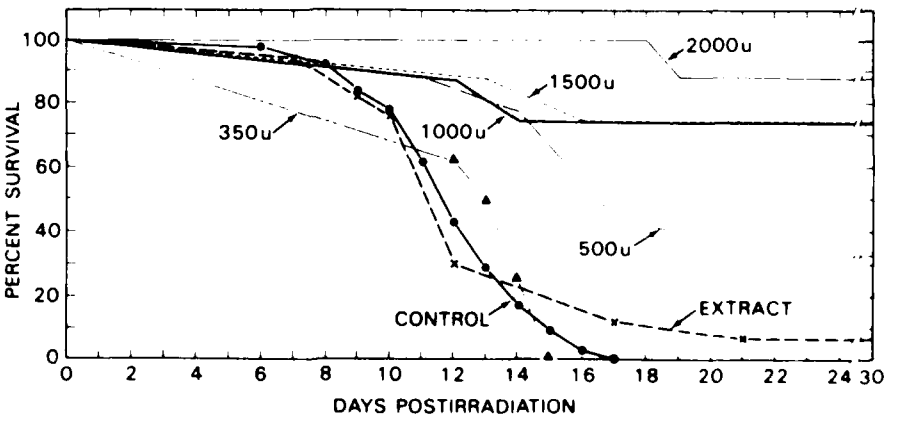

Figure 1. Radioprotective effect of IL 1 on lethally irradiated ($LD_{100/17}$) C57Bl/6 mice. C57Bl/6 mice, 2 to 4 mo old, were placed in Plexiglass restrainers and were given whole body irradiation of 40 rad/min by bilaterally positioned ^{60}Co elements. The total dose was 950 rad. Recombinant IL 1 (*) or *E. coli* extract containing the plasmid without IL 1 cDNA (7) were diluted in pyrogen-free saline and were administered i.p. 20 hr before irradiation. Standard lab chow and HCl acidified water (pH 2-4) were given ad libitum. Results are a compilation of four separate experiments. Control n = 36. Extract (**) n = 28, 350 U = 8, 500 U = 9, 1000 U = 16, 1500 U = 8, 2000 U = 24. * Specific activity 6×10^6 U/mg protein or $2 \cdot 10^6$ U/ml. ** *E. coli* extract dilution parallel that of 1000 U and 2000 U of IL 1. Difference between control and high dose of IL 1 is significant at $p < 0.001$ ($\chi^2 = 38.2$, df = 1) as calculated by chi square test with Yate's correction for continuity.

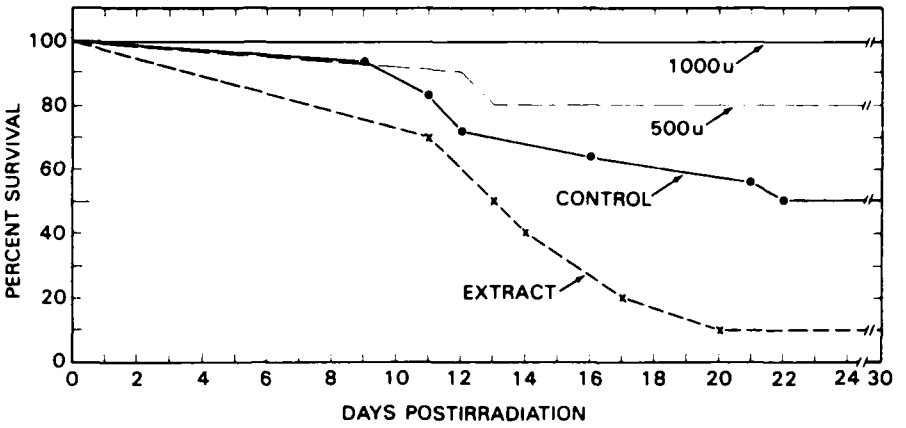

Figure 2. Radioprotective effect of IL 1 on sublethally irradiated ($LD_{50/30}$) DBA/1 mice. DBA/1 mice, 2 to 4 mo old, were treated similarly to C57Bl/6 mice (see Fig. 1). The results are a compilation of two separate experiments. Control n = 18; Extract n = 10; 500 U = 10; 1000 U = 27. Difference between control and high dose (1000 U of IL 1) is significant at $p < 0.001$ level ($\chi^2 = 13.3$, df = 1) as calculated by chi square test.

leukin 2, that induce cell proliferation may be involved in radioprotection in that this lymphokine cascade would initiate entry of the lymphoid and hematopoietic progenitor cells into the S phase of the cell cycle. The fact that the cell cycle time needed for hematopoietic progenitor cells and lymphoid cells has been estimated to last from 6 to 20 hr (17–19) may account for the time lag necessary for IL 1 radioprotection. Another possible radioprotective pathway initiated by IL 1 may be based on its ability to induce acute phase proteins (9, 10) which may have radioprotective effects. In conclusion, the identification of IL 1 as a radioprotective cytokine furthers our understanding of the pathways that mediate endogenous radioprotective events, and may lead to development of new means of radioprotection free of the harmful effects of radioprotective drugs.

Acknowledgments. We thank Drs. T. MacVittie, R. Walker, S. Durum, S. Boggs, B. Mathieson, D. Longo, and P. Neta for helpful suggestions, and Mrs. Betty Markovich and Mrs. Marianne Owens for their excellent assistance in typing the manuscript.

REFERENCES

1. **Anderson, R. W., and N. L. Warner.** 1976. Ionizing radiation and the immune response. *Adv. Immunol. 24:215.*
2. **Elkind, M. M.** 1984. Repair processes in radiation biology. *Radiat. Res. 100:425.*
3. **Nygaard, O. F., and M. G. Simic,** eds. 1983. *Radioprotectors and Anticarcinogens.* Academic Press, New York.
4. **Behling, U. H.** 1983. The radioprotective effect of bacterial endotoxin. In *Beneficial Effects of Endotoxin.* A. Nowotny, ed. Plenum Press, New York. P. 127.
5. **Lomedico, P. T., U. Gubler, C. P. Hellmann, M. Dukovich, J. G. Giri, Y. E. Pan, K. Collier, R. Semionov, A. O. Chua, and S. B. Mizel.** 1984. Cloning and expression of interleukin-1 cDNA in *Escherichia coli. Nature 312:458.*
6. **Manori, I., A. Kushilevsky, S. Segal, and Y. Weinstein.** 1984. Radiosensitivity of isolated subsets of human lymphocytes (E^+, $OKT4^+$, $OKT8^+$): protective role of monocytes and monokines. *Clin. Exp. Immunol. 58:453.*
7. **Lvovsky, E., W. B. Baze, D. E. Hilmas, and H. B. Levy.** 1977. Radiation damage and the interferon system. *Tex. Rep. Biol. Med. 35:388.*
8. **Kampschmidt, R. F., and H. F. Upchurch.** 1980. Rate of clearance of circulating leukocytic endogenous mediator in the rat. *Proc. Soc. Exp. Biol. Med. 164:537.*
9. **Wood, D. D.** 1984. Antigen-nonspecific factors elaborated by macrophages which stimulate lymphocytes: interleukin-1. In *The Reticuloendothelial System: A Comprehensive Treatise.* J. A. Bellanti and H. B. Herscowitz, eds. Plenum Press, New York. P. 201.
10. **Oppenheim, J. J., and I. Gery.** 1982. Interleukin-1 is more than an interleukin. *Immunol. Today 3:113.*
11. **Flynn, A., J. H. Finke, and M. A. Loftus.** 1985. Comparison of interleukin-1 production by adherent cells and tissue pieces from human placenta. *Immunopharmacology 9:19.*
12. **Cannon, J. G., and M. J. Kluger.** 1983. Endogenous pyrogen activity in human plasma after exercise. *Science 220:617.*
13. **Cannon, J. G., and C. A. Dinarello.** 1985. Increased plasma IL-1 activity in women after ovulation. *Science 227:1247.*
14. **Bevilacqua, M. P., J. S. Pober, G. R. Majeau, R. S. Cotran, and M. A. Gimbrone.** 1984. Interleukin-1 (IL-1) induces biosynthesis and cell surface expression of procoagulant activity in human vascular endothelial cells. *J. Exp. Med. 160:618.*
15. **Klempner, M. S., C. A. Dinarello, W. R. Henderson, and J. I. Gallin.** 1979. Stimulation of neutrophil oxygen-dependent metabolism by human leukocytic pyrogen. *J. Clin. Invest. 64:999.*
16. **Sinclair, W. K., and R. A. Morton.** 1966. X-ray sensitivity during the cell generation cycle of cultured Chinese hamster cells. *Radiat. Res. 29:450.*
17. **Boggs, S. S., P. A. Chervenick, and D. R. Boggs.** 1972. The effect of postirradiation bleeding or endotoxin on proliferation and differentiation of hematopoietic stem cells. *Blood 40:375.*
18. **Soren, L.** 1973. Variability of the time in which PHA-stimulated lymphocytes initiate DNA synthesis. *Exp. Cell Res. 78:201.*
19. **Darzynkiewicz, Z., F. Traganos, T. Sharpless, and M. R. Melamed.** 1976. Lymphocyte stimulation: a rapid multiparameter analysis. *Proc. Natl. Acad. Sci. USA 73:2881.*

JOURNAL OF NEUROPHYSIOLOGY
Vol. 55, No. 4, April 1986. Printed in U.S.A.

Histamine Decreases Calcium-Mediated Potassium Current in Guinea Pig Hippocampal CA1 Pyramidal Cells

TERRY C. PELLMAR

Physiology Department, Armed Forces Radiobiology Research Institute, Bethesda, Maryland 20814

SUMMARY AND CONCLUSIONS

1. The action of histamine on CA1 pyramidal cells was studied in a hippocampal slice preparation.

2. In the presence of tetrodotoxin (TTX) and tetraethylammonium (TEA), histamine had little effect on the calcium spikes.

3. Using the single-electrode voltage-clamp technique, the actions of histamine on membrane currents were tested. In TTX, histamine (1 μM) decreased outward current only at potentials more depolarized than approximately −50 mV, where calcium-mediated potassium current is predominant. In the presence of manganese, histamine was without effect.

4. Histamine (10 μM) did not affect the transient outward potassium current (A-current), the inward M-current resulting from small hyperpolarizing steps, or the inward Q-current elicited by larger hyperpolarizing steps.

5. Blocking potassium currents with TEA or replacing calcium with barium revealed a slow inward current normally carried by calcium. With TTX present to block sodium currents, histamine (10 μM) did not reduce the inward current.

6. The outward current reduced by a maximally effective concentration of histamine (10 μM) can be further decreased by manganese.

7. The results support the conclusion that histamine selectively decreases the calcium-mediated potassium conductance in CA1 pyramidal cells of hippocampus. The possibility is raised that there is a component of calcium-mediated potassium current that is insensitive to histamine.

INTRODUCTION

Evidence is accumulating in support of histamine as a neurotransmitter in the hippocampus (29). The synthetic enzyme histidine decarboxylase is present in CA1, CA3, and dentate regions (4). Electrical stimulation and depolarizing agents cause the release of radiolabeled histamine from hippocampal slices (28, 34). Histaminergic inputs enter the hippocampus dorsally through the fimbria and ventrally by way of the amygdala (4). Some of these inputs arise from fibers coursing through the lateral hypothalamus (12, 13). In addition, some histamine of the hippocampal region may be contained in nonneuronal elements (29).

Histamine alters the electrophysiological activity of hippocampal pyramidal cells. Segal (31, 32) found that CA1 and CA3 pyramidal cells respond to histamine with a small calcium-sensitive depolarization and an increase in action-potential firing rate. CA3 neurons fired in a burst pattern in the presence of histamine. Haas and Konnerth (17) demonstrated that the calcium-mediated potassium current underlying the slow afterhyperpolarization is reduced by histamine in CA1 neurons. Haas (16) also found that local application of histamine to hippocampal pyramidal cells often resulted in a hyperpolarization and a small conductance increase. In the present study, voltage-clamp technique was used to further investigate the actions of histamine on hippocampal pyramidal cells. The results reported here suggest that histamine selectively decreases calcium-mediated potassium current

in CA1 pyramidal cells of the guinea pig hippocampus.

METHODS

Male Hartley guinea pigs (250–400 g) were lightly anesthetized with halothane and killed by cervical dislocation. The brain was removed, and the hippocampus of the left hemisphere was dissected out. The hippocampus was then rinsed in iced Krebs solution (composition indicated below) that had been equilibrated with 95% O_2-5% CO_2. Transverse slices 350–400 μm thick were cut, using a McIlwain tissue chopper. The slices were incubated in oxygenated Krebs solution at room temperature (~25°C) for at least 1 h. One slice was then transferred to the recording chamber. The chamber, designed by Dr. K. Zbicz (37), is a low-volume (~0.5-ml) perfusion chamber. The submerged slice rested on a nylon net and was held down by a larger mesh netting secured by silver wires. The bath was constantly perfused with warmed oxygenated Krebs solution at a rate of 1 ml/min. When changing solutions, at least 10 min were allowed for the solutions to equilibrate with the tissue before data were collected. All experiments were done at 30 ± 1°C.

Normal Krebs solution contained (in mM) 124 NaCl, 3 KCl, 2.4 $CaCl_2$, 1.3 $MgSO_4$, 1.24 KH_2PO_4, 10 glucose, and 26 $NaHCO_3$. When barium (2.4 mM) was present, $CaCl_2$ was omitted and 1.3 mM $MgCl_2$ replaced $MgSO_4$. In order to keep 3–4 mM manganese in solution, both sulfate and phosphate were omitted from the solution; $CaCl_2$ and KH_2PO_4 were left out, and 1.3 mM $MgCl_2$ replaced $MgSO_4$. Other pharmacological agents were added without adjusting tonicity. Tetrodotoxin (0.3 μM) was present in all voltage-clamp experiments. Histamine (1 and 10 μM) was applied in the perfusion solutions. The higher dose was used when no effect was observed with a concentration of 1 μM. All solutions were adjusted to pH 7.4. Phenol red (0.00012%) was added to the solutions for a visual check for large changes in pH during the course of the experiment. Phenol red at this concentration had no apparent effect of its own.

Intracellular recording electrodes were pulled from thin-walled capillary tubing (1.2 mm OD, 0.9 mm ID, Omega Dot, Frederick Haer) on a Brown Flaming puller and were filled with 3 M KCl. While in the extracellular solution, electrodes (20–35 MΩ) were tested for their ability to pass current. They were discarded if found to be incapable of passing at least +3 nA for several seconds without developing offset potentials. Microelectrodes were positioned in the CA1 pyramidal cell body layer. An increase in microelectrode resistance indicated the proximity of a cell. A transient increase in capacitance feedback or a large pulse of depolarizing current aided impalement of the neurons. A stainless steel bipolar (concentric) electrode placed in the alveus was used to antidromically stimulate the CA1 pyramidal cells. The presence of an antidromic action potential suggested that all cells used were pyramidal cells. Only neurons with resting potentials more negative than −55 mV and action potentials greater than 70 mV were considered acceptable for this study. Cell parameters (mean ± SE, n = 36) were resting membrane potential −65.3 ± 0.79 mV, action-potential amplitude 88.1 ± 2.15 mV, and membrane resistance 45.0 ± 2.46 MΩ.

Recordings were made through a Dagan 8100 single-electrode voltage clamp. While this technique has its limitations, it does allow analysis of currents in small cells. Because one electrode switches between passing current and recording potential, fast currents cannot be adequately clamped. In the present study, the frequency of switching was set at 3 kHz, and the duty cycle (time spent in current-passing mode) was 25%. No attempts were made to analyze very early currents (<20 ms after the voltage command). Most current measurements were made at the end of a 500-ms step. Another problem associated with clamping a neuron with a complex microanatomy is space clamping. Control of membrane voltage may be adequate at the soma and proximal dendrites but extremely poor at more distal processes. It has been reported that hippocampal pyramidal cells are electrically compact (10, 23), but, as discussed by Johnston and Brown (24), space-clamp considerations cannot be ignored. For this reason, the data here are treated qualitatively. Voltage-clamp control can be optimized by *1*) using relatively low resistance electrodes that can pass substantial currents as described above, and *2*) proper adjustment of capacity compensation to allow the electrode to follow the switching frequency of the clamp. Continual monitoring of headstage output and the unsampled (continuous) current ensured appropriate adjustments of capacitance. Once a cell was impaled, the adequacy of the clamp was always tested by its ability to control membrane potential during a calibrator signal applied between the cell membrane and ground. If the membrane potential fluctuated by >1 mV for a 10-mV calibrator signal, the cell was rejected.

Current-voltage curves were constructed from positive and negative voltage steps (500 ms) from a holding potential usually close to −40 mV. In some cells a holding potential near −70 mV was used. Data were recorded on a Gould 2400 chart recorder and a Gould 4000 digital storage oscilloscope. In addition, current and voltage records were digitized and stored on floppy disks using an LSI 11-03 microcomputer.

RESULTS

Calcium spikes

Haas and Konnerth (17) demonstrated that histamine in concentrations as low as 1 μM

was sufficient to decrease the late afterhyperpolarization (AHP) following a train of action potentials, while the early AHP was unaffected. In agreement with this observation, Fig. 1*A* illustrates the results of a similar experiment. A train of five action potentials was evoked by five short depolarizations (4 ms, 0.85 nA) once every 10 ms. Histamine (1.0 μM) substantially reduced the late AHP that followed the train. This effect was reversed by washing with normal Krebs solution. Since the late AHP is due to a calcium-mediated potassium current (C-current) (3, 18, 19, 22, 30, 35), histamine could be acting directly to decrease C-current or indirectly to decrease the calcium influx that turns on C-current. To evaluate the latter possibility, the effect of histamine on calcium spikes in a solution containing tetrodotoxin (TTX) was tested.

As reported by Haas and Konnerth (17), histamine had little effect on the TTX-resistant spikes when currents near threshold were used to evoke the spikes. With larger currents, the calcium spikes frequently had multiple peaks. In a number of preparations (5, 27), multiple peaks on action potentials have been interpreted as spikes initiated at multiple remote nonisopotential sites. Hippocampal pyramidal cells are known to have calcium spikes on their dendrites (6, 36). Histamine caused the multiple peaks to become more distinct and often increased the frequency of spiking. As seen in the lower traces of Fig. 1*B*, in histamine a second spike appears during the 200-ms current step. This result is consistent with a decrease in potassium conductance that would increase the space constant of the dendritic membrane and thereby allow better somatic invasion of the calcium spikes from the dendrites. Yet the results do not eliminate a possible action of histamine directly on calcium current. Similar results might be expected if histamine reduced

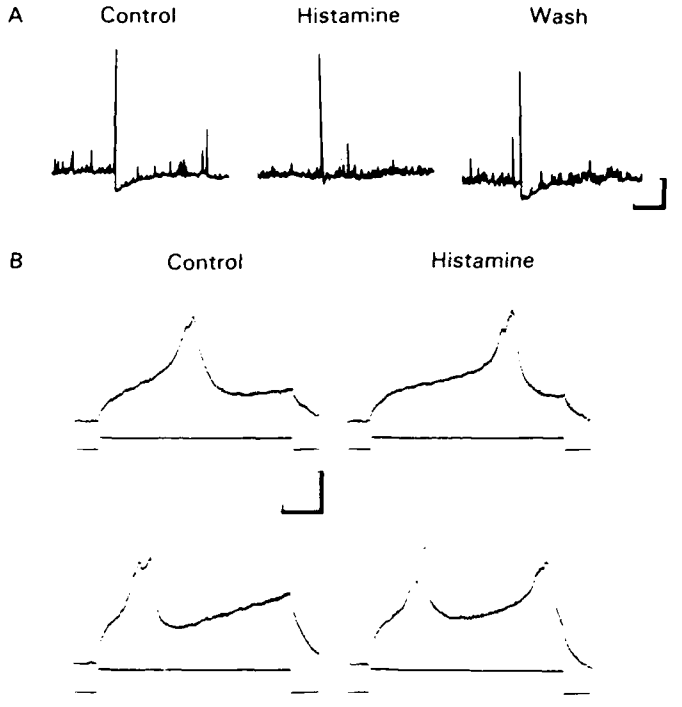

...fect of histamine on posttrain hyperpolarization. Train consisted of 5 action potentials evoked by 5 ...s of 0.85 nA for 4 ms at a frequency of 100 Hz. On this time scale, individual action potentials cannot ...d. Membrane potential was adjusted to −70 mV, and trains were evoked every 20 s. Histamine (1 μM) ...d the slow hyperpolarization following the train. Washing the tissue with normal Krebs solution for 20 min ...sed the effects of histamine. Calibration: 5 mV, 2 s. *B*: effect of histamine on calcium spikes; control on left, 1 μM histamine on right. TTX (0.3 μM) was present to block the sodium action potential. Calcium spikes were elicited with 0.25 nA for 200 ms (*top panels*) and with 0.5 nA for 200 ms (*bottom panels*). Current steps are shown below voltage response. Histamine accentuated double peaks and stimulated second spike with larger current stimulus. Membrane potential was −64 mV. Calibration: 1 nA, 20 mV, 25 ms.

the calcium spikes in the dendrites and consequently decreased C-current. The attenuated calcium spike would more easily invade the soma; it may actually appear larger, or multiple peaks may be enhanced.

Potassium currents

The ionic mechanism of the action of histamine was further studied under voltage-clamp conditions. C-current has been well described by Brown and Griffith (8). This slowly activating outward current is blocked by cadmium, manganese, and removal of calcium from the bathing solution and is reported to constitute the majority of the outward current activated at potentials more positive than −50 mV (8). To study C-current, neurons were voltage clamped to a holding potential near −40 mV. At this membrane potential, the A-current (see below) is inactivated (15) and does not contaminate the current records. The delayed rectifier is also reported to be predominantly inactivated at this holding potential (33) but may contribute slightly to evoked outward

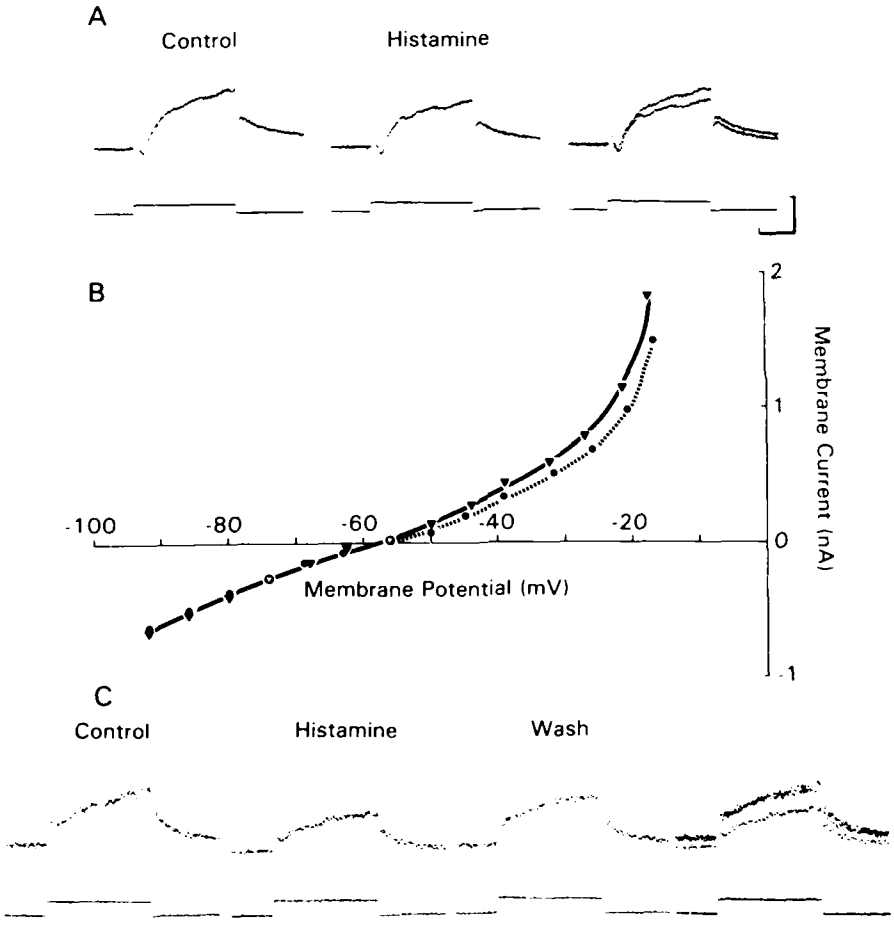

FIG. 2. Sensitivity of outward current to histamine. *A*: CA1 pyramidal cell was voltage clamped to holding potential of −38 mV. Voltage was stepped to −21 mV for 500 ms. TTX (0.3 μM) was present to block sodium spikes. Illustrated currents and voltages are the average of 4 traces. *Lower* traces show actual voltage steps. *Left panel* shows current response to voltage command in control conditions. *Middle panel* was obtained following addition of 1 μM histamine. *Right panel* shows traces with and without histamine superimposed. Calibration: 0.5 nA, 80 mV, 200 ms. *B*: current-voltage relationship of same cell as in *A*. Currents were measured at the end of 500-ms steps to all potentials from a holding potential of −38 mV. *Triangles* show curve for control currents, and *circles* show currents in 1 μM histamine. Notice that only currents at depolarized potentials were reduced by histamine. *C*: data from another cell show reversibility of histamine effects. In the presence of 0.3 μM TTX, CA1 pyramidal cell was voltage clamped to −37 mV. Voltage steps to −23 mV for 500 ms were applied. Histamine (10 μM) reversibly decreased the outward current. Calibration (same bars as in *B*): 0.5 nA, 40 mV, 200 ms.

current (see discussion of delayed rectifier, below). TTX (0.3 μM) was present to block sodium spikes. As would be expected from the results reported above, C-current was substantially reduced by histamine (Fig. 2). The outward current evoked by a depolarizing step was decreased, but the current response to a hyperpolarizing voltage command was usually unaltered by histamine. The current-voltage relationship was affected most in the region where C-current should be greatest: at potentials more depolarized than −50 mV. The decrease in current was greater for larger depolarizations. In all 11 cells tested, histamine reduced this outward current. With steps to a potential near −25 mV, the average decrease was 26.8% ± 4.6% (mean ± SE; $n = 11$).

Other potassium currents were not significantly affected by histamine. A transient outward current blocked by 4-aminopyridine (4-AP) was described by Gustafsson et al. (15) in CA3 pyramidal cells. The current was inactivated with depolarization and was totally inactivated at potentials more positive than −55 mV. A similar outward current was observed in the present study in CA1 neurons. For convenience, this transient outward current will be called A-current because it resembles (in voltage dependence, kinetics, and pharmacology) the A-current described in invertebrate

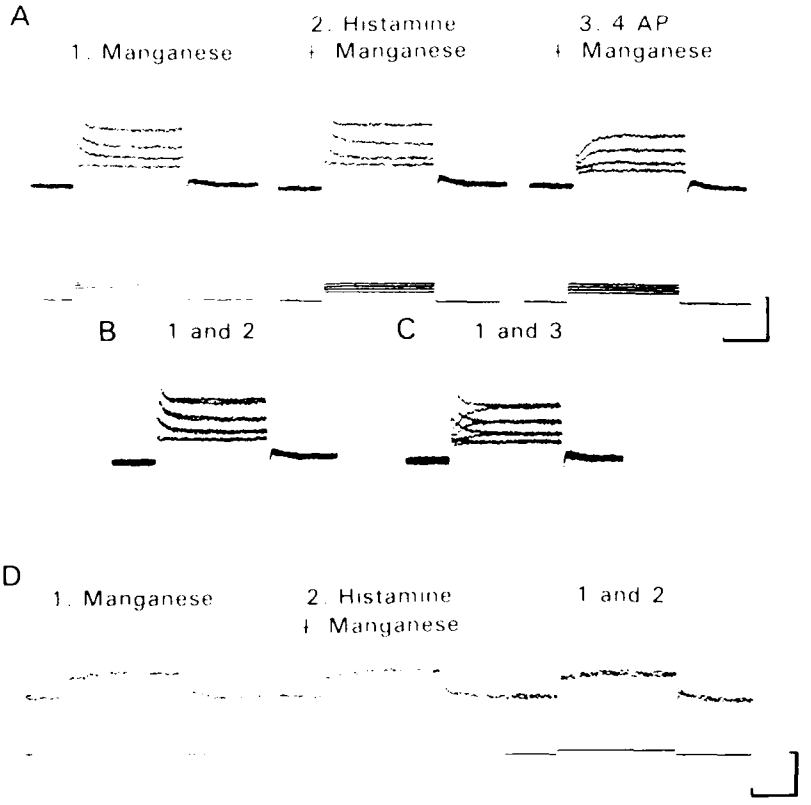

FIG. 3. In 3 mM manganese, outward currents were unaffected by 10 μM histamine. In these experiments, manganese replaced calcium, and 0.3 μM TTX was present in the Krebs solution. *A1*: response of CA1 pyramidal cell to a series of depolarizing steps. Current shown in *top* traces, voltage steps in *lower* traces. Membrane potential was held at −75 mV. Steps go to −58, −52, −46, and −41 mV. *A2*: response of same cell to identical steps after addition of 10 μM histamine. *A3*: response of same cell to identical steps after addition of 500 μM 4-aminopyridine (4-AP) to the solution. *B*: superimposition of current traces of *A1* and *A2* shows that histamine had no effect on outward currents elicited by the depolarizing steps. *C*: superimposition of current traces from *A1* and *A3* shows that 4-AP blocked the fast transient outward current but had no effect on the late outward current. Calibration for *A–C*: 1 nA, 80 mV, 200 ms. *D*: in another CA1 pyramidal cell, fast transient outward current was inactivated by holding membrane potential at −41 mV. Histamine had no effect on outward current elicited by a voltage step to −24 mV. Calibration: 0.5 nA, 80 mV, 200 ms.

neurons (2). The A-current was studied in the presence of manganese (3 mM) to eliminate the C-current contribution to depolarizing steps and to prevent calcium spiking. TTX was again present to block the sodium action potentials. Holding potential was set near −70 mV to allow the current to be well activated (15). Addition of 10 μM histamine to the bathing solution had no effect on A-current (Fig. 3, *A* and *B*). The transient outward current, but not the late outward current, was blocked by 500 μM 4-AP (Fig. 3, *A* and *C*). In the presence of manganese, the effect of histamine on the late outward current was eliminated; this is illustrated in Fig. 3*B*, where the current response to depolarizing steps with and without histamine (Fig. 3, *A1* and *A2*) are superimposed. Similarly, in Krebs solution containing manganese, if A-current was inactivated by changing holding potential to −40 mV, 10 μM histamine did not alter the current evoked by a depolarizing voltage command (Fig. 3*D*). In two of five cells studied in manganese-containing solution, membrane conductance (as measured between −40 and −60 mV) was reduced by 10 μM histamine. Perhaps

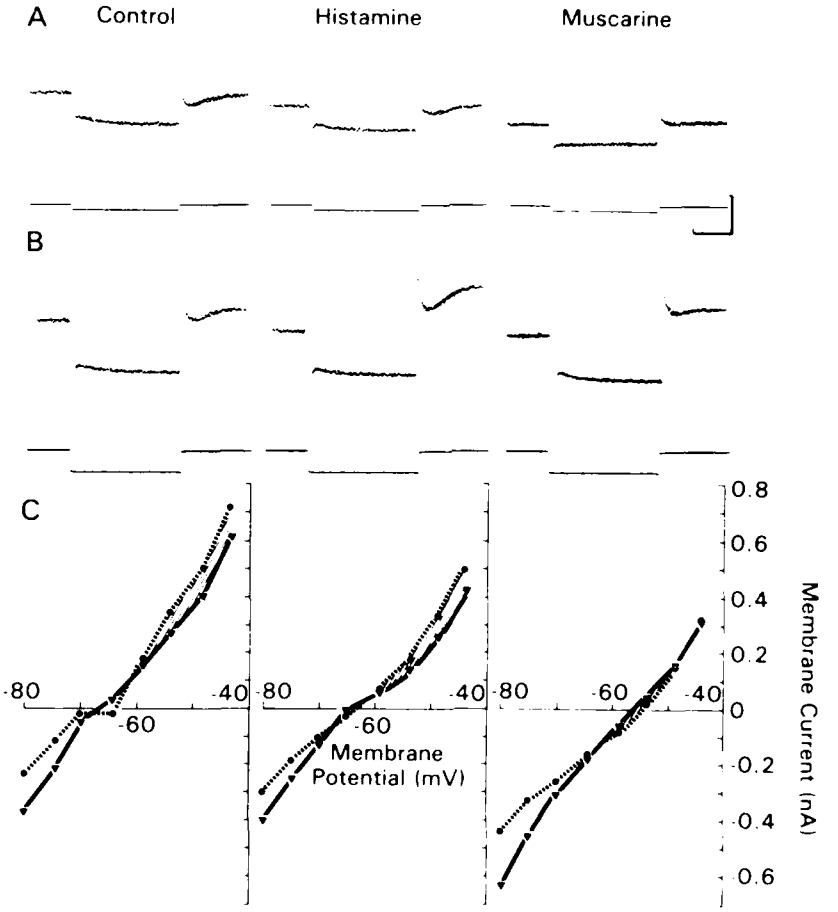

FIG. 4. Histamine (10 μM) does not affect M- or Q-current. TTX (0.3 μM) was present in the Krebs solution. *A*: membrane potential was voltage clamped to −38 mV. Voltage step to −48 mV revealed an inward relaxation (M-current) that was not altered by 10 μM histamine but was blocked by 20 μM muscarine. Traces are average of 4 identical steps. Calibration: 0.5 nA, 80 mV; 200 ms. *B*: larger voltage step (−38 to −80 mV) in same cell as *A* showed inward relaxation (Q-current) that was not affected by either histamine or muscarine. Illustrated currents (upper traces) and voltages (lower traces) are unaveraged single traces. Calibration: 1 nA, 80 mV, 200 ms. *C*: current-voltage curves for same cell as in *A* and *B* under same conditions. Currents at the beginning of hyperpolarizing steps are plotted with *circles*; currents near the end of the 500-ms steps are plotted with *triangles*. *Shaded area* shows M-current region. Histamine does not alter either M-current or Q-current (*middle panel*). Muscarine blocks M-current without affecting Q-current (*right panel*).

histamine has a secondary effect on some pyramidal cells that is not calcium dependent. However, the actions of histamine on voltage-activated currents were eliminated when calcium channels were blocked.

Another potassium current described in hippocampal pyramidal cells is the M-current (20). Hyperpolarizing steps from a holding potential near −40 mV reveal inward relaxations. The relaxations evoked by voltage commands to potentials between −40 and −70 mV resemble M-currents of sympathetic ganglion cells (7) and are blocked by muscarinic agonists (20). Larger hyperpolarizing steps elicit the pharmacologically distinct Q-current, which is dependent on both sodium and potassium ions (20). As shown in Fig. 4, 10 μM histamine did not affect either M- or Q-current. To clearly distinguish between M- and Q-current, 20 μM muscarine was applied. As expected, the inward relaxations resulting from small hyperpolarizing steps were blocked, but those occurring with larger steps were not affected by muscarine. Figure 4C shows the current-voltage curve of one cell treated in this way. The circles represent the current measured early in the 500-ms step, and the triangles represent the current measured at the end of the step. In 10 μM histamine (center panel), the M-current and Q-current were unaltered, whereas in muscarine (right panel), M-current was blocked but Q-current remained.

Segal and Barker (33) recently described, in cultured rat hippocampal neurons, a delayed rectifier that is inactivated at potentials more positive than −50 mV. An outward current with similar voltage and pharmacological sensitivity has been observed in pyramidal cells

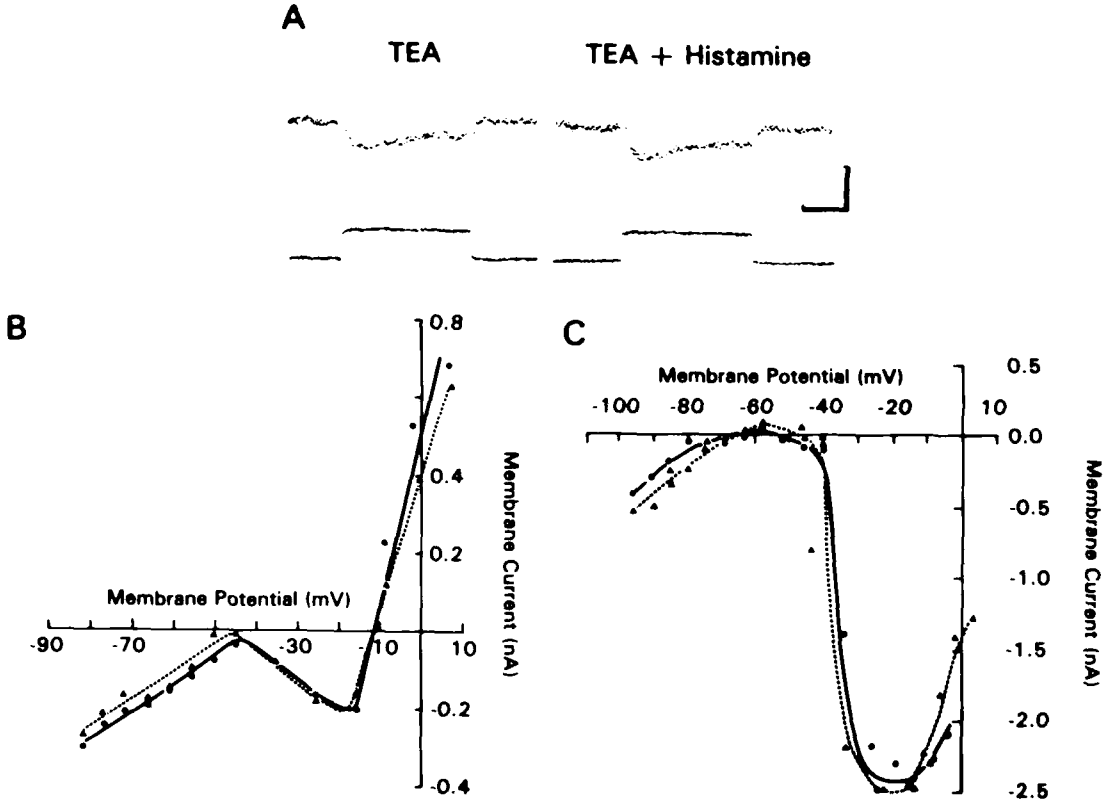

FIG. 5. No effect of histamine (10 μM) on membrane currents in Krebs solution containing 10 mM TEA and 0.3 μM TTX. *A*: voltage step from −45 mV to −25 mV induced an inward current. Histamine was without effect. Two traces are averaged. Calibration: 40 mV, 0.5 nA, 200 ms. *B*: current-voltage curves for same cell. Current at the end of the 500-ms voltage step is plotted against the step potential. *Dotted line* shows relationship without histamine. *Solid line* shows curve in 10 μM histamine. *C*: use of CsCl electrode with 10 mM TEA, to further reduce potassium currents in different cell, revealed similar inability of 10 μM histamine to reduce inward current. Holding potential is −53 mV. Currents at the end of the steps are plotted. *Symbols* are same as in *B*.

of hippocampal slices (K. Zbicz, personal communication). With a holding potential of −40 mV, the delayed rectifier should not contribute substantially to the recorded outward currents. Yet, in the presence of manganese, which does not block the delayed rectifier but does block C-current, a small outward current and outward tails remain (see Figs. 3*D* and 7*A*). This might suggest that the recorded outward currents may be contaminated with uninactivated delayed rectifier. The delayed rectifier reactivates with steps to potentials more negative than −70 mV and is in evidence as an outward tail when membrane potential returns to −40 mV from negative voltage steps (see Fig. 4*B*). Preliminary analysis of this tail current (unpublished observations) suggests that it is carried by the same current as the delayed rectifier described by Zbicz and by Segal and Barker (33). It is not blocked by manganese and is inactivated at potentials depolarized to −50 mV. Although the outward tail current was often variable in amplitude during the course of an experiment, histamine did not have any systematic effect on this current (increased 1.3% ± 5.7; mean ± SE; n = 10). The small outward current and outward tails remaining in the presence of manganese (zero calcium) were also insensitive to histamine (Fig. 3*D*).

Inward calcium current

To evaluate the effect of histamine on the inward calcium current, the potassium currents were pharmacologically blocked. In the present study, 10–15 mM tetraethylammonium (TEA) was used to reveal an underlying inward current as reported by Brown and Griffith (9) in CA1 pyramidal cells. In all cells, 0.3 μM TTX was present to prevent sodium-dependent spiking. Johnston, Hablitz, and Wilson (25) and Brown and Griffith (9) reported that the slow inward current revealed by potassium channel blockers was sensitive to divalent cations; cobalt, manganese, and cadmium blocked the current. Similarly, the inward current observed in the present series of experiments was absent when manganese was in the Krebs solution. These data suggest that the inward current was carried by calcium.

Using a holding potential of −40 mV, inward current was observed with voltage steps to more positive potentials. In some cells, small hyperpolarizing commands resulted in an outward current, suggesting the turning off of a persistent inward current. In TEA, the inward current frequently peaked at 50–200 ms and decayed slowly over the course of the 500-ms step. Inward current was reflected in the current-voltage curve by a negative-slope region. In four of eight cells tested in TEA (2 with CsCl electrodes to further block outward currents), 10 μM histamine had no effect on the inward current (Fig. 5). In the remaining four cells, the peak inward current and, to a lesser degree, the inward current at the end of the 500-ms step were slightly reduced by histamine. However, when this decrease occurred, it was never reversed by a wash period of at least 20 min. The labile nature of neuronal calcium currents may account for the observation.

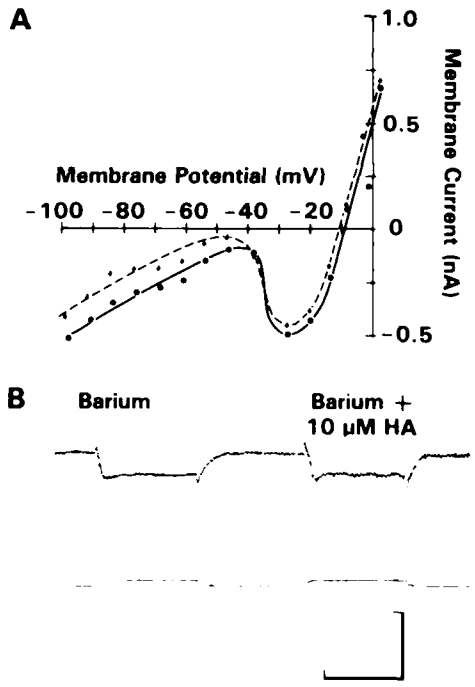

FIG. 6. No effect of histamine (10 μM) on membrane currents in presence of Krebs solution containing 2.4 mM barium (no calcium) and 0.3 μM TTX. *A*: negative-slope region of current-voltage relationship reflects inward current carried by divalent cation. This inward current was unaffected by 10 μM histamine. At hyperpolarized potentials, the current-voltage curve shifted in the inward direction when 10 μM histamine were present. *Dashed line* shows relationship without histamine. *Solid line* shows curve in 10 μm histamine. *B*: sample currents resulting from voltage steps from −39 to −26 mV in same cell as *A*. Histamine (10 μM) was without effect.

In the presence of TEA and TTX, depolarizing steps frequently resulted in a spike-like current superimposed on the slow inward current. This spike often produced a very slow inward tail, which persisted for a variable length of time and ended abruptly. Similar results have been reported by Brown and Griffith (9). This spike contamination sometimes made the current records and the actions of histamine in TEA solutions difficult to interpret.

Substituting barium for calcium eliminated spike contamination (at holding potentials near −40 mV) and further decreased residual C-current. Barium is capable of carrying inward current through calcium channels but does not activate potassium current (11, 14). In fact, it acts as a potassium channel blocker (1, 21). With barium and TTX present, the current-voltage curve showed a negative-slope region. Under these conditions, 10 μM histamine did not reduce the inward current but caused an inward shift of the current at potentials between −50 and −100 mV (n = 4) (Fig. 6). The significance of this current shift is not clear. Under the same experimental conditions, 1 μM histamine had no effect on the current-voltage curve in two cells tested. These results suggest that histamine does not affect the calcium current. The histamine-induced decrease in C-current, therefore, is likely to be a direct effect of the transmitter.

Maximal histamine effect

Histamine in concentrations from 1 to 50 μM was evaluated on the outward current of CA1 pyramidal cells in the presence of TTX to block sodium spikes. As reported above, histamine at 1 μM reduced the outward current. Addition of histamine to concentrations of 5, 10, and 50 μM produced little further decrease of the outward current; a concentration of ~5 μM appeared to be maximally effective.

To test if histamine was fully blocking C-current, 10 μM histamine were applied in the presence of normal calcium concentration. (Phosphate and sulfate salts were replaced with chloride.) After achieving the maximal histaminergic effect, the calcium was replaced with manganese; 10 μM histamine were still present. Since manganese decreased the conductance of the cell in the hyperpolarized region, the leak conductance was subtracted

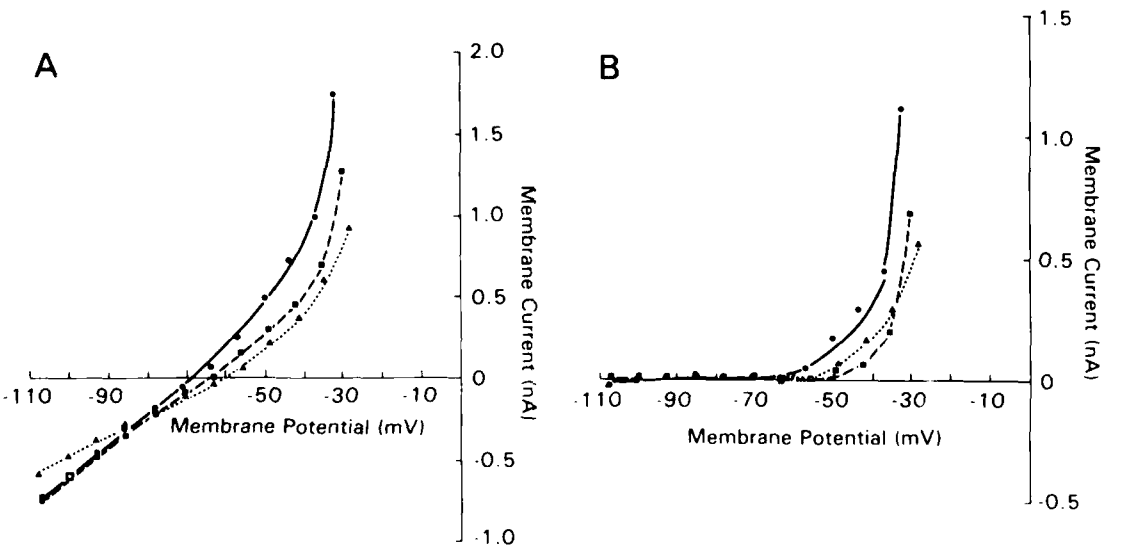

FIG. 7. Effect of manganese on a cell exposed to 10 μM histamine. Holding potential was −50 mV. *A*: current-voltage relationship of neuron in Krebs solution containing normal calcium but without sulfate or phosphate (*solid line*). At a concentration of 10 μM, histamine produced a maximal decrease in outward current (*dashed line*). Replacement of calcium with manganese (histamine still present) increased the resistance of the cell (from 56 to 89 MΩ) and appeared to further decrease the outward current (*dotted line*). *B*: current-voltage curves with the leak current subtracted for the curves in *A*. (*Graph symbols* in *B* correspond to the same condition symbolized in *A*.) Manganese increased the outward current between −55 and −35 mV but decreased the outward current at more depolarized potentials.

from the current-voltage curves in order to evaluate the effects of manganese on the outward current (Fig. 7). In all three cells tested, manganese increased the outward current in the range of −55 to −30 mV. This can be explained by the block of inward current causing an outward shift of the current-voltage curve. At potentials depolarized to −30 mV, manganese decreased the outward current. At these potentials, the effect of manganese to decrease the outward current might overwhelm the decrease in the inward current. Manganese appeared to be capable of further decreasing the outward current in the presence of a maximally effective dose of histamine. These results suggest that histamine, although blocking much of the C-current, does not block all C-current.

Notice that even in the presence of manganese, an outward current remains. It is possible that the residual current is delayed rectifier that was not inactivated by the depolarized holding potential. Near −28 mV, this current constituted 63% ± 6 (n = 3) of the total outward current. This may be an overestimate of the delayed rectifier contribution, however, because of the outward shift produced by the blocking action of manganese of the inward current. Despite the difficulties of quantification, correcting for the presence of an outward current in addition to C-current would increase the calculated effectiveness of histamine to decrease C-current.

DISCUSSION

Previous investigations revealed that histamine affected calcium-mediated processes (17, 31, 32). The present study confirmed that histamine blocked the calcium-dependent hyperpolarization following a train of spikes. Voltage-clamp data revealed that the slowly activating potassium current, which is predominantly C-current (8), was reduced by histamine. The effect on C-current was fairly specific. M-, Q-, and A-currents were unaltered by histamine. The delayed rectifier also appeared to be insensitive to histamine. The effect on C-current is not a consequence of a block of calcium current. Histamine had no effect on calcium inward current or on calcium spikes. In CA1 neurons of hippocampus, histamine appears to decrease calcium-mediated potassium current in a very selective manner.

It is clear from the results reported here that histamine selectively blocks the C-current, although the effect appears to be small (a 27% decrease). This is in contrast to the dramatic effect of histamine on the afterhyperpolarization. The voltage-clamp analysis may provide an underestimate of the effectiveness of histamine for a variety of reasons. First, despite attempts to inactivate delayed rectifier with a holding potential near −40 mV, this histamine-insensitive potassium current may contribute to the total outward current used in calculation of histamine effectiveness. From the data in Fig. 7 it appears that in manganese a substantial outward current remains (63% of total at −28 mV). If C-current actually constitutes only 37% of the total outward current measured, the effectiveness of histamine might be closer to 70% than to 27%.

A second explanation for the apparently small effect of histamine might be that histamine is not blocking all of C-current. If it were, the addition of manganese following exposure to a maximal concentration of histamine either should have no further effect or should increase the net outward current by blocking the inward calcium current. The action of histamine was maximal at concentrations above 5 μM. At potentials positive to −30 mV, manganese was able to further reduce the outward current. This suggests that the histamine is not blocking all of the manganese-sensitive current. Two possibilities can explain this finding. Manganese might be attenuating outward currents other than C-current. There is no evidence, however, that manganese has a direct blocking action on any potassium current; its effect on the C-current is through prevention of calcium influx. Alternatively, only a portion of C-current might be histamine sensitive. An abstract by Lancaster and Adams (26) suggests that a subset of calcium-mediated potassium current is sensitive to norepinephrine. They termed this slow current I(AHP) since it seemed also to be the component of calcium-mediated potassium current responsible for the slow afterhyperpolarization. The residual component had a faster time course, observed as a more quickly decaying tail current following a depolarizing step. In the present study, such a distinction could not be made. After application of histamine, no distinctly faster tail current was revealed.

A third factor complicates the comparison

of the effectiveness of histamine to reduce C-current and to block the afterhyperpolarization. To elicit C-current, the voltage-clamp data uses voltage steps to potentials less positive than approximately −25 mV. Large depolarizations were precluded because the very large outward currents could not be clamped. Yet C-current is not maximally activated in the potential range studied. In contrast, an action potential depolarizes the cell to +30 or +40 mV where C-current is turned on more fully. The difference in the voltages used to elicit C-current in the two experimental paradigms might make comparisons difficult.

Haas (16) reported that histamine applied by iontophoresis caused a hyperpolarization possibly due to an increase in potassium conductance. In the present study, some cells responded to histamine with a change in membrane conductance in the voltage range of −50 to −80 mV. In solutions containing manganese, 10 μM histamine caused a decrease in conductance in two of five cells; in barium, 10 μM histamine consistently produced a reversible inward shift in the current-voltage relationship in this hyperpolarized range (see Fig. 6). A hyperpolarizing action of histamine was never observed in the present study. The absence of this response might be a consequence of the method of application of histamine. With prolonged exposure, as occurs with bath perfusion, the hyperpolarizing response might desensitize. It is also possible that this hyperpolarizing current makes only a minor contribution to the total current of the cell and therefore goes unnoticed.

As reported by Haas and Konnerth (17), the action of histamine to reduce C-current underlying the slow afterhyperpolarization would reduce accommodation of action potentials and increase neuronal excitability. The action of histamine on CA1 pyramidal cells would depend on the actual distribution of histaminergic inputs and the associated histamine receptor/channel complex. Haas (16) suggested that the hyperpolarization resulting from iontophoretically applied histamine is restricted to certain sites. It is possible that the action of histamine on C-current also is restricted to particular locations on the cell. The net effect of histamine may actually be a sensitive balance of excitatory and inhibitory actions.

ACKNOWLEDGMENTS

I thank Dr. J. E. Freschi, Dr. J. M. Sarvey, Dr. A. M. Williamson, H. E. Scharfman, and P. K. Stanton for helpful discussions.

Received 5 April 1985; accepted in final form 30 October 1985.

REFERENCES

1. ADAMS, D. J. AND GAGE, P. W. Divalent ion currents and the delayed potassium conductance in an *Aplysia* neurone. *J. Physiol. Lond.* 304: 297–313, 1980.
2. ADAMS, D. J., SMITH, S. J., AND THOMPSON, S. H. Ionic currents in molluscan soma. *Annu. Rev. Neurosci.* 3: 141–167, 1980.
3. ALGER, B. E. AND NICOLL, R. A. Epileptiform burst after-hyperpolarization: calcium-dependent potassium potential in hippocampal CA1 pyramidal cells. *Science* 210: 1122–1124, 1980.
4. BARBIN, G., GARBARG, M., SCHWARTZ, J. C., AND STORM-MATHISEN, J. Histamine synthesizing afferents to the hippocampal region. *J. Neurochem.* 26: 259–263, 1976.
5. BARRETT, E. F. AND BARRETT, J. N. Separation of two voltage-sensitive potassium currents, and demonstration of a tetrodotoxin-resistant calcium current in frog motoneurones. *J. Physiol. Lond.* 255: 737–774, 1976.
6. BENARDO, L. S., MASUKAWA, L. M., AND PRINCE, D. A. Electrophysiology of isolated hippocampal pyramidal dendrites. *J. Neurosci.* 2: 1614–1622, 1982.
7. BROWN, D. A. AND ADAMS, P. R. Muscarinic suppression of a novel voltage-sensitive K current in a vertebrate neurone. *Nature Lond.* 183: 673–676, 1980.
8. BROWN, D. A. AND GRIFFITH, W. H. Calcium-activated outward current in voltage-clamped hippocampal neurones of the guinea-pig. *J. Physiol. Lond.* 337: 287–301, 1983.
9. BROWN, D. A. AND GRIFFITH, W. H. Persistent slow inward calcium current in voltage-clamped hippocampal neurones of the guinea-pig. *J. Physiol. Lond.* 337: 303–320, 1983.
10. BROWN, T. H., FRICKE, R. A., AND PERKEL, D. H. Passive electrical constants in three classes of hippocampal neurons. *J. Neurophysiol.* 46: 812–827, 1981.
11. CONNOR, J. A. Calcium current in molluscan neurones: measurement under conditions which maximize its visibility. *J. Physiol. Lond.* 286: 41–60, 1979.
12. GARBARG, M., BARBIN, G., BISCHOFF, S., POLLARD, H., AND SCHWARTZ, J. C. Dual localization of histamine in an ascending neuronal pathway and in non-neuronal cells evidenced by lesions in the lateral hypothalamic area. *Brain Res.* 106: 333–348, 1976.
13. GARBARG, M., BARBIN, G., FEGER, J., AND SCHWARTZ, J. C. Histaminergic pathway in rat brain evidenced by lesions of the medial forebrain bundle. *Science* 186: 833–835, 1974.
14. GORMAN, A. L. F. AND HERMANN, A. Internal effects of divalent cations on potassium permeability in mol-

luscan neurones. *J. Physiol. Lond.* 296: 393–410, 1979.

15. GUSTAFSSON, B., GALVAN, M., GRAFE, P., AND WIGSTROM, H. A transient outward current in a mammalian central neurone blocked by 4-aminopyridine. *Nature Lond.* 299: 252–254, 1982.
16. HAAS, H. L. Analysis of histamine actions by intra- and extracellular recording in the hippocampal slices of the rat. *Agents Actions* 11: 125–128, 1981.
17. HAAS, H. L. AND KONNERTH, A. Histamine and noradrenaline decrease calcium-activated potassium conductance in hippocampal pyramidal cells. *Nature Lond.* 302: 432–434, 1983.
18. HABLITZ, J. J. Altered burst responses in hippocampal CA3 neurones injected with EGTA. *Exp. Brain Res.* 42: 483–485, 1981.
19. HABLITZ, J. J. Effects of intracellular injections of chloride and EGTA on postepileptiform burst-hyperpolarizations in hippocampal neurones. *Neurosci. Lett.* 22: 159–163, 1981.
20. HALLIWELL, J. V. AND ADAMS, P. R. Voltage-clamp analysis of muscarinic excitation in hippocampal neurons. *Brain Res.* 250: 71–92, 1982.
21. HERMANN, A. AND GORMAN, A. L. F. Blockage of voltage-dependent and Ca-dependent K current components by internal Ba in molluscan pacemaker neurons. *Experientia* 35: 229–231, 1979.
22. HOTSON, J. R. AND PRINCE, D. A. A calcium-activated hyperpolarization follows repetitive firing in hippocampal neurons. *J. Neurophysiol.* 43: 409–419, 1980.
23. JOHNSTON, D. Passive cable properties of hippocampal CA3 pyramidal neurons. *Cell. Mol. Neurobiol.* 1: 100–110, 1981.
24. JOHNSTON, D. AND BROWN, T. H. Interpretation of voltage-clamp measurements in hippocampal neurons. *J. Neurophysiol.* 50: 464–486, 1983.
25. JOHNSTON, D., HABLITZ, J. J., AND WILSON, W. A. Voltage clamp discloses slow inward current in hippocampal burst-firing neurones. *Nature Lond.* 286: 391–393, 1980.
26. LANCASTER, B. AND ADAMS, P. R. Components of Ca-activated K current in rat hippocampal neurones in vitro (Abstract). *J. Physiol. Lond.* 362: 23P, 1985.
27. LLINAS, R. AND HESS, R. Tetrodotoxin-resistant dendritic spikes in avian Purkinje cells. *Proc. Natl. Acad. Sci. USA* 73: 2520–2523, 1976.
28. MULDER, A. H., VAN AMSTERDAM, R. G. M., WILBRINK, M., AND SCHOFFELMEER, A. N. M. Depolarization-induced release of [3H]histamine by high potassium concentrations, electrical stimulation and veratrine from rat brain slices after incubation with the radiolabelled amine. *Neurochem. Int.* 5: 291–297, 1983.
29. SCHWARTZ, J. C. Histaminergic mechanisms in brain. *Annu. Rev. Pharmacol. Toxicol.* 17: 325–339, 1977.
30. SCHWARTZKROIN, P. A. AND STAFSTROM, C. E. Effects of EGTA on the calcium-activated hyperpolarization in hippocampal CA3 pyramidal cells. *Science* 210: 1125–1127, 1980.
31. SEGAL, M. Histamine produces a Ca-sensitive depolarization of hippocampal pyramidal cells in vitro. *Neurosci. Lett.* 19: 67–71, 1980.
32. SEGAL, M. Histamine modulates reactivity of hippocampal CA3 neurons to afferent stimulation in vitro. *Brain Res.* 213: 443–448, 1981.
33. SEGAL, M. AND BARKER, J. L. Rat hippocampal neurons in culture: potassium conductances. *J. Neurophysiol.* 51: 1409–1433, 1984.
34. SUBRAMANIAN, N. Electrically induced release of radiolabeled histamine from rat hippocampal slices: opposing roles for H1- and H2-receptors. *Life Sci.* 31: 557–562, 1982.
35. WONG, R. K. S. AND PRINCE, D. A. Afterpotential generation in hippocampal pyramidal cells. *J. Neurophysiol.* 45: 86–97, 1981.
36. WONG, R. K. S., PRINCE, D. A., AND BASBAUM, A. I. Intradendritic recordings from hippocampal neurons. *Proc. Natl. Acad. Sci. USA* 76: 986–990, 1979.
37. ZBICZ, K. L., AND WEIGHT, F. F. Transient voltage and calcium-dependent outward currents in hippocampal CA3 pyramidal neurons. *J. Neurophysiol.* 53: 1038–1058, 1985.

Neuroscience Vol. 17, No. 4, pp. 1139–1146, 1986
Printed in Great Britain

0306-4522/86 $3.00 + .00
Pergamon Press Ltd

CYTOCHEMICAL STUDY OF DEVELOPING NEUROTRANSMITTER PROPERTIES OF DISSOCIATED SYMPATHETIC NEURONS GROWN IN CO-CULTURE WITH DISSOCIATED PINEAL CELLS

C. E. PHILLIPS† and J. E. FRESCHI*
Physiology Department, Armed Forces Radiobiology Research Institute, Bethesda, MD 20814, U.S.A.

Abstract—We studied the development of neurotransmitter phenotype in sympathetic neurons grown in the presence of pinealocytes, a target tissue having adrenergic but not cholinergic receptors. Neurons, dissociated from neonatal rat superior cervical ganglia, were grown in co-culture with dissociated pineal cells. Both ganglionic and pineal non-neuronal background cells were allowed to grow nearly to confluency. Electron microscopic cytochemical techniques were used to examine sets of co-cultures at weekly intervals over 5 weeks. Adrenergic vesicles were identified by their dense granular precipitate following potassium permanganate fixation. We found that the percentage of small granular vesicles, both in synaptic boutons onto other neurons and in axonal varicosities, declined very little over 5 weeks. After an initial drop from 75 to 65%, the percentage of small granular vesicles remained remarkably constant. Throughout the 5 weeks, more than 70% of the boutons and varicosities contained a predominance of small granular vesicles; fewer than 20% contained a predominance of clear vesicles. Although both somal synaptic boutons and axonal varicosities retained a predominantly adrenergic ultrastructure, at certain weeks there was a statistically significant shift in the percent distribution of adrenergic vesicles in somal boutons compared with the distribution in axonal varicosities.

Because these cultures were grown under conditions known to favor an induction of acetylcholine metabolism and a suppression of catecholamine metabolism, we conclude that the maintainence of adrenergic ultrastructure over 5 weeks may be due to the presence of the pineal cells.

Sympathetic neurons in tissue culture display considerable plasticity in expression of neurotransmitter phenotype. Depending on tissue culture environment, they may remain adrenergic or they may undergo cholinergic differentiation.[11] The two transmitter phenotypes are not mutually exclusive, however, and the neurons can synthesize, store and release both transmitters at the same time.[4,13,19] It is well established that various nonneuronal background cells can produce one or more diffusable substances, presently uncharacterized,[18] that induce a shift from adrenergic to cholinergic transmitter synthesis in sympathetic neurons in culture.[6,11,12] On the other hand, sympathetic neurons retain their adrenergic phenotype when grown in the absence of background cells or when presynaptic input is mimicked by chronically depolarizing the neurons in elevated potassium.[11,17] Differentiation of neurotransmitter properties is also influenced by identified growth factors and hormones. Epidermal growth factor enhances cholinergic differentiation whereas glucocorticoids antagonize this effect. Both substances, however, act indirectly on the neuron by affecting the production of cholinergic conditioning factor by background cells.[3]

The influence of direct neuronal contact with target tissues on subsequent transmitter metabolism is less clear. Most studies have shown a shift to cholinergic metabolism regardless of the presence of a specific target tissue.[8,11,15] Rowe and Parr[14] found that pineal cells, which have α and β-adrenoreceptors but no acetylcholine receptors, caused an increase in choline acetyltransferase activity in co-cultured sympathetic neurons 10 times over that found in neurons in cultures alone. This effect was not reproduced when the neurons were treated with pineal conditioned media. Previous studies from our laboratory indicate that sympathetic neurons develop dural transmitter function when co-cultured with pineal cells. After 2.5 weeks in culture the sympathetic neurons formed functional cholinergic synapses onto each other, as assessed by electrophysiological techniques, yet still released a β-adrenergic agonist that caused an increase in pineal *N*-acetyltransferase activity.[10]

In these studies we wished to extend our previous electrophysiological and biochemical studies by using ultrastructural techniques to determine what effect pinealocytes have on co-cultured sympathetic neurons. We asked if the dual neurotransmitter state in this particular co-culture system is maintained or transient. We also sought evidence for morphological contacts between sympathetic neurons and pinealocytes.

*To whom correspondence should be sent at present address: Department of Neurology, 401 Woodruff Memorial Research Building, Emory University School of Medicine, Atlanta, GA 30322, U.S.A.
†Present address: Stroke and Trauma Program, NINCDS, National Institutes of Health, Bethesda, MD 20205, U.S.A.

Abbreviations: CV, clear vesicles; SCG, superior cervical ganglion; SGV, small granular vesicles.

EXPERIMENTAL PROCEDURES

Tissue culture

We have previously published detailed descriptions of our culture methodology.[1,2] For these experiments we plated dissociated pineal cells onto collagen-coated plastic coverslips one week before adding the dissociated superior cervical ganglion (SCG) neurons. Feeding medium comprised modified F12 medium (F12K, GIBCO) supplemented with 5% (v v) fetal bovine serum (Hyclone) nerve growth factor (kindly supplied by Dr Gordon Guroff) and additional glutamine and ascorbic acid (Sigma). Background cell proliferation was controlled by periodically adding 5-fluorodeoxyuridine plus uridine (Sigma) to the feeding medium. The purpose of this treatment was not to completely eliminate background cells but rather to prevent their overgrowth. Thus, in addition to pinealocytes and SCG neurons, the culture dishes contained a nearly confluent monolayer of various background cells, including fibroblasts and Schwann cells, from pineal glands and SCG. For these experiments only cultures of the same plating (sister cultures) were used for comparative analysis.

Microscopy

Two dishes of sister co-cultures were fixed each week during the 5 weeks of study. Culture dishes were rinsed several times with *N*-2-hydroxyethylpiperazine-*N'*-2-ethanesulfonic acid (HEPES) buffered Hanks saline, pH 7.35. Cells were fixed in freshly prepared 4% (w v) potassium permanganate ($KMnO_4$) in HEPES-buffered Hanks saline and then placed on ice for 1 h. The cultures were then rinsed first in cold HEPES-buffered Hanks saline, then in cold sodium acetate buffer, pH 5, and stained *en bloc* with uranyl acetate for 1.5 h at 4 C. Tissues were then dehydrated through a series of ethanol concentrations and embedded in Taab 812. Some cultures were incubated for 30 min, with constant gentle agitation, in 5×10^{-4} M L-norepinephrine (Sigma) at 37 C prior to fixation. This did not increase the density or number of granular vesicles over that seen in cultures not preincubated with norepinephrine. Control cultures were prepared as above but with the additional preincubation in 2 μM reserpine (Sigma) for 2.5 h before fixation. Suitable areas, at least two from each coverslip, were scored, cut out and mounted so that sections were cut parallel to the collagen surface. Thin sections were collected on Formvar-coated slit grids and photographed in a Philips 400 electron microscope at 60 kV. Micrographs were taken at a magnification of 46,600 and printed at a final magnification of 116,500.

Data analysis

Synaptic vesicles were photographed, classified, and counted both in synaptic boutons contacting neuron somata (somal synapses) and in axonal swellings relatively remote from nerve cell bodies (axonal varicosities). (For clarity and convenience, we shall hereafter refer to both somal synapses and axonal varicosities as terminals or varicosities.) A total of 50 such terminals were counted at each of the 5 weeks. Terminals were chosen at random but were rejected if they contained fewer than 10 vesicles total. Adrenergic vesicles were identified by their dense granular precipitate. The number of clear vesicles (CV) and small granular vesicles (SGV) present in each varicosity was counted and expressed as a percentage of the total number of vesicles in the terminal (% SGV = SGV (SGV + CV) × 100).

Distribution histograms were made for both axonal and somal varicosities at each week. The histograms display the distribution of varicosities containing various percentages of SGV. The distributions for the different weeks were then compared by applying the Chi-square analysis to the data entered in $r \times c$ contingency tables.[9] In the rows were entered the weeks in culture, in columns were entered the percent of varicosities grouped according to the percentage of SGV they contained (0–25%, 25–50%, 50–75%, and 75–100%). In addition, sets of sister co-cultures from a second plating were fixed to test the repeatability of our experiments across platings. Counts of axonal varicosities were made from the second plating of co-cultures fixed at 3, 4 and 5 weeks.

RESULTS

We found that SCG neurons, when co-cultured with dissociated pinealocytes over a 5-week period, retained ultrastructural characteristics of adrenergic neurotransmitter metabolism, suggesting ongoing uptake, synthesis and storage of norepinephrine.

Vesicle cytochemistry

As previously described,[10] SCG neurons, alone and in small clusters, send out processes in bundles which ramify throughout the culture dish. The neurites are especially tortuous and display numerous varicosities at sites of synaptic contacts at other neuron clusters and, to a lesser extent, over regions of pineal cell nests. We found that the ultrastructure of the varicosities at these locations was similar: swelling of the axon with accumulation of vesicles.

Adrenergic vesicles reacted strongly in $KMnO_4$ over the entire 5 weeks of the study. Figure 1 shows photographs of representative synapses and varicosities from cultures at each of the 5 weeks. The preponderance of SGV in the terminals is clearly evident at each week. Less frequently seen were terminals containing a predominance of CV (Fig. 2a). Even at five weeks, neurons fixed directly in $KMnO_4$ (Fig. 1f) contained SGV that had as dense a precipitate as those preincubated in norepinephrine (Fig. 1a–e). Thus, the ability of vesicles to precipitate with $KMnO_4$ (reflecting endogenous stores) remained qualitatively constant over the 5 weeks. In the reserpine-treated control cultures studied at each of the 5 weeks, we found no SGV.

Because $KMnO_4$ fixation does not preserve synaptic densities, we could not precisely determine the relationship of vesicles to release sites. Nevertheless, we did not see vesicles clustered at presumptive release sites. This was true even for varicosities containing a predominance of clear vesicles, in which typical synaptic release sites and vesicle clustering might be expected (Fig. 2a). We found, in areas remote from SCG neuron somata, varicosities abutting pineal cells (Fig. 2b). These presumably can serve as release sites of functional significance.[10]

Statistical analysis of vesicle counts

In order to quantify the ultrastructural data, the synaptic vesicles in 50 varicosities from co-cultures at each week were classified and counted, as described in the Experimental Procedures. We found that the total percentage of SGV in the co-cultures remained remarkably constant throughout the study. Figure 3a shows the total percentage of SGVs from the 50 varicosities counted at each week. After an initial

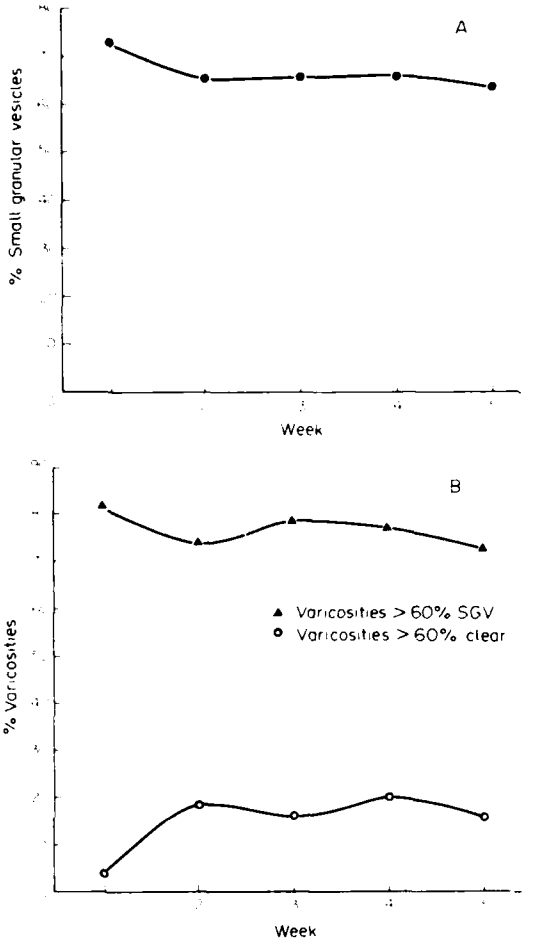

Fig. 3. Stability of vesicle population over 5 weeks. (A) Total percentage of SGV at each week. Fifty varicosities, 25 somal and 25 axonal, were counted at each week for 5 weeks. The percent SGV of the total of all vesicles counted in all 50 varicosities is plotted. (B) Percentage of varicosities that contain more than 60% SGV (triangles) or more than 60% CV (circles) at each week.

drop between weeks 1 and 2, the percentage of SGVs remained constant at about 65%. Furthermore, we found that the vesicles within any given varicosity remained predominantly of one type. Figure 3b shows the percentage of terminals that contained more than 60% SGV or more than 60% CV at each of the 5 weeks. More than 70% of the terminals contained predominantly SGV and fewer than 20% contained predominantly CV over the entire course of the study.

In order to compare in greater detail the vesicle counts from week to week, the data were entered in frequency histograms. The distributions of varicosities having different percentages of SGV for each week are shown in Fig. 4. Separate distributions were constructed for somal and axonal varicosities. It appears from inspection of the histograms that the distribution of axonal varicosities was similar for each of the 5 weeks. For the somal synapses the distributions displayed some variation. The somal histograms for weeks 1, 3 and 4 appeared similar and resembled those of the axonal varicosities. The somal histogram for week 2 and possibly week 5, however, appeared different. For the somal varicosities pooled over the 5 weeks, the Chi-square (χ^2) for the 5×4 contingency table was 23.53 ($P < 0.05$), indicating significant differences within this group (all somal varicosities). A contingency table for weeks 2 and 5 did not show a significant χ^2, indicating that the percentage counts in each of the four categories for these 2 weeks were not statistically different. χ^2 for a contingency table for weeks 1, 3 and 4 was also not significant. Weeks 2 and 5 were therefore combined, as were weeks 1, 3 and 4. The same analysis done on the axonal counts at each week showed that they were not significantly different ($P > 0.05$). Therefore, all of the axonal counts were combined. The frequency histograms of the three combined groups are shown in Fig. 5. The next step in analysis was to statistically compare the three combined groups. The combined somal counts for weeks 2 and 5 were found to be significantly different from each of the other two combined groups ($P < 0.01$). In Fig. 5 it appears that the principal difference occurred as a reversal of the percentages of SGV in categories 50–75% and 75–100% (i.e. more boutons with 50–75% SGV and fewer with 75–100% SGV). When the distribution of these two categories for the weeks 2 and 5, combined somal counts was compared with the same distribution from each of the other two combined groups, the reversal seen in the histograms was found to be significant ($P < 0.05$). The same comparisons made between the 0–25% and 25–50% distributions showed no significant difference.

To summarize, statistical analysis confirmed that, overall, there was no significant decline in numbers of SGV between weeks 1 and 5. This was unequivocably true for axonal varicosities. Somal varicosities showed some variability, but differences were in the groups containing greater than 50% SGV. Overall, the somal varicosities remained predominantly adrenergic.

To check the reproducibility of some of these results, we counted axonal varicosities from sets of sister cultures from another plating at weeks 3, 4 and 5. The vesicle population comprised 65% SGV. The combined distribution histogram for the three weeks was the same as that obtained from analysis of the combined axonal varicosities from the first plating reported above.

Finally, we compared results obtained with and without norepinephrine loading. We counted vesicles from 25 randomly selected unloaded somal and axonal varicosities at week 5. Distribution histogram and Chi-square analysis of the data showed these unloaded terminals to be statistically identical to the loaded somal terminals of weeks 1, 3, 4 and all loaded axonal varicosities.

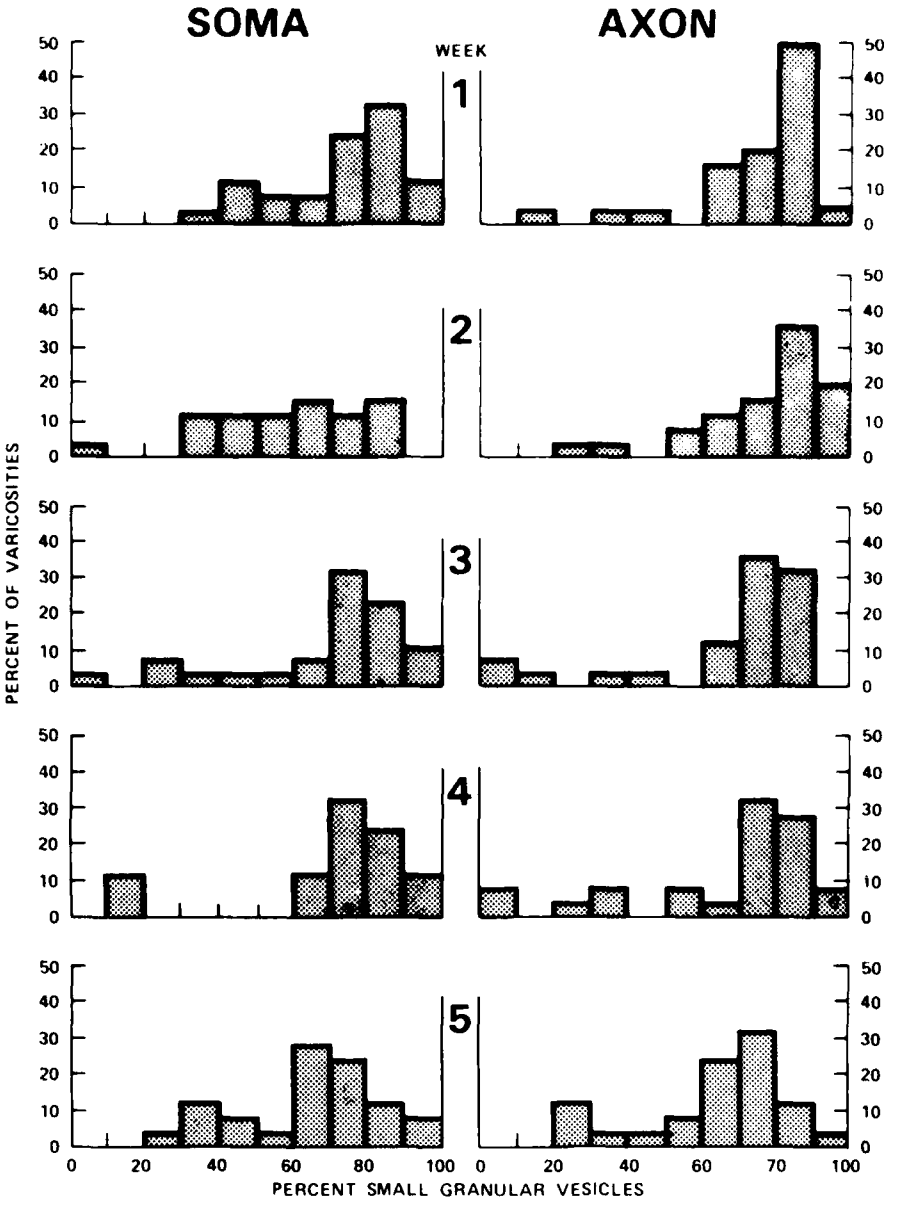

Fig. 4. Frequency histograms showing distribution of varicosities having different percentages of SGV. Histograms were constructed for somal synapses (left column) at each week and for axonal varicosities (right column) at each week.

DISCUSSION

Pineal cells in co-culture with superior cervical ganglion neurons may help conserve neuronal adrenergic ultrastructure

We found that, in the presence of pinealocytes and background cells of SCG and pineal origin, sympathetic neurons maintained their adrenergic ultrastructural characteristics. Based on data in the literature, one would have predicted that the population of synaptic vesicles would have shifted to one of predominantly clear vesicles for the following reasons. Our cultures were grown in medium with fetal calf serum and bicarbonate buffer, and had nearly con-

Fig. 1. Representative varicosities from the 5 weeks of study. Note that the $KMnO_4$ causes strong precipitation in the vesicles at all times. (A) (E) were preincubated in L-norepinephrine 30 min prior to fixation, the culture in (F) was fixed directly in permanganate. (A) Somal varicosity 1 week in co-culture. (B) Axonal varicosity 2 weeks in co-culture. (C) Somal varicosity 3 weeks in co-culture. (D) Somal varicosity 4 weeks in co-culture. (E) (F) Somal varicosities 5 weeks in co-culture. Axons (A), somata (S), and varicosities (V) are identified.

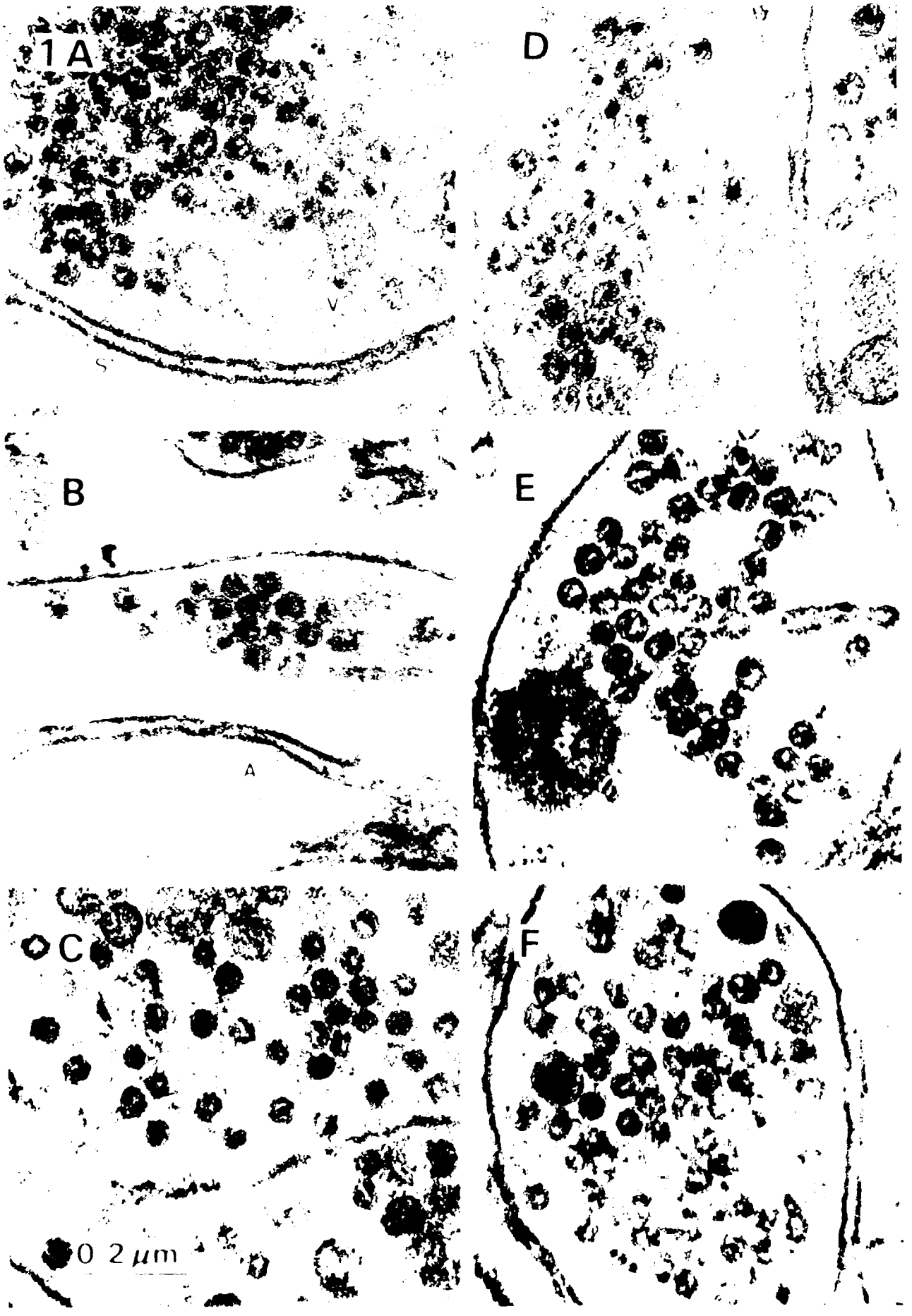
1A
D
B
E
C
F
0 2 μm

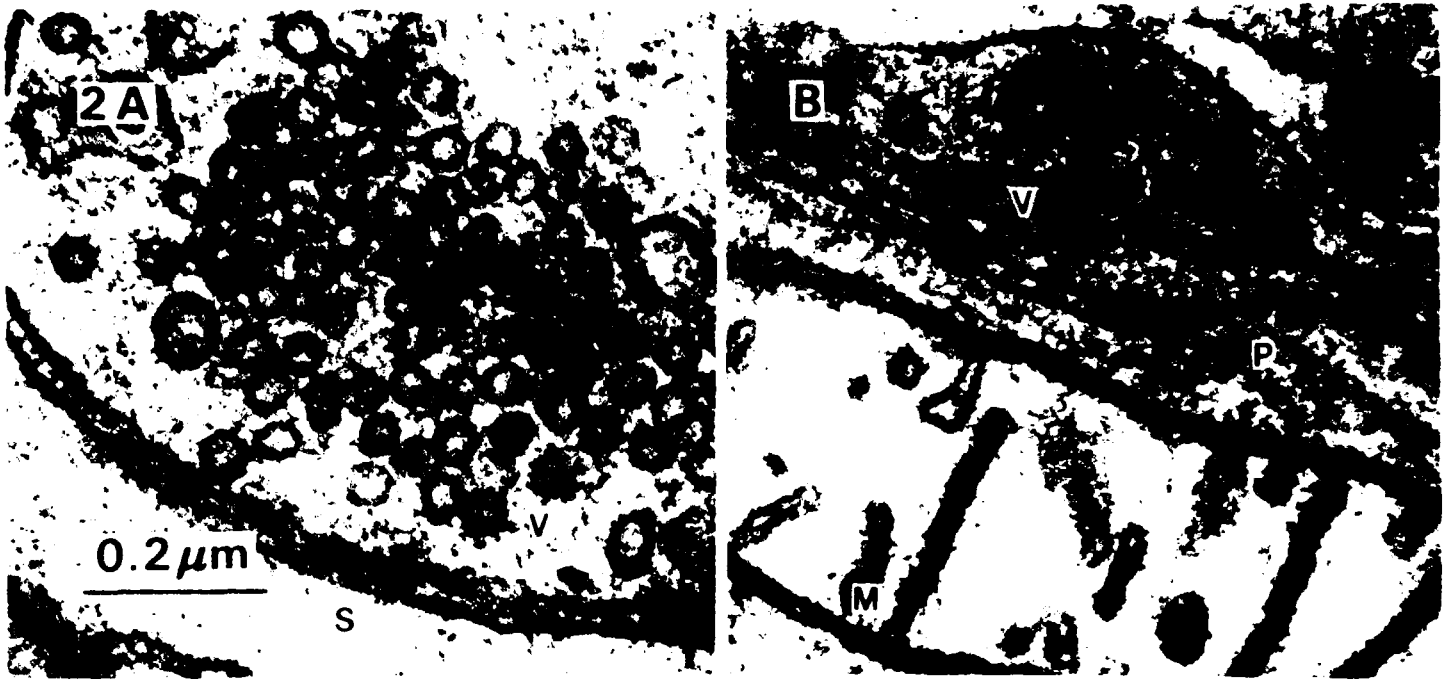

Fig. 2. (A) After 4 weeks in co-culture, a somal varicosity with predominantly clear vesicles. Note the absence of vesicle clustering at sites along the presynaptic membrane. (B) Axonal varicosity with predominantly small granular vesicles adjacent to a pinealocyte after 2 weeks in co-culture. Mitochondrion (M), pinealocyte (P), neuronal soma (S), and varicosities (V) are shown.

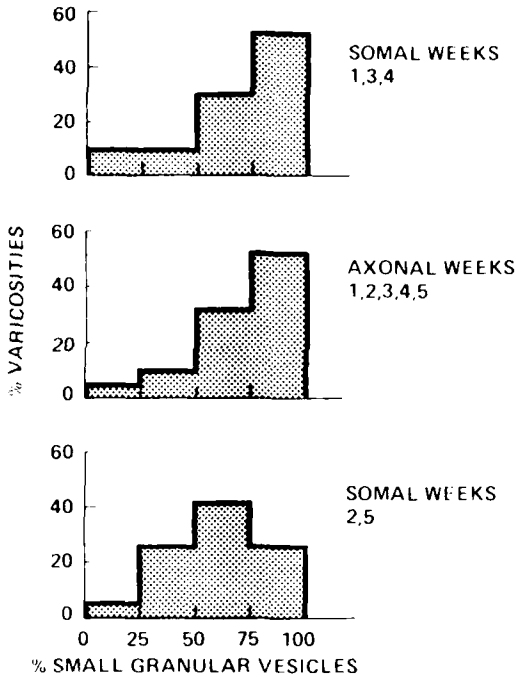

Fig. 8. Combined frequency histograms. Within each of the two categories of varicosities, somal and axonal, the histograms at each week (Fig. 4) were compared. Those that did not statistically differ were combined. The pooled histogram of somal counts from weeks 1, 3 and 4 was not significantly different from the pooled histogram of axonal counts from weeks 1–5 ($P > 0.05$). The combined histogram of somal counts from weeks 2 and 5 was significantly different from the other two combined histograms ($P < 0.01$ in both cases).

fluent layers of background cells. These conditions are known to induce neuronal cholinergic differentiation. Landis found that sympathetic neurons grown in culture conditions similar to ours (but without co-cultured pinealocytes) showed a shift in the percentage of SGV vesicles from 88% at day 4 to 34% at day 21 in culture. When preloaded with 5-hydroxydopamine, these same cultures declined from 93% at day 7 to 63% at day 21 in culture. Extrapolating to 5 weeks, one may predict that the loaded vesicles in Landis's study would have declined to 45%. Our co-cultures, however, showed no difference between loaded and unloaded vesicles at 5 weeks. This indicates that the neurons retained the capacity for synthesis, storage and uptake of norepinephrine. Whether one compares our data with the loaded or unloaded data of Landis, the conservation of adrenergic ultrastructure in our co-cultures is apparent. Furthermore, our co-cultures contained pineal cells which, like nonneuronal background cells, have been reported to induce a shift to cholinergic transmitter metabolism in SCG neurons. Rowe and Patt [5] reported that the presence of pineal cells caused an increase in choline acetyltransferase in co-cultured sympathetic neurons. Since they did not attempt to eliminate background cells of either pineal or SCG origin, it is difficult to assess to what extent the cholinergic induction was due to pinealocytes rather than the background cells. In contrast, we found that, although the sympathetic neurons displayed cholinergic electrophysiological activity, they remained histochemically predominantly adrenergic. In addition, in an earlier study we confirmed that the SCG neurons in co-culture release a β-adrenergic agonist which induces a rise in pineal *N*-acetyltransferase.[10]

Our data suggest that the presence of cells from the dissociated pineal glands helps stabilize the population of adrenergic vesicles within co-cultured sympathetic neuron varicosities. The dissociated pineal cells then, may counteract the cholinergic-inducing influence of the other nonneuronal background cells. Whether this requires the production of a diffusable factor or a closer functional contact between neuron and pinealocyte we cannot infer. Perhaps relevant to our results is the recent abstract by Kessler wherein he reported that conditioned medium from pineal cultures influenced the phenotypic expression of peptide synthesis in dissociated SCG neurons. This effect was apparently different from those produced by SCG nonneuronal background cells.

Can sympathetic neurons in culture store and release the two transmitters in different amounts appropriate to the target?

In preliminary studies done on horseradish peroxidase-injected SCG neurons in co-culture with pinealocytes, the glutaraldehyde-fixed vesicle populations appeared different in somal synaptic terminals compared with axonal varicosities overlying nests of pinealocytes. In somal synaptic boutons the vesicles were electron-clear and of uniform size. In the axonal varicosities the vesicles were pleomorphic (W. Shain, A. G. Parfitt, J. E. Freschi and C. L. Rieder, unpublished data). These findings suggested the unusual possibility that the same neuron may shift transmitter synthesis to variable degrees in different terminals depending on the type of target tissue it contacts. Ko *et al.*[7] also reported variability in vesicle phenotype in sympathetic neurons in co-culture with brown fat cells, a target tissue with adrenoreceptors. Vesicles in varicosities near the fat tissue were uniformly large and clear after aldehyde fixation and contained dense cores after $KMnO_4$ fixation. Those in somal boutons, however, were of variable size and density. In the present study we found no statistically significant segregation of vesicle population, but there was more intragroup variation among the somal varicosities than among the very stable axonal varicosities. Thus, it is possible that under some conditions the shift toward cholinergic transmitter metabolism may be greater in those varicosities contacting neuronal somata (acetylcholine receptor target) than in those varicosities overlying nests of pinealocytes (adrenoreceptor target).

Our results do not exclude other explanations for the differences between somal and axonal varicosities. Jaim-Etcheverry and Zieher[5] found that noradrenergic sympathetic terminals in rat pineal glands can take up and store serotonin in the same vesicles that store norephrine. This occurred, however, only when extracellular serotonin concentration was high and when intravesicular norepinephrine was depleted. By using appropriate inhibitors of norepinephrine and serotonin synthesis, this possibility is experimentally testable. Alternatively, the variation among somal histograms might be caused by a subpopulation of cholinergic neurons which make preferential contact with the other neurons because of the presence of acetylcholine receptors. This seems unlikely because all somal and axonal histograms showed the same low percentage of clear vesicles; the difference was between somal varicosities that were predominantly adrenergic in ultrastructure.

Acknowledgements—We are grateful for the assistance and discussions provided by Dr Andrew G. Parfitt. We thank William Jackson for his assistance in the statistical analysis of the data. We thank Guy Bateman for excellent graphics support.

REFERENCES

1. Freschi J. E. (1982) Effect of serum-free medium on growth and differentiation of sympathetic neurons in culture. *Devl Brain Res.* **4,** 455–464.
2. Freschi J. E., Parfitt A. G. and Shain W. G. (1979) Electrophysiology and pharmacology of striated muscle fibres cultured from dissociated neonatal rat pineal glands. *J. Physiol., Lond.* **293,** 1–10.
3. Fukada K. (1980) Hormonal control of neurotransmitter choice in sympathetic neurone cultures. *Nature* **287,** 553–555.
4. Furshpan E. J., MacLeish P. R., O'Lague P. H. and Potter D. D. (1976) Chemical transmission between rat sympathetic neurons and cardiac myocytes developing in microcultures: evidence for cholinergic, adrenergic and dual-function neurons. *Proc. Natn Acad. Sci. U.S.A.* **11,** 4225–4229.
5. Jaime-Etcheverry G. and Zieher L. M. (1974) Localizing serotonin in central and peripheral nerves. In *The Neurosciences: Third Study Program* (eds Schmitt F. O. and Worden F. G.), pp. 917–924. MIT Press, Cambridge, Massachusetts.
6. Johnson M. I., Ross C. D., Meyers M., Spitznagel E. L. and Bunge R. P. (1980) Morphological and biochemical studies on the development of cholinergic properties in cultured sympathetic neurons– I. Correlative changes in choline acetyltransferase and synaptic vesicle cytochemistry. *J. Cell Biol.* **59,** 346–360.
7. Kessler J. A. (1984) Environmental regulation of peptide neurotransmitter phenotypic expression. *Soc. Neurosci. Abst* **10,** 13.
8. Ko C-P., Burton H., Johnson M. I. and Bunge R. P. (1976) Synaptic transmission between rat superior cervical ganglion neurons in dissociated cell culture. *Brain Res.* **117,** 461–485.
9. Landis S. C. (1980) Developmental changes in the neurotransmitter properties of dissociated sympathetic neurons: a cytochemical study of the effects of medium. *Devl Biol.* **77,** 349–361.
10. Parfitt A. G., Freschi J. E., Shain W. G., Schmechel D. E., Auerbach D. A. and Turner J. N. (1982) Pineal cells: culture and co-culture with neurons from the superior cervical ganglia. In *Melatonin Rhythm Generating System* (ed. Klein D. C.), pp. 62–83. Karger, Basel.
11. Patterson P. H. (1978) Environmental determination of autonomic neurotransmitter functions. *Annu. Rev. Neurosci.* **1,** 1–17.
12. Patterson P. H. and Chun L. L. Y. (1977) The induction of acetylcholine synthesis in primary cultures of dissociated rat sympathetic neurons. *Devl Biol.* **56,** 263–280.
13. Potter D. D., Furshpan E. J. and Landis S. C. (1983) Transmitter status in cultured rat sympathetic neurons: plasticity and multiple function. *Fedn Proc.* **42,** 1626–1632.
14. Rowe V. and Parr J. (1980) Pineal cells enhance choline acetyltransferase activity in sympathetic neurons. *J. Neurobiol.* **11,** 547–556.
15. Rowe V. D., Parr J. and Fernandez H. L. (1982) Developmental interaction of pineal target cell and sympathetic neurons in tissue culture. In *Melatonin Rhythm Generating System* (ed. Klein D. C.), pp. 84–96. Karger, Basel.
16. Snedecor G. W. and Cochran W. G. (1980) *Statistical Methods*, pp. 208–210. Iowa University Press, Iowa.
17. Wallicke P. A., Campenot R. B. and Patterson P. H. (1977) Determination of transmitter function by neuronal activity. *Proc. Natn Acad. Sci. U.S.A.* **74,** 5767–5771.
18. Weber M. J. (1981) A diffusible factor responsible for the determination of cholinergic functions in cultured sympathetic neurons: partial purification and characterization. *J. biol. Chem.* **256,** 3447–3453.
19. Wolinsky E. and Patterson P. H. (1983) Tyrosine hydroxylase activity decreases with induction of cholinergic properties in cultured sympathetic neurons. *J. Neurosci.* **1,** 685–690.

(*Accepted* 24 *August* 1985)

Physiology & Behavior, Vol. 36, pp. 1173–1178. Copyright © Pergamon Press Ltd., 1986. Printed in the U.S.A.

0031-9384/86 $3.00 + .00

Angiotensin II-Induced Taste Aversion Learning in Cats and Rats and the Role of the Area Postrema[1]

BERNARD M. RABIN,*†[1] WALTER A. HUNT,* ALEXANDRA C. BAKARICH,‡[2]
ALAN L. CHEDESTER‡[3] AND JACK LEE*

**Behavioral Sciences and ‡Veterinary Medicine Departments*
Armed Forces Radiobiology Research Institute, Bethesda, MD 20814-5145
and †Department of Psychology, University of Maryland Baltimore County, Catonsville, MD 21228

Received 19 August 1985

RABIN, B. M., W. A. HUNT, A. C. BAKARICH, A. L. CHEDESTER AND J. LEE. *Angiotensin II-induced taste aversion learning in cats and rats and the role of the area postrema.* PHYSIOL. BEHAV. 36(6) 1173–1178, 1986.—The capacity of angiotensin II (AII, 1 mg/kg, IP) to produce a taste aversion was studied in cats and rats with and without lesions of the area postrema. Using a one-bottle test, injection of AII produced an aversion in cats but not in rats. Using a two-bottle test, injection of AII produced a slight, but significant, decrease in sucrose preference in intact rats, but had no effect on rats with area postrema lesions. Lesions of the area postrema prevented the acquisition of a taste aversion in cats. These results, which show a clear species difference in the capacity of AII to produce a taste aversion, are discussed as supporting the hypotheses that there is a relationship between the sensitivity of the area postrema to a compound and the capacity of that compound to produce a taste aversion; and that excitation of the area postrema constitutes a sufficient condition for taste aversion learning to occur.

Angiotensin II Conditioned taste aversion Area postrema Cats Rats

A conditioned taste aversion (CTA) is produced when a novel tasting solution is paired with an unconditioned stimulus such as exposure to ionizing radiation [21] or treatment with a variety of toxic and nontoxic compounds, including lithium chloride and amphetamine [9,10]. Previous research has shown that the area postrema (AP), the chemoreceptive trigger zone for emesis [3], mediates the acquisition of a CTA when the unconditioned stimulus is irradiation [14,16] or injection of compounds such as lithium chloride or methylscopolamine [1, 16, 18]. In contrast, the AP is not involved in the acquisition of an amphetamine-induced CTA [1,18]. In this role the AP apparently serves as the transfer point by which information about potential toxins in the blood and cerebrospinal fluid is transmitted to the central nervous system [17].

These studies suggest that the area postrema may be a critical component of the neural system leading to the acquisition of a CTA for one class of unconditioned stimuli, and that any unconditioned stimulus which excites the AP would also lead to CTA learning. The present experiments were designed to test the hypothesis that excitation of the AP constitutes a sufficient condition for the acquisition of a CTA by using injections of angiotensin II (AII) to produce a CTA in cats and rats. Previous research has established that injection of AII produces changes in AP unit activity in cats [4], but has no effect on unit activity in the AP of the rat [5]. Concordant with these electrophysiological studies, other research has shown that the AP mediates the cardiovascular effects of AII in the cat, but not in the rat (e.g., [19]). These studies therefore suggest that the AP of the cat is sensitive to exogenously administered AII while the AP of the rat is not sensitive to exogenous AII. If excitation of the AP is a suffi-

[1]A preliminary report of some of the data was presented at the 14th Meeting of the Society for Neuroscience, Anaheim, CA, 1984. This research was conducted according to the principles described in the "Guide for the Care and Use of Laboratory Animals" prepared by the Institute of Laboratory Animal Research, National Research Council.

[2]Present Address: Naval Ocean Systems Center, San Diego, CA 92152.

[3]Present Address: Walter Reed Army Institute of Research, Washington, DC 20307.

[†]Requests for reprints should be addressed to Bernard M. Rabin, Department of Psychology, University of Maryland Baltimore County, Catonsville, MD 21228.

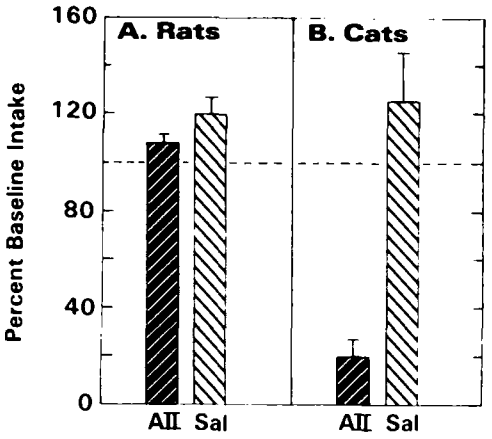

FIG. 1. Effects of injection of AII (1 mg/kg, IP) or saline on sucrose intake in rats (A) and cats (B) using a one-bottle test. Error bars indicate the standard error of the mean.

cient condition for CTA learning, then injection of AII should lead to the acquisition of a CTA in cats but have little or no effect in rats.

EXPERIMENT 1

Subjects

The subjects were 20 male Sprague-Dawley rats weighing 250–350 g, and 18 cats weighing 3.5–5.0 kg at the start of the experiment. All animals were housed in individual cages in a room with a 12:12 light:dark cycle. Food and water were continuously available except as required by the experimental protocol.

Methods

The initial taste aversion procedures for both rats and cats utilized a single-bottle test so that the data would be directly comparable. For the rats, the procedure involved placing them on a 23.5 hr water deprivation schedule for 10 days during which water was available for 30 min a day during the early light phase of the diurnal cycle. On the conditioning day (day 10), the water bottle was replaced by a calibrated tube containing 10% sucrose solution as the conditioned stimulus (CS) and intake measured. Immediately following the drinking period, 10 rats were given a single intraperitoneal injection of 1 mg/kg AII, while the remaining 10 rats were given an injection of an equivalent volume of isotonic saline. On the test day (day 11), the rats were given access to the single calibrated tube containing 10% sucrose and their intake recorded.

For cats, a CTA was produced by removing all food and water 20 hr prior to the conditioning day. On the conditioning day, all cats were given a single dish containing a measured amount of the CS, chocolate milk, and their intake recorded. Immediately following a 1 hr drinking period, 9 cats were given a single injection of AII, 1 mg/kg, IP, and the remaining 9 cats were injected with an equivalent volume of isotonic saline. Four hours after the injection food and water were returned for 24 hr. Food and water were then removed 20 hr prior to testing for the acquisition of a CTA.

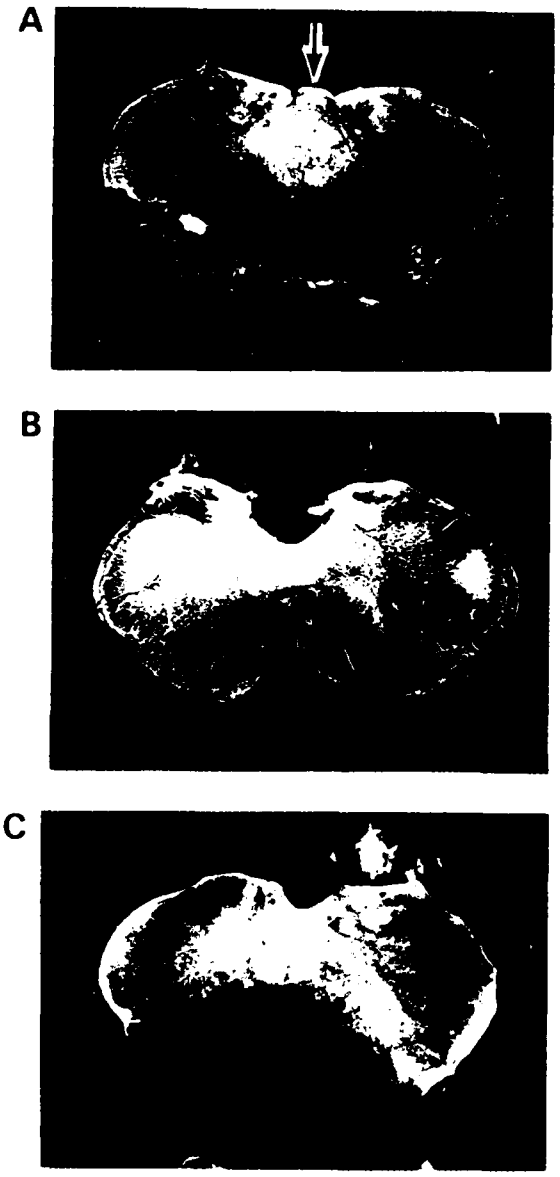

FIG. 2. Photomicrographs of the brainstem of the rat showing the area postrema (A, arrow) and representative lesions (B,C).

Results and Discussion

Test day CS intake is presented as the percentage of the baseline intake on the conditioning day. As shown in Fig. 1, injection of AII did produce a reduction in test day CS intake in cats but did not do so in rats. Analysis of the data using t-tests indicates that there were no significant differences in CS intake between the rats injected with AII and those injected with saline, $t = 1.15$, $p > 0.10$. In contrast, the cats injected with AII showed a significantly reduced CS intake compared to the cats given saline injection, $t = 4.75$, $p < 0.001$.

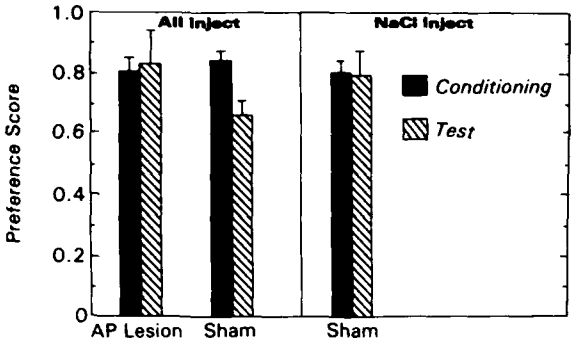

FIG. 3. Effects of AP lesions on sucrose preference in rats using a two-bottle test. The scores to the left of the line were from animals injected with AII; those from the right were injected with saline. Error bars indicate the standard error of the mean.

These results show that a single injection of AII produces a CTA in cats but not in rats. Since the research cited above indicates that the AP of the cat, unlike that of the rat, is responsive to exogenously administered AII, these results suggest that activation of the AP by treatment with a compound is an adequate unconditioned stimulus for the acquisition of a CTA. As such, these results would be consistent with the hypothesis that excitation of the AP constitutes a sufficient condition for CTA learning.

There are, however, several limits on this conclusion. First, because the AP of the rat does contain binding sites for AII [12,20], it may be that the behavioral procedures were not sensitive enough to permit observation of the AII-induced effects. Second, it may be that the AP of the rat, unlike that of the cat, exerts inhibitory effects on this behavior, thereby masking the effects of the AP on behavior. An inhibitory effect of the rat AP has been shown for rotation-induced CTA learning, such that the AP lesions cause an enhanced CTA [15]. A third possibility is that the AII-induced CTA observed in cats is not mediated by the AP but involves a different neural structure. The experiments described below attempted to evaluate these alternative hypotheses.

EXPERIMENT 2

As indicated above, the failure to observe an AII-induced CTA in rats may have resulted from a lack of sensitivity of the behavioral CTA procedures or because the AP exerts an inhibitory effect on the behavior. This experiment was designed to evaluate these hypotheses by using the more sensitive two-bottle procedure [7,11] and by examining the effect of AP lesions on the acquisition of an AII-induced CTA.

Subjects

The subjects were 38 male rats weighing 275–350 g at the start of the experiment.

Methods

The behavioral procedures were identical to those described above, except that a two-bottle test was utilized. On both the conditioning and test days the animals were presented with two calibrated drinking tubes, one containing tap water and the other containing a 10% sucrose solution, and the intake of each recorded. Any rat which did not show a greater sucrose intake than water intake on the conditioning day was discarded from the experiment. This procedure was adopted to assure that all rats had sampled a sufficient quantity of the CS to provide a valid baseline for the observation of a CTA. Five rats with AP lesions and 4 control rats did not meet this criterion and were excluded from the experiment. Given the relatively equal numbers of lesion and control rats which were discarded, it is not likely that this procedure influenced any observed differences between these groups.

Lesions were made in the AP of 15 rats using procedures detailed previously [16,17]. Briefly, the rats were anesthetized with a combination of ketamine (120 mg/kg, IP) and pentobarbital (21 mg/kg, IP), and the AP was exposed and cauterized under direct visual control. An additional 15 rats served as sham-operated controls, in which the AP was exposed but not cauterized. Following surgery, the rats were given a prophylactic injection of Bicillin (60,000 units, IM) and allowed to recover for 2–3 weeks before starting the next phase of the experiment. The remaining 8 rats served as an unoperated saline-injected comparison group.

At the conclusion of the experiment, all operated rats were anesthetized with pentobarbital (50 mg/kg, IP) and perfused with isotonic saline and 10% formalin saline. The brains were fixed in 10% formalin saline and cut through the brainstems at the level of the AP at 50 μm. Photomicrographs of the AP and representative lesions are presented in Fig. 2.

Results and Discussion

Average conditioning day sucrose intake for the sham-operated control rats was 21.53±1.12 ml (mean±standard error) while for the rats with AP lesions it was 25.13±2.18 ml. This difference was not significant, $t=1.47$, $p>0.10$, possibly because of the short drinking period and because water was also available, so that the rats, which typically display neophobia to the presentation of a novel stimulus, were not restricted to drinking the more palatable, but novel, sucrose CS.

The results for the acquisition of a CTA are presented as preference scores, sucrose intake divided by total fluid intake, and summarized in Fig. 3. Injection of AII produced a reduced sucrose preference in sham-operated control rats but had no effect in rats with lesions of the AP. The response to injection of AII of the rats with AP lesions was similar to that of unoperated controls injected with isotonic saline. Analysis of the data for the AII-treated animals using a mixed two-way analysis of variance showed that the main effect for surgery for the comparison between the rats with AP lesions and sham-operated controls was not significant, $F(1,28)=1.32$, $p>0.10$. In contrast, the main effect for the comparison between the conditioning and test days was significant, $F(1,28)=6.28$, $p<0.05$, indicating that there was a significant change in preference score on the test day in response to treatment with AII. The significant surgery by day interaction, $F(1,28)=6.54$, $p<0.05$, would indicate that the rats with AP lesions responded to AII differently than did the control rats.

Histological examination of the brains of the operated rats showed that all rats had complete destruction of the AP. The extent of the lesions ranged from small lesions that were restricted to the AP itself (Fig. 2C) to larger lesions that

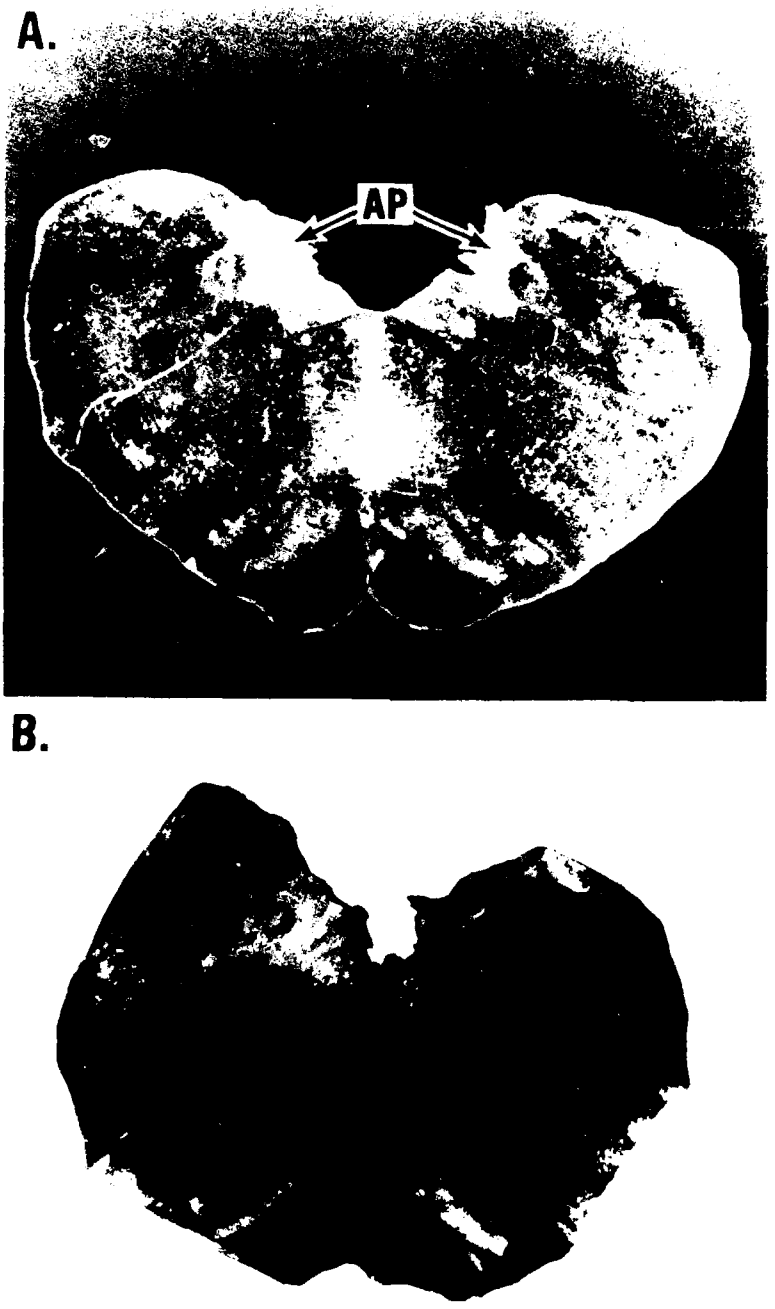

FIG. 4. Photomicrographs of the brainstem of the cat showing the AP (A, arrow) and representative lesions (B).

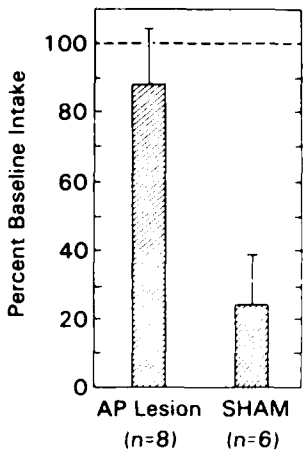

FIG. 5. Effects of injection of AII in cats with lesions of the AP and in sham-operated controls. Error bars indicate the standard error of the mean.

included parts of the nucleus of the solitary tract (Fig. 2B). There was no apparent correlation between the extent of the lesion and the disruption of the AII-induced reduction in sucrose preference.

These results indicate that injection of AII in rats does have a slight, but significant, effect on sucrose preference when the behavioral response utilizes the more sensitive two-bottle procedure. While injection of AII in the rat does not produce an aversion to the CS, in the sense that the rats actively avoided the CS by ingesting more water than sucrose, there was a consistent decrease in sucrose preference across all subjects. An analysis of individual preference scores of the sham-operated rats indicates that while only 3 of the 15 sham-operated rats showed an active aversion to the sucrose, an additional 9 rats showed a decrease in sucrose preference compared to their conditioning day scores. Since this reduction in preference was not observed in rats with AP lesions, the AP must be involved in the acquisition of the response in the intact animal. As such, the present results would be consistent with the observation of AII binding sites in the AP [12,20] and would indicate some limited behavioral responsiveness of the rat AP to exogenously administered AII.

EXPERIMENT 3

As indicated above, the observation of an AII-induced CTA in cats does not necessarily mean that the acquisition of this response is mediated by the AP even though neurons in the AP of the cat are sensitive to exogenously administered AII [4,19]. If the AP of the cat mediates AII-induced CTA learning, it should be possible to disrupt the acquisition of a CTA by producing lesions of the AP.

Subjects

The subjects were 14 cats weighing between 3.2–4.8 kg. They were maintained in individual cages with food and water continually available except as required by the experimental protocol.

Methods

Lesions were made in the AP of 8 cats using the procedures detailed by Borison and his coworkers [2, 22, 23]. Briefly, the cats were anesthetized with halothane and the AP exposed and cauterized under direct visual control. For the control cats, the AP was exposed, but not cauterized. All cats were given a minimum of 2–3 months to recover from the effects of the surgery before beginning the next phase of the experiment. The behavioral testing was identical to that described for Experiment 1, except that for some cats the CS was chocolate milk while for other cats the CS was a 10% sucrose solution. As before, aversions were produced by injections of AII, 1 mg/kg, IP.

At the conclusion of the experiment, the cats were sacrificed with T-61 and perfused intracardially with isotonic saline and 10% formalin saline. Sections were cut through the brainstem at 50 μm at the level of the AP and stained with thionin. Representative photomicrographs are presented in Fig. 4.

Results and Discussion

Average conditioning day CS intake was 74.25 ± 16.33 ml (mean ± standard error) for the cats with AP lesions while the control cats showed an average intake of 47.50 ± 17.01 ml. Although there is the suggestion that cats with AP lesions show increased intake of a palatable CS, as reported for rats using similar procedures [8], the difference in CS intake between control and lesion cats was not significant, $t = 1.19$, $p > 0.10$, probably as a result of the large individual variability.

The results of AP lesions on the acquisition of a CTA are summarized in Fig. 5. Injection of AII in cats with lesions of the AP produced a slight, but nonsignificant, $t = 0.76$, $p > 0.10$, decrease in sucrose intake relative to their conditioning day baseline intake. In contrast, injection of AII in sham operated control cats produced a significant decrease in test day sucrose intake compared to the operated cats, $t = 2.58$, $p < 0.05$. These results, therefore, support the hypothesis that the acquisition of an AII-induced CTA in cats is mediated by the AP.

Histological examination of the brains of the operated cats showed that the lesions tended to be somewhat variable in extent. These ranged from small lesions which were restricted to the AP and which may have left small amounts of AP tissue intact to large lesions which included portions of the nucleus of the solitary tract and the dorsal motor nucleus of the vagus. There was no apparent relationship between the extent of the lesion beyond the AP and the effects of the lesion on behavior since the smallest lesion was sufficient to produce a complete disruption of the AII-induced CTA.

GENERAL DISCUSSION

As indicated above, the AP is a critical component of the neural system leading to the acquisition of a CTA for one class of unconditioned stimuli [1, 14, 16, 17, 18]. As such, it might be predicted that any classes of stimuli that affect the AP would result in the acquisition of a CTA. The results of the present experiments support that prediction.

The AP of the cat is responsive to treatment with exogenous AII, both in terms of its electrophysiological characteristics [4] and in terms of mediating the behavioral responsiveness of the organism [19]. Concordant with this previous research is the present observation that treating cats with

AII produces a CTA which is dependent upon the integrity of the AP. In rats, to the contrary, the AP is not sensitive to exogenously administered AII [5], despite the reported presence of AII binding sites [12,20]. Concordant with these findings is the present observation that that treatment with AII does not produce a reliable CTA in the rat. However, as might be expected given the observation of AII binding sites in the rat AP, injection of AII does cause some reduction in sucrose preference, but only when the more sensitive two-bottle procedure is utilized.

Another possibility, given the observation of AII binding sites in the rat AP [12,20], may be that the physiological response produced by AII in the rat AP is not the response necessary to produce CTA learning. The AP has other functions [6,13] in addition to its role as the chemoreceptive trigger zone for emesis [3]. It is possible, therefore, that the effects of AII on the rat AP may be related to these other functions and not to its role in monitoring the blood and cerebrospinal fluid for potential toxins. However, this interpretation would not be consistent with the observation of a reduction in sucrose preference in control rats tested using a two-bottle procedure. Because of this observation, the present results would be most consistent with the hypothesis that AII exerts qualitatively similar effects on both the rat and the cat AP, but that there are species differences in the sensitivity of the AP to AII which in turn results in the acquisition of a CTA in cats but not in rats.

Overall, the present results which show a clear species difference in the capacity of AII to produce CTA learning in cats and rats, are consistent with the hypothesis of a relationship between the sensitivity of the AP to a given compound and the capacity of that compound to produce a CTA. As such, these results would support the hypothesis that excitation of the AP constitutes a sufficient condition for the acquisition of a CTA.

ACKNOWLEDGEMENTS

We wish to acknowledge the support of the Computer Science Center facilities of the University of Maryland.

REFERENCES

1. Berger, B. D., C. D. Wise and L. Stein. Area postrema damage and bait shyness. *J. Comp Physiol Psychol* **81**: 21–26, 1972.
2. Borison, H. L. Site of emetic action of X-radiation in the cat. *J Comp Neurol* **107**: 439–453, 1957.
3. Borison, H. L. Area postrema: Chemoreceptive trigger zone for vomiting—is that all? *Life Sci* **14**: 1807–1817, 1974.
4. Borison, H. L., M. J. Hawken, J. L. Hubbard and N. E. Sirett. Unit activity from cat area postrema influenced by drugs. *Brain Res* **92**: 153–156, 1975.
5. Brooks, M. J., J. L. Hubbard, and N. E. Sirett. Extracellular recording in rat area postrema in vitro and the effects of cholinergic drugs, serotonin and angiotensin II. *Brain Res* **261**: 85–90, 1983.
6. Contreras, R. J., T. Kosten and E. Bird. Area postrema: Part of the autonomic circuitry of caloric homeostasis. *Fed Proc* **43**: 2966–2968, 1984.
7. Dravoin, W., G. E. McCleary, and P. McCleary. A comparison of two methods of measuring conditioned taste aversions. *Behav Res Meth Instr* **3**: 309–310, 1971.
8. Edwards, G. L., and R. C. Ritter. Ablation of the area postrema causes exaggerated consumption of preferred foods in the rat. *Brain Res* **216**: 265–276, 1981.
9. Garcia, J., W. G. Hankins, and K. W. Rusiniak. Behavioral regulation of the milieu interne in man and rat. *Science* **185**: 824–831, 1974.
10. Goudie, A. J. Aversive stimulus properties of drugs. *Neuropharmacology* **18**: 971–979, 1979.
11. Grote, F. W. and R. T. Brown. Conditioned taste aversions: Two stimulus tests are more sensitive than one-stimulus tests. *Behav Res Meth Instr* **3**: 311–312, 1971.
12. Harding, J. W., L. P. Stone and J. W. Wright. The distribution of angiotensin II binding sites in rodent brain. *Brain Res* **205**: 265–274, 1981.
13. Miselis, R. R., T. M. Hyde and R. E. Shapiro. Area postrema and adjacent solitary nucleus in water and energy balance. *Fed Proc* **43**: 2969–2971, 1984.
14. Ossenkopp, K.-P. Taste aversions conditioned with gamma radiation: attenuation by area postrema lesions in the rat. *Behav Brain Res* **7**: 295–305, 1983.
15. Ossenkopp, K.-P. Area postrema lesions in rats enhance the magnitude of body rotation-induced conditioned taste aversions. *Behav Neural Biol* **38**: 82–96, 1983.
16. Rabin, B. M., W. A. Hunt and J. Lee. Attenuation of radiation- and drug-induced conditioned taste aversions following area postrema lesions in the rat. *Radiat Res* **93**: 388–394, 1983.
17. Rabin, B. M., W. A. Hunt and J. Lee. Recall of a previously acquired conditioned taste aversion in rats following lesions of the area postrema. *Physiol Behav* **32**: 503–506, 1984.
18. Ritter, S., J. L. McGlone and K. W. Kelly. Absence of lithium-induced taste aversion after area postrema lesions. *Brain Res* **201**: 501–506, 1980.
19. Simpson, J. B. The circumventricular organs and the central actions of angiotensin. *Neuroendocrinology* **32**: 248–256, 1981.
20. Sirett, N. E., A. S. McLean, J. J. Bray and J. L. Hubbard. Distribution of angiotensin II receptors in rat brain. *Brain Res* **122**: 299–312, 1977.
21. Smith, J. C. Radiation: Its detection and its effects on taste preferences. In: *Progress in Physiological Psychology* vol 4, edited by E. Stellar and J. M. Sprague. New York: Academic Press, 1971, pp. 73–117.
22. Thron, C. D., J. A. Riancho and H. L. Borison. Lack of protection against ouabain cardiotoxicity after chronic ablation of the area postrema in cats. *Exp Neurol* **85**: 574–583, 1984.
23. Wang, S. C. and H. L. Borison. The vomiting center: A critical experimental analysis. *Arch Neurol Psychiatry* **63**: 928–941, 1950.

Neurobehavioral Toxicology and Teratology, Vol. 8, pp. 83–87, 1986. Ankho International Inc. Printed in the U.S.A. 0275-1380/86 $3.00 + .00

Effects of Area Postrema Lesions on Taste Aversions Produced by Treatment With WR-2721 in the Rat

BERNARD M. RABIN,*†[1] WALTER A. HUNT* AND JACK LEE*

**Behavioral Sciences Department, Armed Forces Radiobiology Research Institute, Bethesda, MD 20814-5145*
†Department of Psychology, University of Maryland Baltimore County, Catonsville, MD 21228

Received 14 January 1984

RABIN, B. M., W. A. HUNT AND J. LEE. *Effects of area postrema lesions on taste aversions produced by treatment with WR-2721 in the rat.* NEUROBEHAV TOXICOL TERATOL 8(1) 83–87, 1986.—The conditioned taste aversion procedure was used to further assess some behavioral effects of treatment with the putative radioprotectant WR-2721 and the role of the area postrema in mediating the behavioral effects of treatment. Treatment with 40, 150 or 300 mg/kg WR-2721 produced dose-dependent changes in sucrose intake in both control rats and rats with area postrema lesions. The effectiveness of the lesion in disrupting the acquisition of an aversion varied as a function of the dose administered, with the lesions producing the greatest disruption of aversion learning at the lowest dose and little disruption at the highest dose tested. At all dose levels, sucrose intake was greater for the rats with area postrema lesions than for the sham-operated control rats. Treatment with WR-2721 also produced significant decreases in total fluid intake, particularly at the higher dose levels. The results are discussed as indicating that treatment with WR 2721 produces highly toxic effects on behavior and that the use of the compound as a radioprotectant for radiotherapy requires additional assessment of its effects on brain function and behavior.

WR-2721 Conditioned taste aversion Area postrema Radioprotection Behavior

USING a variety of physiological endpoints, the compound WR-2721 [S-2-(3-aminopropylamino)ethylphosphorothioic acid] at doses ranging between 200 mg/kg to 400 mg/kg has been reported to provide significant protection against physiological damage caused by exposure to ionizing radiation (e.g., [10, 18, 20, 21]). Despite this, there has been relatively little research on the behavioral effects of treatment with WR-2721. These studies do, however, indicate that the compound is highly toxic, causing a conditioned taste aversion (CTA) in rats [7], and nausea and vomiting in human patients [4,8] at doses of less than 15 mg/kg, well below those required for therapeutic radioprotection. These toxic behavioral side-effects could function to limit the usefulness of WR-2721 as a therapeutic radioprotectant by causing increased behavioral distress in those receiving the compound which could, in turn, result in decreased tolerance to procedures utilizing continued treatment. Behavioral studies of WR-2721 are therefore a necessary component for the evaluation of this compound.

The CTA procedure has been increasingly used as a means of assessing a variety of compounds for potentially toxic effects on behavior (e.g., [1, 9, 12, 14]). A CTA is produced when a normally preferred stimulus, such as saccharin or sucrose, is paired with a toxic unconditioned stimulus, such as lithium chloride or ionizing radiation, resulting in the avoidance of the conditioned stimulus on a subsequent presentation [11].

Using the procedure Cairnie [7] has reported a dose-dependent decrease in saccharin intake in rats following repeated treatment with WR-2721 at doses of 40 mg/kg and 200 mg/kg, but not at 8 mg/kg. Additionally, combining injections of WR-2721 with exposure to non-lethal levels of ionizing radiation produced a stronger CTA than was produced by either treatment alone. These findings suggest that, in terms of its effects on behavior at least, WR-2721 administered prior to radiation exposure provides no protection for the organism, but rather that its use may actually increase the toxic effects of radiation on behavior.

Previous research has shown that destruction of the area postrema (AP), the chemoreceptive trigger zone that functions to monitor the blood and cerebrospinal fluid for toxins [5], can disrupt CTA learning following exposure to ionizing radiation or treatment with toxic chemicals [15, 16, 19]. Lesions of the AP similarly disrupt emetic responses following injection of toxic drugs [3,13], and following exposure to ionizing radiation in monkeys [6]. Because treatment with WR-2721 produces some effects on behavior that are similar to those produced by radiation and by treatment with toxic drugs, and because treatment with WR-2721 has additive effects when combined with irradiation, similar mechanisms involving the AP may mediate the behavioral effects of both radiation and treatment with WR-2721. If WR-2721 does produce CTA learning and emesis by interacting with the AP, this could mean that WR-2721 does not provide behav-

[1]Requests for reprints should be addressed to Bernard M. Rabin, Department of Psychology, University of Maryland Baltimore County, Catonsville, MD 21228.

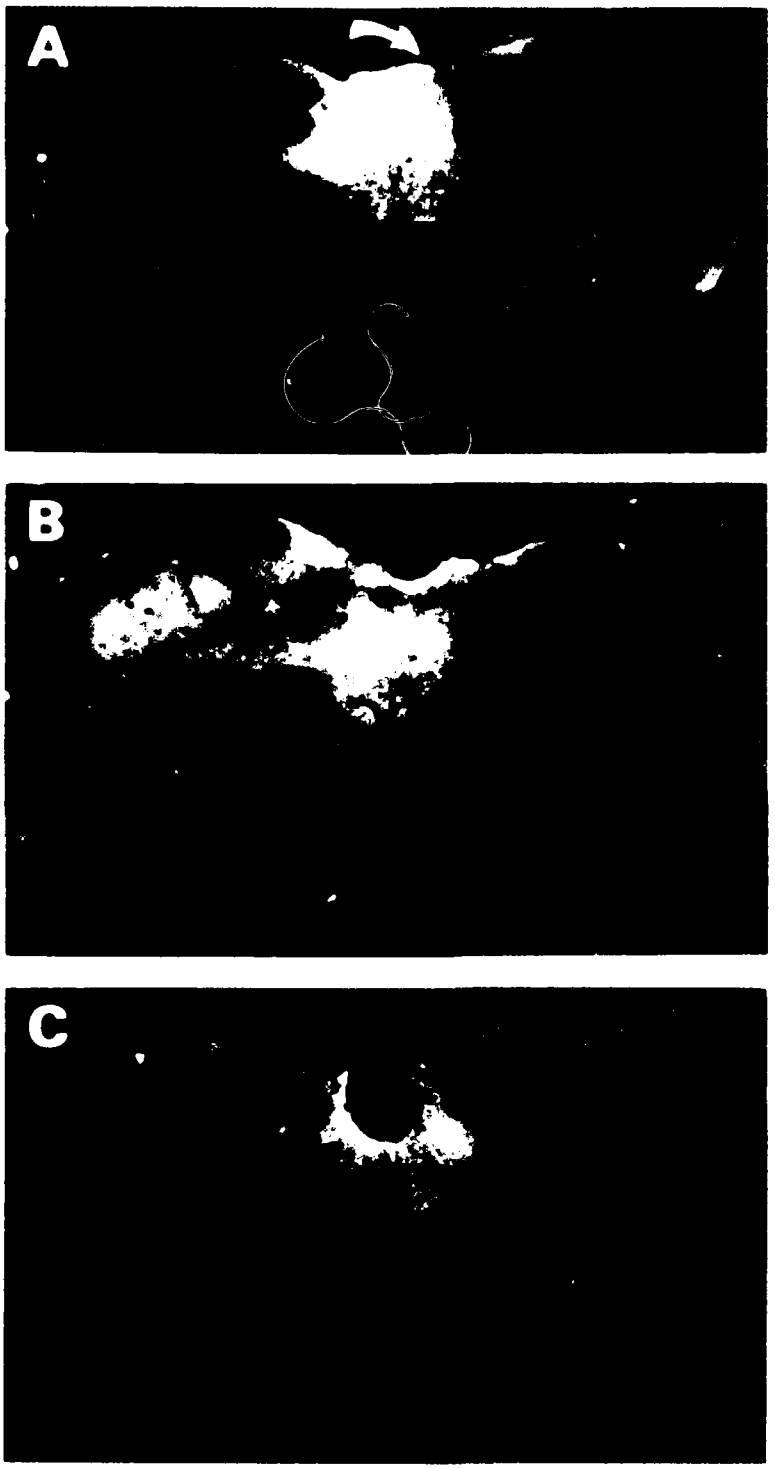

FIG. 1. Representative samples of the brainstem of the rat at the level of the area postrema. A: Section from the brainstem of a sham-operated control showing the area postrema (arrow). B,C: Examples of lesions of the area postrema.

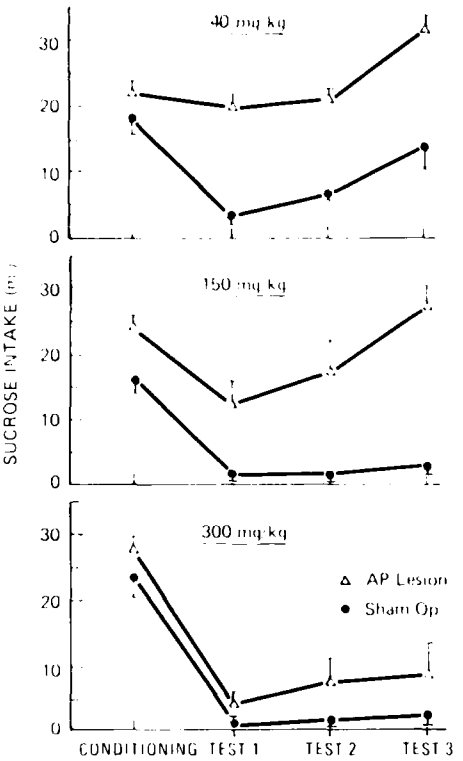

FIG. 2. Effects of treatment with three doses of WR-2721 on sucrose intake of rats with lesions of the area postrema (triangles) and sham-operated controls (circles). A single injection of the drug was administered after ingestion of the sucrose solution on the conditioning day. Variance bars indicate the standard error of the mean.

ioral radioprotection and that treatment with WR-2721 might generally potentiate some of the toxic effects of exposure to ionizing radiation on behavior, thereby limiting its usefulness as a therapeutic radioprotectant. The present experiment, therefore, was designed to evaluate the effects of a single treatment with different doses of WR-2721 on the acquisition of a CTA and to determine whether or not lesions of the AP would ameliorate the toxic effects of the treatment.

METHOD

Subjects

The subjects were 39 male Sprague-Dawley rats, weighing 300–400 g at the start of the experiment. They were housed in individual cages in a room with a 12:12 light:dark cycle. Food and water were continually available except as required by the experimental protocol.

Procedures

Histologically confirmed lesions were placed in the AP of 21 rats using procedures described previously [16]. Briefly, the rats were anesthetized with a combination of sodium pentobarbital (21 mg/kg, IP) and ketamine (120 mg/kg, IP), the brain stem exposed and the AP cauterized under direct visual control. An additional 18 rats in which the AP was exposed, but not cauterized, served as sham-operated controls. After surgery the rats were given a prophylactic injection of bicillin (60,000 units) and allowed to recover for 3–4 weeks.

Following recovery, the rats were placed on a 23.5 hr water deprivation schedule for 10 days during which water was available for 30 min a day during the early light part of the diurnal cycle. On the conditioning day (day 10), the rats were presented with two calibrated drinking tubes, one containing a 10% sucrose solution and the other containing tap water, and the intake of each recorded. Any rat which did not show a greater sucrose intake than water intake was eliminated from the study. Immediately after the drinking period, the rats were given one of three doses of WR-2721: 40 mg/kg, 150 mg/kg or 300 mg/kg administered as a single intraperitoneal injection. Seven rats with AP lesions and 6 control rats received each dose. They were then returned to their home cages for 48 hr. Three test days were run on days 12, 16 and 17 in order to get a measure of the intensity and duration of the WR-2721-elicited response. On the intervening days, the rats were given the standard 30 min access to water.

Histology

At the conclusion of the experiment, the rats were sacrificed with an overdose of pentobarbital (50 mg/kg, IP) and perfused with isotonic saline followed by 10% formalin saline. The brains were removed and fixed in formalin saline. Serial sections were cut through the brainstem at 50 μm and stained with thionin. Figure 1 presents photomicrographs of the brainstem of rats showing the AP and representative lesions.

RESULTS

A single dose of WR-2721 induced a dose-dependent reduction of sucrose intake in both the rats with AP lesions and the control rats (Fig. 2). For the sham-operated controls, a single injection produced significant decreases in sucrose intake at all three dose levels, although some recovery in intake was apparent in the rats given the 40 mg/kg dose by the third test day. AP lesions prevented the WR-2721-induced decrease in sucrose intake only with the rats given 40 mg/kg, the lowest dose tested. At 150 mg/kg there was an initial decrease in sucrose intake which returned to the level of intake observed on the conditioning day by the third test day, while 300 mg/kg of WR-2721 produced a severe decrease in sucrose intake which showed little recovery over the 3 test days.

Statistical analysis of the data using a 3-way analysis of variance with one repeated factor showed that the main effects for the comparisons between the rats with AP lesions and controls, $F(1,33)$ 44.40, $p < 0.001$ for dose, $F(2,33)$ 7.52, $p < 0.01$, and for days, $F(3,99)$ 57.39, $p < 0.001$, were all highly significant. This would indicate that there were consistent significant differences between the control rats and the rats with AP lesions, that the 3 doses of WR-2721 had different effects on behavior, and that there were consistent differences in sucrose intake between the conditioning and test days. In addition, the significant dose by lesion interaction, $F(2,33)$ 3.88, $p < 0.05$, would indicate that the effectiveness of the lesion in disrupting the acquisition of a CTA varied as a function of the dose of WR-2721 that was administered. Similarly, the significant day by dose, $F(6,99)$ 11.15, $p < 0.001$, and day by lesion, $F(3,99)$ 6.80,

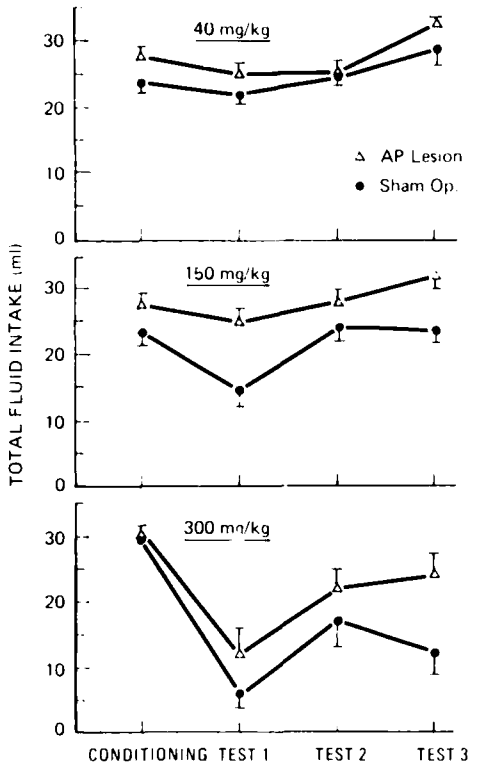

FIG. 3. Effects of treatment with WR-2721 on total fluid intake (sucrose plus water). Variance bars indicate the standard error.

$p < 0.001$, interactions would indicate that both the dose of WR-2721 and the presence of an AP lesion affected the response of the animal to the sucrose solution across the 4 days of the experiment. The triple interaction, $F(6,99) = 2.03$, $p < 0.05$ was not significant.

Figure 3 summarizes the effects of injection of WR-2721 on total fluid intake (water plus sucrose solution). Transient decreases in fluid intake were observed in control rats given either the 40 mg/kg or 150 mg/kg dose of WR-2721, while a more permanent decrease in fluid intake was observed in the rats given 300 mg/kg. Lesions of the AP attenuated this treatment-induced decrease in fluid intake at the lower two doses, but had only a slight protective effect after the highest dose of WR-2721. A comparison of Fig. 3 with Fig. 2 indicates that the decrease in fluid intake resulted from the fact that the animals, particularly at the higher doses, did not compensate for the reduced sucrose solution intake by increasing their intake of tap water to the preconditioning day average of 22.00 ± 0.71 ml. In this regard, it might be noted that 3 control rats that received 300 mg/kg died prior to the second test day without having shown any fluid intake after the conditioning day and had to be excluded from the study. This total lack of fluid intake following treatment with WR-2721 was not observed in any rat having histologically confirmed lesions of the AP.

The statistical analysis of the data on fluid intake using a 3-way analysis of variance with one repeated factor showed that the main effects for dose, $F(2,33) = 8.16$, $p < 0.01$, for lesion, $F(1,33) = 12.48$, $p < 0.01$, and for day, $F(3,99) = 27.94$, $p < 0.001$, were all highly significant, indicating that all three of these factors were consistently involved in determining the fluid intake of the animal following treatment with WR-2721. Unlike the data for sucrose intake, the dose by lesion interaction was not significant, $F(2,33) = 0.41$, $p > 0.10$, indicating that changes in fluid intake were consistently observed in all groups of animals, both control and lesion. The significant day by dose interaction, $F(3,99) = 9.89$, $p < 0.001$ would indicate that the pattern of drinking across days was different for the three tested doses, while the significant day by lesion interaction, $F(3,99) = 3.79$, $p < 0.05$, would indicate that the rats with AP lesions showed a different pattern of fluid intake across days than the sham-operated controls.

DISCUSSION

The results of the present experiment show that a single injection of WR-2721 at doses of 40 mg/kg, 150 mg/kg or 300 mg/kg can consistently produce a CTA in a dose-dependent manner. However, in the intact rats there was no difference between the 150 mg/kg and 300 mg/kg doses because of a floor effect, with both groups showing a nearly total avoidance of the sucrose. As such these results are consistent with the view that WR-2721 is a highly toxic compound that can have a variety of effects on behavior [4, 7, 8].

The effects of treatment with WR-2721 on fluid intake were not predicted. While a transient decrease in total fluid intake below the level of the preconditioning day water intake was first observed in the intact rats treated with 150 mg/kg, a more severe and prolonged decrease in fluid intake was observed in the rats given 300 mg/kg WR-2721. This reduction in fluid intake involved the avoidance of both sucrose solution, the conditioned stimulus, and tap water. Because it is not a novel stimulus, it is extremely difficult to establish a learned aversion to tap water. As such, it is likely that the reduction in fluid intake represents a direct toxic effect of the drug on the mechanisms regulating water intake, perhaps at the level of the kidney. Consistent with this hypothesis is the observation that the kidneys take up and retain the largest amounts of radiolabelled WR-2721 [18].

In contrast to the results with intact rats, the results from the rats with AP lesions were not completely as predicted. While at every dose level rats with AP lesions did show a significantly weaker CTA, it was only at the lowest dose, 40 mg/kg, that the lesions produced the complete disruption of CTA learning that has been observed with treatment with other toxins and with ionizing radiation [15, 16, 19]. At the intermediate dose, 150 mg/kg, the rats acquired a CTA, but showed a rapid extinction of the response, indicating that the AP lesions provided some protection from the toxic effects of the drug. The data from these two doses would be consistent with the hypothesis that the AP plays a role in mediating the toxic behavioral effects of WR-2721 leading to the acquisition of a CTA. It is not certain how the observation of a severe and long-lasting CTA in the rats with AP lesions treated with 300 mg/kg WR-2721 fits into this hypothesis, although the data do indicate that the rats with AP lesions did show a reduced CTA compared to the sham-operated controls. Under normal conditions, the AP functions to limit the intake and/or absorption of toxic substances by initiating either the acquisition of a CTA or an emetic response [17] following ingestion of much smaller quantities of a toxic substance than can be provided under experimental conditions. It may be that the toxicity of this dose of WR-2721 is so great as to completely overwhelm the system that nor-

mally functions to protect the organism. Some data consistent with this hypothesis is provided by the data on fluid intake from the present experiment which showed that the larger doses of WR-2721 produced significant decreases in water intake in addition to the decreased sucrose intake. Also consistent with this interpretation is the observation by Rauschenberger (cited in [2]) who reported that while lesions of the AP disrupted CTA learning to copper sulfate at 5 mg/kg, these lesions were not effective when the dose was increased to 50 mg/kg.

Overall, the present data are consistent with those of Cairnie [7] who reported that repeated treatment with 40 mg/kg and 200 mg/kg WR-2721 resulted in the acquisition of a CTA in rats. As such, the results of the studies using the CTA procedure would be consistent with the limited clinical data which indicates that treatment of human volunteers with doses of WR-2721 of less than 15 mg/kg produces nausea and emesis [4,8]. The present results indicate that the mechanism by which WR-2721 exerts these effects on behavior, at least at low and intermediate doses, involves the mediation of the AP. Since the CTA learning and the emesis seen following exposure to non-lethal levels of ionizing radiation depend upon the integrity of the AP [15,16], the present data indicating that the AP also mediates the toxic effects of WR-2721 on behavior would be consistent with the observation of additive effects when treatment with WR-2721 is combined with exposure to ionizing radiation [7]. The present data would suggest that the additive effects of WR-2721 with ionizing radiation derive from the common involvement of the AP in mediating the behavioral responses following their use. The implication of this finding is that, whatever the radioprotectant effects of WR-2721 on physiological systems within the organism, treatment with WR-2721 prior to exposure to ionizing radiation will not provide protection against the behavioral effects of irradiation, but may instead function to intensify the toxic effects of exposure to ionizing radiation on behavior. While the present results would suggest a limited usefulness for pretreatment with WR-2721 in radiotherapy because of the possible potentiation of behavioral side-effects of the treatment, more neurobehavioral toxicological research is needed, particularly at doses within the therapeutic range of 200 mg/kg to 400 mg/kg, to further assess the toxic effects of WR-2721 on the brain and on behavior.

ACKNOWLEDGMENTS

We wish to acknowledge the support of the Computer Science Center facilities of the University of Maryland, and to thank Col. David E. Davidson, Jr. of the Walter Reed Army Institute for Research for providing the WR-2721. This research was conducted according to the principles described in the "Guide for the Care and Use of Laboratory Animals" prepared by the Institute of Laboratory Animal Research, National Research Council.

REFERENCES

1. Anderson, C. E., H. A. Tilson and O. L. Mitchell. Conditioned taste aversion following acutely administered acrylamide. *Neurobehav. Toxicol. Teratol.* **4**: 497–499, 1982.
2. Ashe, J. H. and M. Nachman. Neural mechanisms in taste aversion learning. In: *Progress in Psychobiology and Physiological Psychology*, vol. 9, edited by J. M. Sprague and A. N. Epstein. New York: Academic Press, 1980, pp. 233–262.
3. Bhargava, K. P. and K. S. Dixit. Role of the chemoreceptive trigger zone in histamine-induced emesis. *Br. J. Pharmacol.* **34**: 508–513, 1968.
4. Blumberg, A. L., D. E. Nelson, M. Gramkowski, D. Glover, J. H. Glick, I. M. Yuhas and M. M. Kligerman. Clinical trials of WR-2721 with radiation therapy. *Int. J. Radiat. Oncol. Biol. Phys.* **8**: 561–563, 1982.
5. Borison, H. L. Area postrema: Chemoreceptive trigger zone for emesis—is that all? *Life Sci.* **14**: 1807–1817, 1974.
6. Brizzee, K. R. Effects of localized brain stem lesions and supradiaphragmatic vagotomy on X-irradiation emesis in the monkey. *Am. J. Physiol.* **187**: 567–570, 1956.
7. Cairnie, A. B. Adverse effects of the radioprotector WR-2721. *Radiat. Res.* **94**: 221–226, 1983.
8. Czerwinski, A. W., A. B. Czerwinski, M. L. Clark and L. L. Whitsett. *A Double Blind Comparison of Placebo and WR 2721 Use in Normal Adult Volunteers*. Report No. MCA-1-33, U.S. Army Medical Research and Development Command, Washington, DC, 1972.
9. Dacanay, R. L., P. Mastropaolo, D. A. Olm and A. L. Riley. Sex differences in taste aversion learning: An analysis of the minimal effective dose. *Neurobehav. Toxicol. Teratol.* **6**: 9–11, 1984.
10. Donaldson, S. S., P. S. Moskowitz, J. W. Evans and E. Equardo. Protection from radiation neuropathy by WR-2721. *Radiat. Res.* **97**: 414–423, 1984.
11. Garcia, J., W. G. Hankins and K. W. Rusniak. Behavioral regulation of the milieu interne in man and rat. *Science* **185**: 824–831, 1974.
12. Kellman, M. J., M. R. Lynch and M. R. Landauer. Taste aversions to several halogenated hydrocarbons. *Neurobehav. Toxicol. Teratol.* **5**: 23–27, 1983.
13. McCarthy, L. E., and H. L. Borison. Cisplatin-induced vomiting eliminated by ablation of the area postrema in cats. *Cancer Treat. Rep.* **68**: 401–404, 1984.
14. Miyagawa, M., T. Honma, M. Sato and H. Hasegawa. Conditioned taste aversion induced by toluene administration in rats. *Neurobehav. Toxicol. Teratol.* **6**: 33–37, 1984.
15. Ossenkopp, K. P. Taste aversions conditioned with gamma radiation: Attenuation by area postrema lesions in rats. *Behav. Brain Res.* **7**: 297–305, 1983.
16. Rabin, B. M., W. A. Hunt and J. Lee. Attenuation of radiation- and drug-induced conditioned taste aversions following area postrema lesions in the rat. *Radiat. Res.* **93**: 388–394, 1983.
17. Rabin, B. M., W. A. Hunt and J. Lee. Recall of a previously acquired conditioned taste aversion in rats following lesions of the area postrema. *Physiol. Behav.* **32**: 503–506, 1984.
18. Rasey, J. S., N. J. Nelson, P. Mahler, K. Anderson, K. A. Krohn and T. Menard. Radioprotection of normal tissues against gamma rays and cyclotron neutrons with WR-2721: LD_{50} studies and ^{35}S-WR-2721 biodistribution. *Radiat. Res.* **97**: 598–607, 1984.
19. Riffer, S., J. F. McGlone and K. W. Kelly. Absence of lithium-induced taste aversion after area postrema lesion. *Brain Res.* **201**: 501–506, 1980.
20. Stewart, F. A. and A. Rojas. Radioprotection of mouse skin by WR-2721 in single and fractionated treatments. *Br. J. Radiol.* **55**: 42–47, 1982.
21. Utley, J. F., C. A. Quinn, E. C. White, N. A. Seaver and C. M. Bloor. Protection of normal tissue against late radiation injury by WR-2721. *Radiat. Res.* **85**: 408–415, 1981.

AFRRI SPECIAL REPORT

DoD nuclear mishaps

H. L. Reese

AFRRI SP86-2

DEFENSE NUCLEAR AGENCY
ARMED FORCES RADIOBIOLOGY RESEARCH INSTITUTE
BETHESDA, MARYLAND 20814-5145

The following information concerning U.S. nuclear weapon accidents has been collected from materials released by the Department of Defense (DoD) in 1977, 1980, and 1981, and also from several media references. This publication is intended to be a source document in the course "Medical Effects of Nuclear Weapons," which is sponsored by the Armed Forces Radiobiology Research Institute.

The United States has never had an inadvertent nuclear detonation, even a partial one, despite the very severe stresses imposed on the weapons that might be involved in accidents. All "detonations" reported in the DoD summaries involved only conventional high explosives. Only two accidents, those at Palomares and Thule, resulted in widespread dispersal of nuclear materials.

Nuclear weapons are never carried on training flights. Most of the aircraft accidents described here occurred during logistic/ferry missions or airborne alert flights by Strategic Air Command (SAC) aircraft. Airborne alert was terminated in 1968 because of

- Accidents, particularly those at Palomares and Thule;
- The rising cost of maintaining a portion of the SAC bomber force constantly on airborne alert;
- The advent of a responsive and survivable intercontinental ballistic missile force, which relieved the manned bomber force of a part of its more time-sensitive responsibilities. (A portion of the SAC force remains on nuclear ground alert.)

Since the location of a nuclear weapon is classified defense information, it is DoD policy, normally, to neither confirm nor deny the presence of a nuclear weapon at any specific location. In the case of an accident involving a nuclear weapon, the weapon's presence may or may not be divulged at the time, depending on the possibility of public hazard or alarm. Therefore, for some of the events summarized in this publication, the presence of a nuclear weapon or material may not have been confirmed at the time. Furthermore, due to diplomatic considerations, it is not possible to specify the locations of the accidents that occurred overseas, except for Palomares and Thule.

Most of the weapon systems involved in these accidents are no longer in the active inventory. Those include the B-29, B-36, B-47, B-50, B-58, C-124, F-100, and P-5M aircrafts and the Minuteman I Missile.

With some early models of nuclear weapons, it was a standard safety procedure during most operations to keep a capsule of nuclear material separate from the weapon. Although a weapon with the capsule removed did contain a quantity of natural (not enriched) uranium with an extremely low level of radioactivity, the accidental detonation of the high-explosive element would not cause a nuclear detonation or contamination. Modern designs incorporate improved safety features, to ensure that a nuclear explosion does not occur as the result of an accident.

MANAGEMENT OF THE NUCLEAR WEAPON STOCKPILE

The management of nuclear weapons is shared by the Department of Energy (DOE) and DoD. The Secretary of Energy and the Secretary of Defense are directly responsible to the President, who retains the sole authority for weapons employment. DOE, as successor of the Atomic Energy Commission, is responsible for all research, development, test, and production of nuclear weapons. DOE is the only Government agency that is authorized by statute to engage in these activities. By law, DOE is required also to control and account for all active nuclear material, including the U.S. stockpile of war-reserve nuclear weapons. These weapons have been entrusted to DoD for employment readiness in case the President orders their use in the interest of national security. Ownership, however, is retained by DOE.

To carry out these responsibilities, the DOE organization includes a network of Government-owned laboratories, plants, and test sites in nine states, all operated by private industry or institutions under Government contract. There are three design and development laboratories, manufacturing facilities, and a field test capability.

At the policy level, DOE's Division of Military Applications (DMA) interfaces with DoD's Military Liaison Committee (MLC). DMA is DOE's primary liaison with DoD, and it provides major program guidance and direction for weapons research and development directly to the weapons laboratories. The Defense Nuclear Agency (DNA) provides some elements of the DoD liaison function with DOE. DNA is a joint service agency under the Joint Chiefs of Staff, with headquarters in Washington, DC, and its operating unit, Field Command, Defense Nuclear Agency, located in Albuquerque, New Mexico.

The MLC Chairman is the Assistant to the Secretary of Defense for Atomic Energy, and is responsible for management and control policies for all nuclear weapon functions within DoD. MLC consists of two senior officers from each Service, with the DNA Director and DOE's DMA Director acting as observers. The DoD nuclear weapon program and requirements are provided to DOE through MLC.

WEAPON SAFETY CONCEPTS

Since DOE designs, develops, and produces all nuclear weapons, it is primarily responsible for the safety features and devices within the weapons. DoD is responsible for safe and secure operations external to the weapon. Considerable overlap and interaction exist, with DoD participating in weapon design (for familiarity and to coordinate requirements) and DOE assisting in the development of safety rules for operating the total nuclear weapon system.

To understand the philosophy of nuclear weapon safety, it is important to first understand the basic nuclear physics involved. Unlike conventional explosives that derive their sensitive properties from their basic chemical makeup, a nuclear device must be specifically designed to bring about an explosion. To obtain a nuclear reaction or explosion through fission, an amount of active material sufficient to produce a continuous, self-sustaining nuclear reaction must be assembled so that a "supercritical mass" can be attained. One technique used to achieve a supercritical mass is called "implosion." In contrast to the outward burst of an explosion, implosion is an inward compression. In a nuclear weapon, high

explosive surrounds the nuclear material. A simultaneous firing of detonators mounted on the surface of the high explosive produces a shock wave that compresses the nuclear material. The important feature is the simultaneous firing of the detonators and control of the shock wave to achieve symmetrical compression of the nuclear material, and thus attain a supercritical mass.

The implosion process used to detonate a nuclear weapon, by its very nature, has a built-in safety feature. If the high explosive detonates at any single point for any reason, including fire or shock as a result of an accident, there would be no symmetrical implosion. The shock wave moving from a single point on the high-explosive surface would explode and destroy the device. This would release and perhaps scatter the active material, but would not result in a nuclear explosion.

In our latest weapons, a new, insensitive high explosive is used, which is extremely stable and will not explode on impact or in a fire. This will dramatically reduce the possibility of nuclear materials being scattered in an accident.

The current DOE safety-design concept packages the weapon-detonation subsystem into an "exclusion region." This feature follows a design philosophy intended to prevent undesired electrical energy from reaching the nuclear weapon detonator system. Included in this concept is a series of "weak links" and "strong links" to obtain predictably safe responses in abnormal environments such as fire, deep water, lightning, cruising impacts, or impact from high-velocity projectiles. The strong links are open switches that close only when the proper signals are received. The weak links are elements vital to the operation of the detonator system. These links are packaged together so that both strong and weak links experience the same environment. Safety is achieved in abnormal environments because the vital components (weak links) are designed to fail first, destroying the detonator system, before the open switches (strong links) can possibly fail to a closed position.

Associated with the exclusion region concept is the design of the strong links to respond only to unique signals. These open switches will not respond to the weapon system's electrical power sources, which might become connected through short circuits during an accident. The unique signals required can be generated by the weapon system only when intended by the human operator.

Nuclear weapons also contain environment-sensing devices that prevent firing of the detonators unless the required environment is experienced. The devices include such items as

- Pullout cables that maintain an open circuit until the cable is physically pulled from the weapon upon release from the aircraft;
- Accelerometers that maintain open circuits until they sense the acceleration or deceleration for a required period of time, as would be produced by a rocket motor or a retarding parachute;
- Barometric switch devices that remain open until they sense the pressure differential that is anticipated in desired release conditions;
- Timers that maintain open switches for a specific time interval after weapon release;

- Electromechanical switches that remain open until a positive action is taken by a human operator.

These safety features and others are designed into the weapon with stringent quality and reliability controls by DoD.

The DoD Safety Program is based on four nuclear safety standards. The standards require that, in the design, development, and employment of a nuclear weapon system, there be positive measures to

- Prevent jettisoned weapons or weapons involved in accidents or incidents from producing a nuclear yield;

- Prevent deliberate prearming, arming, launching, firing, or releasing of nuclear weapons except upon execution of emergency war orders or when directed by competent authority;

- Prevent inadvertent prearming, arming, launching, firing, or releasing of nuclear weapons;

- Ensure adequate security of nuclear weapons.

To satisfy these DoD nuclear safety standards, the Safety Program addresses safety-design engineering for each nuclear weapon system, its logistic and operational environment, and the human factors involved in the maintenance and operation of the weapon system. The various considerations of the program are listed below to give a perspective of their relationships and a feeling for the extent of the Safety Program. The program considerations include

- Requirements and design guidance for safety considerations in nuclear weapon system development;

- Safety engineering evaluation and formal certification before the system can be used with a nuclear weapon;

- Nuclear safety analysis and certification of all computer programs developed for use in the control of the nuclear weapon system;

- Engineering, operational, and logistic studies and reviews of the complete weapon system and its intended environment from storage to target, resulting in weapon system safety rules that prescribe authorized procedures and impose limitations for operation of the nuclear weapon system;

- Approved technical data and maintenance procedures that must be precisely followed in the operation or maintenance of the nuclear weapon system;

- Engineering evaluation and safety certification of all equipment used in the maintenance, movement, and operation of the nuclear weapon system;

- Reporting and analysis of accidents, incidents, and deficiencies that involve the nuclear weapon system, support equipment, and procedures;

- Safing and sealing of critical nuclear weapon system switches;

- Evaluation of all personnel associated with the nuclear weapon system to ensure their emotional stability and proper security clearance before being authorized access to a nuclear weapon, nuclear weapon system, or nuclear command and control facility;

- A "two-man" or "no lone zone" concept around the nuclear weapon and the nuclear weapon system;

- An inspection system to monitor compliance not only with the four DoD safety standards but also with all nuclear safety rules and technical data in all operations involving a nuclear weapon or nuclear weapon system.

In addition to the safety devices contained within the nuclear weapon, the weapon carrier contains devices that prevent prearming or release unless intended. Examples of these devices are

- Dual switches that force two-man consent for both prearm and launch (or release);

- Intent switches that prevent a prearm signal until manually closed by the human operators;

- A unique signal generator, activated by the prearm intent switch, that produces the unique signal required by the weapon's strong links described earlier;

- Intent switches that prevent a nuclear weapon release signal until manually closed by the human operators (separate from the prearm switches);

- Arm-inhibit switches that require a "good guidance" signal from the missile guidance system before warhead arming can occur;

- In-flight reversible mechanical locks on the weapon carriage rack that physically prevent weapon release until electrically activated by the human operators;

- A monitor system to provide the operator the arm/safe status of the nuclear weapon and lock/unlock status of the carriage rack.

Devices such as these prevented weapon arming in the Goldsboro and Palomares accidents. In early bomb racks such as those involved in the accidents at Kirtland Air Force Base, New Mexico, and at Florence, South Carolina, one means to prevent inadvertent release was the insertion of safety pins in the carriage rack. These pins were removed during takeoff and landing to permit emergency jettison. When the safety pins were removed, however, a single failure in the rack could cause an inadvertent release of the nuclear weapon, as shown by these accidents.

A cockpit-controlled, in-flight, reversible lock is now required which, when locked, prevents inadvertent weapon release even though the normal release force is applied. This design allows safe takeoff and landing with the rack in the locked position. The device is designed to fail to the locked position, and also requires an independent positioning of intent switches by two crew members in multiplace aircraft before the rack holding the weapon can be unlocked.

RADIOACTIVE MATERIALS IN NUCLEAR WEAPON ACCIDENTS

Nuclear weapons contain three principal types of radioactive materials: plutonium, uranium, and tritium. Other types of radioactive materials may also be present in lesser and varying amounts, depending on the type and age of the weapon. For accidental contamination, the initial public health risks and protective/corrective actions are the same as those for contamination by particles of plutonium, uranium, and tritium (see below).

The risks to the public from radioactive contamination caused by a nuclear weapon accident are not like fallout from a nuclear bomb blast, and are not like contamination from a major nuclear power plant accident. However, contamination from a nuclear weapon accident could be serious and could require both immediate and long-term protective and corrective cleanup measures. The potential harm to the public and the environment can be controlled best by an effective response to the accident and by providing the public with timely information and instructions about protection from contamination.

Public instructions and appropriate actions will depend on the severity of the accident, the type of material involved, and the length of time between occurrence of the accident and initiation of protective action.

ACCIDENT SEVERITY FACTORS

If nuclear weapons are involved in an accident and the condition of the weapon is not known, the potential for contamination must be assumed. Besides the immediate response around the accident site, protective measures (possible evacuation) for the general public may be necessary within 1 day.

Instructions on basic protective measures should allow time to respond to the accident, to determine the condition of the weapon, and to disseminate supplementary information and instructions to the public.

If damage to a nuclear weapon is known but the weapon is still structurally intact, any potential contamination would be limited to the immediate area of the accident site, and would probably be of very short duration (a few minutes). Keeping the public clear of the accident site and providing information to relieve unwarranted fears (prevent panic) should be sufficient for public protection.

If a nuclear weapon accident results in severe structural damage (scattering of small chunks of the warhead), fire (melting and burning of the warhead), or detonation of the conventional (chemical) high explosive, then more widespread contamination is probable and larger scale protective actions will be necessary. In this case, information and instructions provided to the public will depend on the type of radioactive material and the time since the accident.

PLUTONIUM

Contamination by plutonium particles dispersed by conventional (chemical) explosion or burning of a weapon would pose the most serious health hazard to the public, and could impact the environment over a wide area.

Plutonium is both a poison and a radiation hazard. The radiation given off consists of "alpha particles" (like very fast moving helium atoms), which do not have sufficient energy to penetrate buildings, most clothing, or even the outer skin. Therefore, short-term exposure (up to a few days) to contamination outside of the body will pose only a small health risk.

Plutonium radiation is considered a serious health risk if small "dust-like" pieces are inhaled or ingested and remain as deposits in the body. Even a very small quantity (equivalent to a single piece of dust) inside the body could cause concern as a health risk over the long term. No immediate "radiation sickness" symptoms are expected from this type of contamination.

Unless it is possible to immediately (within minutes) evacuate the area around the accident site and several miles downwind, the best initial public response will probably be to stop outside activity, seek shelter in well-sealed buildings (with little or no use of outside air for heating or cooling), and delay evacuation until the dust cloud has passed and particles have had time to settle out of the air. Besides being medically sound, this procedure will reduce casualties that result from panic and will least affect the critical and essential services.

Any evacuation of the public that does take place must be in a controlled manner, thereby reducing the risk of resuspension of the contaminant and the risk of collateral injury to the civilian population. Any person evacuating an area should breathe through a filter (such as a common dust mask or even several layers of a wet handkerchief), and move with care to avoid stirring up the dust. If resources and time permit, evacuation should include the use of protective outer clothing that can be cleaned for reuse or discarded.

The best direction and timing for travel can be specified for population centers or zones in the area. Factors such as population density, transportation, and facilities in the contaminated area must be considered in deciding whether and when to move the public out of an area.

Whether evacuation is immediate or delayed, panic of the population may result in some injury, death, or property damage. Every effort should be made to state the problem in a way that will inform the public, keep the problem in context, and avoid confusion.

The determination of cleanup requirements and techniques will involve extensive surveys and coordination with experts in several government agencies (Federal Emergency Management Agency, Environmental Protection Agency, DOE, DoD, etc.). Cleanup efforts may extend over several months, and monitoring requirements over several years.

URANIUM

Contamination by uranium fragments or small particles dispersed by a conventional (chemical) explosion or by the burning of a weapon is primarily a chemical health hazard (heavy metal poison similar to the lead poisoning associated with some paints), not a radiological hazard. The short-term risk to health occurs only if a relatively large quantity of uranium is deposited inside the body by inhaling or ingesting the dust. A short-term public hazard from radiation (alpha particles) from uranium is very unlikely. Determination of any long-term radiation (or chemical) hazard will require detailed and extensive surveys.

It is unlikely that uranium contamination, even though dispersed over a wide area, would add significantly to the overall exposure that man normally receives from radioactive materials found in most environments.

TRITIUM

The radiation given off by tritium is a low-energy "beta particle," which is stopped by the outer layers of skin. Thus external exposure is not a hazard. Contamination by tritium gas would pose a health hazard only in a closed or confined space. Tritium released by a weapons accident will dissipate and be diluted so rapidly in open air that no internal hazard would result. Monitoring (air sampling) of the immediate site of the accident is sufficient to assure prevention of exposure to accident-response personnel. Tritium from a weapons accident will not affect the public or the environment.

CLEANUP AFTER A NUCLEAR WEAPON ACCIDENT

An accident that causes a nuclear weapon to structurally break apart, burn, or chemically detonate will contaminate an area of indeterminate size with potentially hazardous materials. These materials may include plutonium, uranium, or high explosive.

The cleanup of explosive and chemical hazards will be relatively straightforward, but the decontamination of any radioactive materials will depend on technically sophisticated surveys and risk assessments.

DETERMINATION OF CONTAMINATION LEVEL

An initial estimate of the size and shape of the contaminated area and of the level of contamination within the area can be provided within a few hours by computer models. This information can be used to determine the actions necessary to protect the public and the scope of the cleanup problem. Then the determination of actual cleanup requirements and preferred techniques will depend on the material involved, field survey measurements of actual contamination levels, and careful assessment of any associated potential health risk.

Cleanup requirements may be minimized if contamination levels are low, or if the contaminating material is trapped and therefore not a hazard to plants, animals, or man. If contamination levels are high and/or the material is a health risk to man, then cleanup requirements may be quite stringent over an extensive area. The cleanup of scattered plutonium would probably present the greatest difficulty.

THE CLEANUP PROCESS

If initial estimates of the contamination level and subsequent field survey measurements indicate radiological contamination in the soil above a screening level of 0.2 microcuries/square meter (or above 1 fCi/m^3), then a careful assessment of health risks is necessary and cleanup may be necessary. Below this screening level, cleanup actions may not be necessary.

SUMMARY OF ACCIDENTS INVOLVING U.S. NUCLEAR WEAPONS, 1950-1980

An "accident involving a nuclear weapon" may be defined as an unexpected event involving a nuclear weapon or nuclear weapon components that results in any of the following:

- Accidental or unauthorized launching, firing, or use by U.S. forces or supported allied forces of a nuclear-capable weapon system that could create the risk of an outbreak of war;
- Nuclear detonation;
- Nonnuclear detonation or burning of a nuclear weapon or radioactive weapon component, including a fully assembled nuclear weapon, an unassembled nuclear weapon, or a radioactive nuclear weapon component;
- Seizure, theft, or loss, including jettison, of a nuclear weapon or radioactive nuclear weapon component;
- Public hazard, actual or implied.

Accidents involving U.S. nuclear weapons from 1950 to 1980 are summarized in the following paragraphs.

1. 13 February 1950 / B-36 / Pacific Ocean, Off Coast of British Columbia

A B-36 aircraft was en route from Eielson AFB to Carswell AFB on a simulated combat profile mission. The weapon aboard the aircraft had a dummy capsule installed. After 6 hours of flight, the aircraft developed serious mechanical difficulties, making it necessary to shut down three engines. The aircraft was at 12,000 feet altitude. Icing conditions complicated the emergency, and level flight could not be maintained. The aircraft headed out over the Pacific Ocean and dropped the weapon from 8,000 feet into the ocean. A bright flash occurred on impact, followed by a sound wave and a shock wave. Only the weapon's high-explosive material detonated. The aircraft was then flown over Princess Royal Island, where the crew bailed out. The aircraft wreckage was later found on Vancouver Island.

2. 11 April 1950 / B-29 / Manzano Base, New Mexico

A B-29 aircraft departed Kirtland AFB at 9:38 p.m. and approximately 3 minutes later crashed into a mountain on Manzano Base, killing the crew. Detonators were installed in the bomb on board the aircraft. The bomb case was

demolished, and some high-explosive material burned in the gasoline fire. Other pieces of unburned high explosive were scattered throughout the wreckage. Four spare detonators in their carrying case were recovered undamaged. Contamination did not occur, and there were no recovery problems. The recovered components of the weapon were returned to the Atomic Energy Commission. The capsule of nuclear material was on board the aircraft but had not been inserted into the weapon for safety reasons. A nuclear detonation was not possible.

3. 13 July 1950 / B-50 / Lebanon, Ohio

A B-50 aircraft was on a training mission from Biggs AFB, Texas, flying at 7,000 feet on a clear day. The aircraft nosed down and flew into the ground, killing 4 officers and 12 airmen. The high-explosive portion of the weapon aboard detonated on impact. There was no nuclear capsule aboard the aircraft.

4. 5 August 1950 / B-29 / Fairfield-Suisun AFB, California

A B-29 carrying a weapon, but no capsule, experienced two runaway propellers and landing-gear-retraction difficulties on takeoff from Fairfield-Suisun AFB (now Travis AFB). The aircraft attempted an emergency landing, crashed, and burned. Fire was fought for 12-15 minutes before the weapon's high-explosive material detonated. Nineteen crew members and rescue personnel, including General Travis, were killed in the crash or the resulting detonation.

5. 10 November 1950 / B-50 / Over Water, Outside the United States

Because of an inflight aircraft emergency, a weapon containing no capsule of nuclear material was jettisoned over water from an altitude of 10,500 feet. A high-explosive detonation was observed.

6. 10 March 1956 / B-47 / Mediterranean Sea

The aircraft was one of a flight of four scheduled for nonstop deployment from MacDill AFB to an overseas air base. The takeoff from MacDill and the first refueling were normal. The second refueling point was over the Mediterranean Sea. In preparation, the flight penetrated solid cloud formation to descend to the refueling level of 14,000 feet. The base of the clouds was 14,500 feet, and visibility was poor. The aircraft never made contact with the tanker. An extensive search failed to locate any trace of the missing aircraft or crew. No weapons were aboard the aircraft, only two capsules of nuclear weapon material in carrying cases. A nuclear detonation was not possible.

7. 27 July 1956 / B-47 / Overseas Base

A B-47 aircraft with no weapons aboard was on a routine training mission and making a touch-and-go landing, when the aircraft suddenly went out of control. It slid off the runway and crashed into a storage igloo containing several nuclear weapons. The bombs did not burn or detonate; they were in storage configuration. No capsules of nuclear materials were in the weapons or present elsewhere in the building. There were no contamination or cleanup problems. The damaged weapons and components were returned to the Atomic Energy Commission.

8. 22 May 1957 / B-36 / Kirtland AFB, New Mexico

The B-36 aircraft was ferrying a weapon from Biggs AFB, Texas, to Kirtland AFB. At 11:50 a.m., MST, as the aircraft approached Kirtland at an altitude of 1,700 feet, the weapon dropped from the bomb bay, taking the bomb bay doors with it. Weapon parachutes were deployed but apparently did not fully retard the fall because of the low altitude. The impact point was approximately 4.5 miles south of the Kirtland control tower and .3 mile west of the Sandia Base reservation. The high-explosive material detonated, completely destroying the weapon, and making a crater approximately 25 feet in diameter and 12 feet deep. Fragments and debris were scattered as far as 1 mile from the impact point. The release-mechanism locking pin was being removed at the time of release. (It was standard procedure, at that time, to remove the locking pin during takeoff and landing, to allow emergency jettison of the weapon if necessary.) The recovery and cleanup operations were conducted by Field Command, Armed Forces Special Weapons Project. Radiological survey of the area disclosed no radioactivity beyond the lip of the crater, at which point the level was 0.5 milliroentgens. There were no health or safety problems. A nuclear capsule was on board the aircraft but had not been inserted into the weapon for safety reasons. A nuclear detonation was not possible.

9. 28 July 1957 / C-124 / Atlantic Ocean

Two weapons were jettisoned from a C-124 aircraft off the east coast of the United States. The C-124 aircraft was en route from Dover AFB, Delaware, when a loss of power from the number one and number two engines was experienced. Maximum power was applied to the remaining engines, but level flight could not be maintained. At this point, the decision was made to jettison cargo in the interest of safety of the crew and aircraft. Three weapons and one nuclear capsule were aboard the aircraft, and nuclear components had not been installed in the weapons. The first weapon was jettisoned at 4,500 feet altitude. The second weapon was jettisoned at approximately 2,500 feet altitude. No detonation occurred from either weapon. Both weapons are presumed to have been damaged from impact with the ocean surface, and to have submerged almost instantly. The ocean varies in depth in the area of the jettisons. The C-124 landed at an airfield in the vicinity of Atlantic City, New Jersey, with the remaining weapon and the nuclear capsule aboard. A search for the weapons or debris had negative results.

10. 11 October 1957 / B-47 / Homestead AFB, Florida

The B-47 departed Homestead AFB shortly after midnight on a deployment mission. Shortly after lift-off, one of the aircraft's outrigger tires exploded. The aircraft crashed in an uninhabited area approximately 3,800 feet from the end of the runway. The aircraft was carrying one weapon in ferry configuration in the bomb bay and one nuclear capsule in a carrying case in the crew compartment. The weapon was enveloped in flames, and it burned and smoldered for approximately 4 hours, at which time it was cooled with water. Two low-order high-explosive detonations occurred during the burning. The nuclear capsule and its carrying case were recovered intact and only slightly damaged by heat. Approximately one half of the weapon remained. All major components were damaged but were identifiable and accounted for.

11. 31 January 1958 / B-47 / Overseas Base

A B-47 with one weapon in strike configuration was making a simulated takeoff during an exercise alert. When the aircraft reached approximately 30 knots on the runway, the left rear wheel casting failed. The tail struck the runway, and a fuel tank ruptured. The aircraft caught fire and burned for 7 hours. Firemen fought the fire for the allotted 10-minute fire-fighting time for the high-explosive contents of that weapon, and then evacuated the area. The high explosive did not detonate, but some contamination did occur in the immediate area of the crash. No contamination was detected after removal of the wreckage and the asphalt beneath it and after washing down of the runway. One fire truck and one fireman's clothing showed slight alpha contamination before washing. Following the accident, exercise alerts were temporarily suspended and B-47 wheels were checked for defects.

12. 5 February 1958 / B-47 / Savannah River, Georgia

The B-47 was on a simulated combat mission that originated at Homestead AFB, Florida. While near Savannah, Georgia, the B-47 had a mid-air collision with an F-86 aircraft at 3:30 a.m. Following the collision, the B-47, with a weapon aboard, attempted to land three times at Hunter AFB, Georgia. Because of the condition of the aircraft, its airspeed could not be reduced enough to ensure a safe landing. Therefore, the decision was made to jettison the weapon rather than expose Hunter AFB to the possibility of a high-explosive detonation. A nuclear detonation was not possible since the nuclear capsule was not aboard the aircraft. The weapon was jettisoned into the water several miles from the mouth of the Savannah River (Georgia) in Wassaw Sound off Tybee Beach. The precise impact point of the weapon is unknown. The weapon was dropped from an altitude of approximately 7,200 feet at an aircraft speed of 180-190 knots. No detonation occurred. After jettison, the B-47 landed safely. A 3-square-mile area was searched by divers and underwater demolition team technicians using galvanic drag and hand-held sonar devices. The weapon was not found. The search was terminated on 16 April 1958. The weapon was considered to be irretrievably lost.

13. 11 March 1958 / B-47 / Florence, South Carolina

At 3:53 p.m., EST, a B-47E departed Hunter AFB, Georgia, as number three aircraft in a flight of four en route to an overseas base. After level off at 15,000 feet, the aircraft accidentally jettisoned an unarmed nuclear weapon that impacted in a sparsely populated area 6.5 miles east of Florence, South Carolina. The bomb's high-explosive material exploded on impact. The detonation caused property damage and several injuries on the ground. The aircraft returned to the base without further incident. No capsule of nuclear materials was aboard the B-47 or installed in the weapon.

14. 4 November 1958 / B-47 / Dyess AFB, Texas

A B-47 caught fire on takeoff. Three crew members successfully ejected; one was killed when the aircraft crashed from an altitude of 1,500 feet. One nuclear weapon was on board when the aircraft crashed. The resultant detonation of the high explosive made a crater 35 feet in diameter and 6 feet deep. Nuclear materials were recovered near the crash site.

15. 26 November 1958 / B-47 / Chennault AFB, Louisiana

A B-47 caught fire on the ground. The single nuclear weapon on board was destroyed by the fire. Contamination was limited to the immediate vicinity of the weapon residue within the aircraft wreckage.

16. 18 January 1959 / F-100 / Pacific Base

The aircraft was parked on a revetted hardstand in ground alter configuration. The external load consisted of a weapon on the left intermediate station and three fuel tanks (both inboard stations and the right intermediate station). When the starter button was depressed during a practice alter, an explosion and fire occurred when the external fuel tanks inadvertently jettisoned. Fire trucks at the scene put out the fire in about 7 minutes. The capsule was not in the vicinity of the aircraft and was not involved in the accident. There were no contamination or cleanup problems.

17. 6 July 1959 / C-124 / Barksdale AFB, Louisiana

A C-124 on a nuclear logistics movement mission crashed on takeoff. The aircraft was destroyed by fire, which also destroyed one weapon. No nuclear or high-explosive detonation occurred; safety devices had functioned as designed. Limited contamination was present over a very small area immediately below the destroyed weapon. This contamination did not hamper rescue or fire-fighting operations.

18. 25 September 1959 / P-5M / Pacific Ocean Off the Washington Coast

A U.S. Navy P-5M aircraft assigned to Naval Air Station, Whidbey Island, Washington, crashed in the Pacific Ocean about 100 miles west of the Washington-Oregon border. It was carrying an unarmed nuclear antisubmarine weapon containing no nuclear material. The weapon was not recovered.

19. 15 October 1959 / B-52 / KC-135 / Hardinsburg, Kentucky

The B-52 departed Columbus AFB, Mississippi, at 2:00 p.m., CST. The aircraft assumed the number two position in a flight of two. The KC-135 departed Columbus AFB at 5:33 p.m., CST, as the number two tanker aircraft in a flight of two scheduled to refuel the B-52's. Rendezvous for refueling was accomplished in the vicinity of Hardinsburg, Kentucky, at 32,000 feet. It was night; the weather was clear, with no turbulence. Shortly after the B-52 began refueling from the KC-135, the two aircraft collided. The instructor pilot and pilot of the B-52 ejected, followed by the electronic warfare officer and the radar navigator. The copilot, navigator, instructor navigator, and tail gunner failed to leave the B-52. All four crew members in the KC-135 were fatally injured. The B-52's two unarmed nuclear weapons were recovered intact. One had been partially burned, but did not result in dispersion of nuclear material or other contamination.

20. 7 June 1960 / BOMARC / McGuire AFB, New Jersey

A BOMARC air defense missile in ready storage condition (permitting launch in 2 minutes) was destroyed by explosion and fire after a high-pressure helium tank exploded and ruptured the missile's fuel tanks. The warhead was also destroyed by

the fire, although the high explosive did not detonate. Nuclear safety devices functioned as designed. Contamination was restricted to an area immediately beneath the weapon and an adjacent elongated area approximately 100 feet long, caused by drain-off of fire-fighting water.

21. 24 January 1961 / B-52 / Goldsboro, North Carolina

During a B-52 airborne alert mission, structural failure of the right wing resulted in two weapons separating from the aircraft during aircraft breakup at 2,000-10,000 feet. One bomb parachute deployed, and the weapon received little impact damage. The other bomb fell free and broke apart upon impact. No explosion occurred. Five of the eight crew members survived. A portion of one weapon, containing uranium, could not be recovered despite excavation in the waterlogged farmland to a depth of 50 feet. The Air Force subsequently purchased an easement requiring permission for anyone to dig there. No detectable radiation and no hazard exist in the area.

22. 14 March 1961 / B-52 / Yuba City, California

A B-52 experienced failure of the crew compartment pressurization system, forcing descent to 10,000 feet altitude. Increased fuel consumption caused fuel exhaustion before rendezvous with a tanker aircraft. The crew bailed out at 10,000 feet except for the aircraft commander, who stayed with the aircraft to 4,000 feet and steered the plane away from a populated area. The two nuclear weapons on board were torn from the aircraft on ground impact. The high explosive did not detonate. Safety devices worked as designed to prevent nuclear contamination.

23. 13 November 1963 / Atomic Energy Commission Storage Igloo / Medina Base, Texas

An explosion involving 123,000 pounds of high-explosive components of nuclear weapons caused minor injuries to three Atomic Energy Commission employees. There was little contamination from the nuclear components, which were stored elsewhere in the building. The components were from the disassembly of obsolete weapons.

24. 13 January 1964 / B-52 / Cumberland, Maryland

A B-52D was en route from Westover AFB, Massachusetts, to its home base at Turner AFB, Georgia. The crash occurred approximately 17 miles southwest of Cumberland, Maryland. The aircraft was carrying two weapons, which were in a tactical ferry configuration (no mechanical or electrical connections had been made to the aircraft, and the safing switches were in the "SAFE" position). Before the crash, the pilot had requested a change of altitude because of severe air turbulence at 29,500 feet. The aircraft was cleared to climb to 33,000 feet. During the climb, the aircraft encountered violent air turbulence, and aircraft structural failure then occurred. Of the five air-crew members, only the pilot and copilot survived. The gunner and navigator ejected, but died of exposure to subzero temperatures after successfully reaching the ground. The radar navigator did not eject and died upon aircraft impact. The crash site was an isolated mountainous and wooded area. The 14 inches of new snow covered the aircraft wreckage, which was scattered over an area of approximately 100 square yards. The weather during the recovery and cleanup operation involved extreme cold and

gusty winds. Both weapons remained in the aircraft until it crashed, and were relatively intact in the approximate center of the wreckage area.

25. 5 December 1964 / LGM 30B (Minuteman ICBM) / Ellsworth AFB, South Dakota

The LGM 30B Minuteman I missile was on strategic alert at Launch Facility L-02, Ellsworth AFB, South Dakota. Two airmen were dispatched to the Launch Facility to repair the inner zone security system. In the midst of their checkout of the inner zone system, one retrorocket in the spacer below the Reentry Vehicle (RV) fired, causing the RV to fall about 75 feet to the floor of the silo. When the RV struck the bottom of the silo, the arming and fusing/altitude control subsystem containing the batteries was torn loose, thus removing all sources of power from the RV. The RV structure received considerable damage. All safety devices operated properly in that they did not sense the proper sequence of events to allow arming the warhead. There was no detonation or radioactive contamination.

26. 8 December 1964 / B-58 / Bunker Hill (now Grissom) AFB, Indiana

SAC aircraft were taxiing during an exercise alert. As one B-58 reached a position directly behind the aircraft on the runway ahead of it, the aircraft ahead brought advanced power. As a result of the combination of the jet blast from the aircraft ahead, the icy runway surface conditions, and the power applied to the aircraft while attempting to turn onto the runway, control was lost and the aircraft slid off the left side of the taxiway. The left main landing gear passed over a flush-mounted taxiway light fixture, and 10 feet farther along in its travel, grazed the left edge of a concrete light base. After another 10 feet, the left main landing gear struck a concrete electrical manhole box, and the aircraft caught on fire. When the aircraft came to rest, all three crew members aboard abandoned the aircraft. The aircraft commander and defensive systems operator egressed with only minor injuries. The navigator ejected in his escape capsule, which impacted 548 feet from the aircraft. He did not survive. Portions of the nuclear weapon on board burned. Contamination was limited to the immediate area of the crash and was subsequently removed.

27. 11 October 1965 / C-124 / Wright-Patterson AFB, Ohio

The C-124 aircraft was being refueled in preparation for a routine logistics mission when a fire occurred at the aft end of the refueling trailer. The fuselage of the aircraft, containing only components of nuclear weapons and a dummy training unit, was destroyed by the fire. There were no casualties. The resultant radiation hazard was minimal. Minor contamination was found on the aircraft, cargo, and clothing of explosive ordnance disposal and fire-fighting personnel, and was removed by normal cleaning.

28. 5 December 1965 / A-4 / Pacific Ocean

An A-4 aircraft loaded with one nuclear weapon rolled off the elevator of a U.S. aircraft carrier and fell into the sea. The pilot, aircraft, and weapon were lost. The incident occurred more than 500 miles from land.

29. 17 January 1966 / B-52 / KC-135 / Palomares, Spain

The B-52 and the KC-135 collided during a routine high-altitude-air refueling operation. Both aircraft crashed near Palomares, Spain. Four of the eleven crew members survived. The B-52 carried four nuclear weapons. One was recovered on the ground, and one was recovered from the sea on 7 April after extensive search and recovery efforts. Two of the weapons' high-explosive materials exploded on impact with the ground, releasing some radioactive materials. Approximately 1400 tons of slightly contaminated soil and vegetation were removed to the United States for storage at an approved site. Representatives of the Spanish Government monitored the cleanup operation.

30. 21 January 1968 / B-52 / Thule, Greenland

A B-52 from Plattsburgh AFB, New York, crashed and burned approximately 7 miles southwest of the runway at Thule AB, Greenland, while approaching the base to land. Six of the seven crew members survived. The bomber carried four nuclear weapons, all of which were destroyed by fire. Some radioactive contamination occurred in the area of the crash, which was on the sea ice. Some 237,000 cubic feet of contaminated ice, snow, water, and crash debris were removed to an approved storage site in the United States over the course of a 4-month operation. Although an unknown amount of contamination was dispersed by the crash, environmental sampling showed normal readings in the area after the cleanup was completed. Representatives of the Danish Government monitored the cleanup operations.

31. Spring 1968 / Atlantic Ocean

Details remain classified.

32. 19 September 1980 / Titan II ICBM / Damascus, Arkansas

During routine maintenance in a Titan II silo, an Air Force repairman dropped a heavy wrench socket, which rolled off a work platform and fell toward the bottom of the silo. The socket bounced and struck the missile, causing a leak from a pressurized fuel tank. The missile complex and the surrounding area were evacuated, and a team of specialists was called in from Little Rock AFB, the missile's main support base. About 8.5 hours after the initial puncture, fuel vapors within the silo ignited and exploded. The explosion fatally injured one member of the team. Twenty-one other USAF personnel were injured. The missile's reentry vehicle, which contained a nuclear warhead, was recovered intact. There was no radioactive contamination.

NOTE: The events outlined here involved operational weapons, nuclear materials, aircraft, and/or missiles under control of the U.S. Air Force, U.S. Navy, or the Atomic Energy Commission (the DOE predecessor agency). The U.S. Army has never experienced an event classified as an accident involving nuclear weapons. The U.S. Marine Corps does not have custody of nuclear weapons in peacetime, and has not experienced an accident involving them.

AFRRI — TECHNICAL REPORT

AFRRI TR86-1

The TRIGA Reactor Facility at the Armed Forces Radiobiology Research Institute: A simplified technical description

M. L. Moore and S. Elsasser

DEFENSE NUCLEAR AGENCY
ARMED FORCES RADIOBIOLOGY RESEARCH INSTITUTE
BETHESDA, MARYLAND 20814-5145

REVIEWED AND APPROVED

GARY H. ZEMAN
CDR, MSC, USN
Chairman
Radiation Sciences Department

LAWRENCE S. MYERS, Ph.D.
Scientific Director

JAMES J. CONKLIN
Colonel, USAF, MC
Director

CONTENTS

The mission of the Armed Forces Radiobiology Research Institute (AFRRI) is to conduct research in the field of radiobiology and related matters that is essential to the operation and medical support of the Department of Defense and the Military Services. In support of that mission, AFRRI operates a medium-sized research nuclear reactor. The reactor is used to generate radiations, primarily neutrons and gamma rays, which are used to conduct experimental biomedical research and to produce isotopes. The radiations are delivered to the experiments in one of two ways: A pulse operation delivers a very short burst of high power, or a steady-state operation delivers a longer, continuous low- to medium-power exposure. The reactor is also used to train military personnel in reactor operations.

The AFRRI TRIGA Mark-F reactor facility is within the AFRRI complex on the grounds of the Naval Medical Command National Capital Region, in Bethesda, Maryland. TRIGA is an acronym for Training, Research, and Isotope, General Atomics. Mark-F is the specific General Atomics Reactor model, distinguished by a pool, a movable core, exposure room facilities, and the ability to pulse to momentary high powers. A cutaway view of the AFRRI reactor is shown in Figure 1.

Reactor operations at AFRRI began in 1962. In 1965, a change was made from aluminum-clad to stainless steel-clad fuel elements. Currently more than 150 multiple-exposure experiments are performed each year using the reactor.

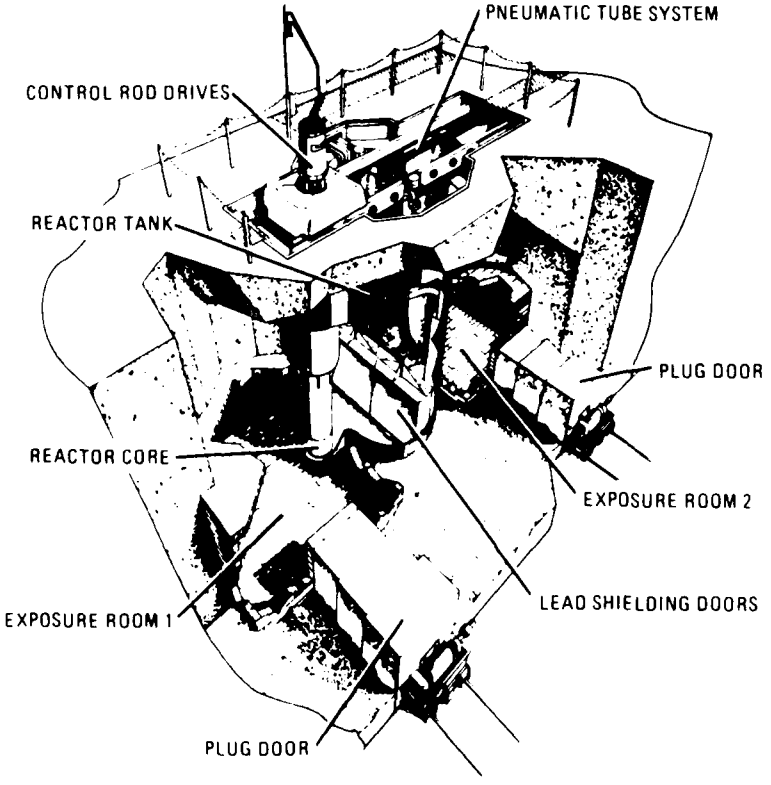

Figure 1. Cutaway view of AFRRI TRIGA reactor

PRINCIPLES OF REACTOR OPERATION

The process of splitting the nucleus of a heavy atom is called fission. Certain elements are ideal for fission because their nucleus splits easily upon absorption of low-energy neutrons. Uranium-235 is such an element, and it is used as fuel in the AFRRI reactor as well as commercial power reactors. When a neutron enters the nucleus of a uranium-235 atom, it disrupts the stability of the nucleus and causes the nucleus to split, generally into two fragments. As fission occurs, neutron, beta, and gamma radiations are emitted, along with other photons and particles. After slowing down in energy, some of the neutrons that result from the fission will enter the nuclei of additional uranium-235 atoms and cause further fissions. If allowed to continue, the resulting series of fissions is called a chain reaction (see Figure 2). The fragments resulting from the fission process have large amounts of kinetic energy, and that energy is transferred to the surrounding medium in the form of heat energy.

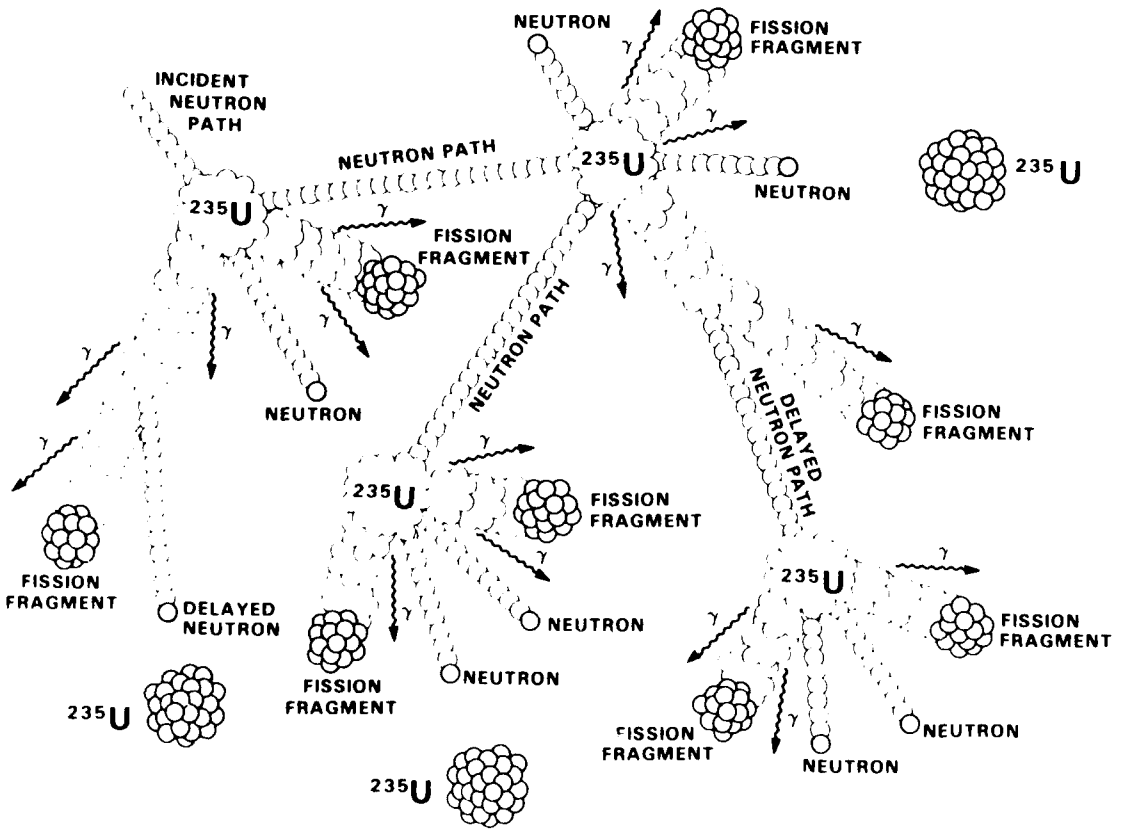

Figure 2. Nuclear fission chain reaction

THE AFRRI REACTOR VERSUS A POWER REACTOR

The AFRRI reactor, classified as a 1-megawatt research reactor, differs from a power reactor in purpose and usage. The AFRRI reactor serves as a source of radiation, mainly neutrons and gammas, for research purposes. The heat energy produced by the fission process is not of concern at AFRRI, because the nominal amounts of heat produced by the AFRRI reactor are dissipated in its cooling system. In contrast, power reactors depend on the heat produced, and channel the heat resulting from fission into steam turbines, which then turn generators to produce power. Conversely, the radiation produced in a power reactor is an unwanted by-product, and must be appropriately controlled. The relative amounts of heat and radiation produced by the AFRRI reactor and a power reactor may be compared in terms of power levels of operation. The AFRRI reactor operates at a maximum of 1 megawatt (thermal), while a power reactor typically operates at power levels of 1000 megawatts electrical or about 3000 megawatts thermal. Power reactors, as all reactors, directly produce thermal power, which is then converted into electrical power at about 30 percent efficiency.

MODES OF OPERATION

The power levels of a reactor directly correspond to the rate at which fission occurs. In turn, the rate of fission is governed by the size of the neutron population in the core (Figure 1). As the neutron source perpetually emits neutrons, and as prompt and delayed neutrons are constantly produced from fission, new neutron generations continually occur in the reactor core. The reactivity of the core is described in terms of criticality; that is, when the number of neutrons from generation to generation is constant, the reactor is said to be critical. When the neutron population is decreasing, the reactor is said to be subcritical. When the neutron population is increasing, the reactor is said to be supercritical.

The AFRRI reactor is licensed to operate in a variety of power levels, which are characterized by two modes: steady-state mode and pulse mode. Each of these operational modes is accompanied by particular power levels and individual configurations of control rods (the transient rod, safe rod, shim rod, and regulating rod). Each mode simulates a general type of radioactive occurrence or dose delivery to the experiment, described as follows.

STEADY-STATE MODE

The steady-state mode is characterized by low levels of power, up to 1 megawatt, which occur for a designated length of time, from several seconds to hours. The reactor may be automatically set to shut down after a particular amount of time, or it may be manually shut down after achieving a desired radiation dose in an exposure facility. In the steady-state mode, the reactor is brought to a specific power, and is then controlled to run constantly at that power until shut down. The reactor is brought to power by first partially withdrawing the transient rod, then partially withdrawing the safe rod and shim rod, and finally withdrawing the regulating rod a sufficient amount to produce the power sought. Depending on the position of the core, the rod heights may be adjusted so that the majority of the radiation is thrown in a particular direction. The steady-state mode simulates a relatively low-level, long-term exposure to radioactivity.

PULSE MODE

The pulse mode is characterized by a rapid rise in power, up to 3000 megawatts. In order to be able to pulse the reactor, or bring the power to momentary high levels, the reactor must first be brought to criticality at a low level of power. In order to accomplish this, the safe rod and shim rod are usually completely withdrawn and the regulating rod is partially withdrawn so that the reactor will be steady at the desired power. Following this, calculations are made of the rod drive position for the required pulse value, and the anvil (part of the rod drive that limits upward movements) is raised to the appropriate height. The transient rod is then fired, driven by compressed air. The transient rod hits the anvil, and the anvil drops down by the force of gravity. This is followed automatically by shutdown of the reactor. The entire process takes place in less than 500 milliseconds, and results in a short burst of high-level radiation.

THE AFRRI REACTOR

REACTOR CORE

The core (see Figure 1) is the heart of a reactor. The core is composed primarily of fuel elements (containing the uranium fuel), a neutron source, and neutron-absorbing control rods. The core is the site of fission, which produces the radiation sought by research investigators. The AFRRI reactor is equipped with a movable core. The core is suspended under 16 feet of water from a dolly just above the reactor pool. Movement of the core dolly along the track from one side of the pool to the other is controlled from the reactor console. Approximately 5 minutes are required to move the core from one side of the pool to the other, a distance of 13 feet.

Located next to the base of the tank pool (two floors below the control room) are two exposure rooms (Figure 1). Exposure rooms are dry exposure areas into which experiments are placed. One is located at each end of a pool shaped like a cloverleaf. The advantages to having a movable core are that (a) the quantity and character of the radiation reaching these exposure facilities may be controlled, and (b) more than one exposure facility may be used at the same time. The primary types of radiation produced by the AFRRI reactor are neutron and gamma. The ratio of neutron radiation to gamma radiation may be controlled by movement of the core and by shielding. In order for personnel to enter an exposure room to set up or change experiments, the core is moved to the opposite side of the pool. The lead shield doors are then closed for additional shielding.

The core support structure provides a means to suspend the reactor core. The core housing structure encloses the control rod drives (Figure 1), which are gear systems to lower or withdraw the control rods into or from the core. Connecting rods connect the rod drives to the actual control rods, which are located within the core, 16 feet under water.

As stated, the core is composed of cylindrical fuel elements, control rods, and a neutron source held in place by two grid plates. In each grid plate (see Figure 3), holes for the fuel elements and control rods are arranged in six concentric rings labeled A thru F. The four control rods occupy four holes, and 87 fuel elements occupy the remaining holes. A guide tube to hold the neutron source is placed immediately outside the sixth or "F" ring.

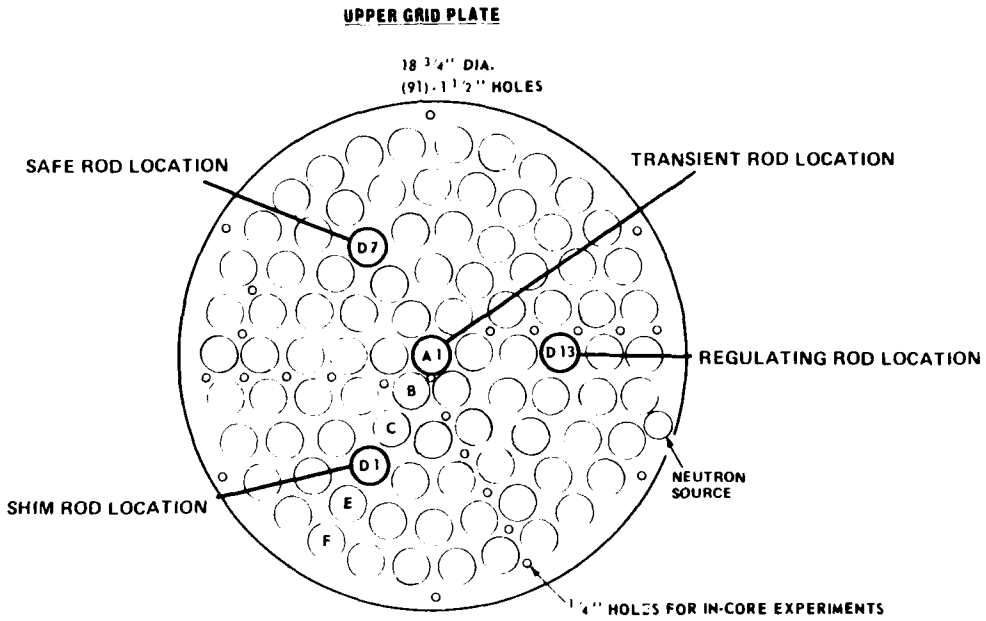

Figure 3. Overhead view of AFRRI reactor. Remaining holes are filled with 87 fuel elements.

FUEL ELEMENTS

An AFRRI TRIGA fuel element is shown in Figure 4. The fuel elements are principally composed of a cylinder of zirconium hydride mixed with uranium-235, the actual fuel of the reactor. Uranium-235 will fission upon the absorption of neutrons, thereby producing more neutrons as well as gamma radiation and heat. Uranium-235 has a much greater probability of absorbing a low-energy or "slow" neutron than a fast neutron. As a result, zirconium hydride, a moderator, is used to slow down the fast neutrons emitted from the neutron source and the fissioning uranium-235. A rod of zirconium is placed inside the fuel cylinder to ensure structural integrity. Graphite plugs are placed at each end of the fuel element in order to reflect fast neutrons back into the core, which then requires fewer fissions to sustain the chain reaction.

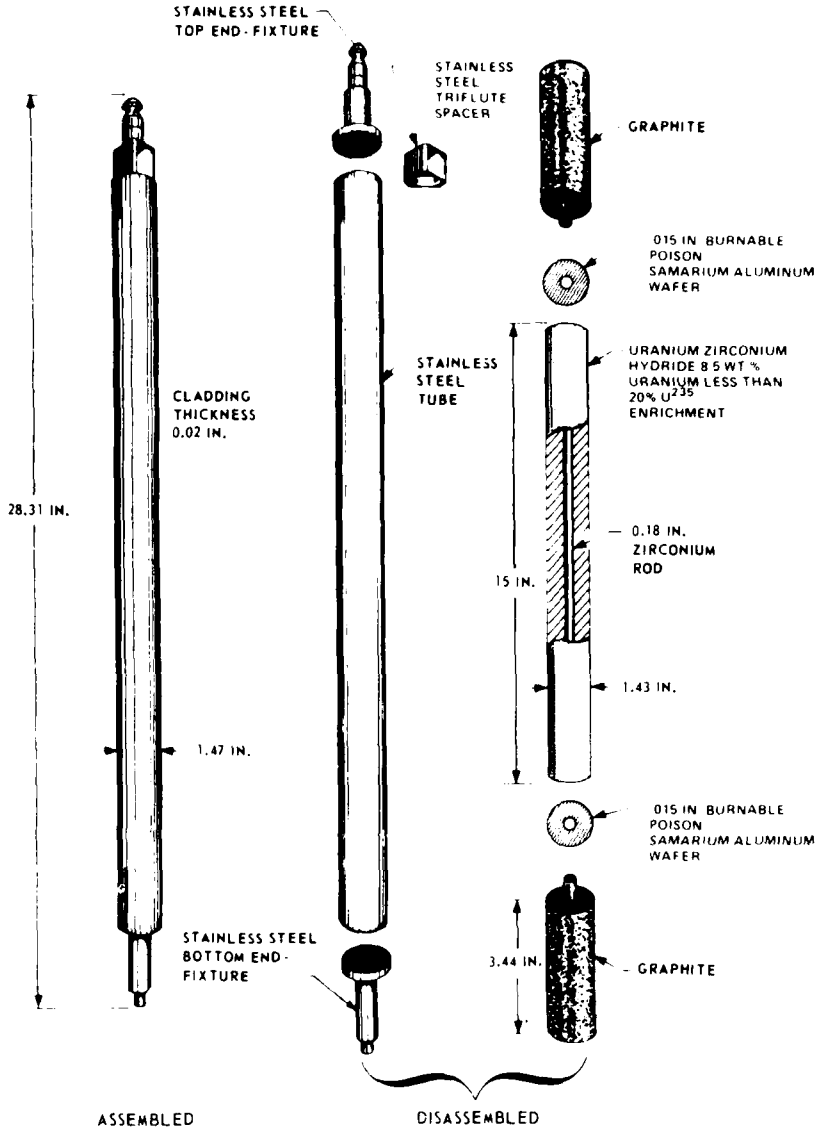

Figure 4. Standard fuel element

Samarium wafers are placed between the fuel cylinder and the graphite plugs, in order to extend the life of the fuel elements. The wafers do so because they absorb neutrons and burn out in proportion to the rate of fuel burnup.

An instrumented fuel element is similar in construction to a standard fuel element. It differs in that three thermocouples are placed within the center portion of the fuel element. These thermocouples measure the temperature of the fuel, which is then monitored at the reactor console.

CONTROL RODS

To be of maximum use in experimentation, the rate of fission must be controlled, thereby controlling the amounts of radiation and heat that are generated. The fission rate is controlled by absorbing the neutrons resulting from fission, thus decreasing the number of neutrons available to the fuel elements for subsequent fissioning. In the AFRRI reactor, the absorption of neutrons is regulated by control rods, which are mainly composed of borated graphite. (Boron is an effective neutron absorber, and graphite is a viable means for the suspension of boron, which is brittle and powdery in pure form.) These control rods are moved in or out of the core by means of rod drives, which are operated from the reactor console. The amount of control rod present in the core regulates the fission rate. That is, a greater length of control rod in the core results in a greater number of absorbed neutrons and, finally, a lower fission rate. If neutrons are being absorbed at a greater rate than they are being produced, the fissions will decrease and the production of power and radiation will be terminated. On the other hand, if neutrons are being produced at a faster rate than they are being absorbed, the fissions will increase along with the power level and corresponding radiations. By withdrawing just enough of the control rods to match the neutron absorption rate with the neutron production rate, a steady-state power level may be achieved.

As mentioned, there are four control rods in the core of the AFRRI reactor. One control rod is placed in the center position (Figure 3) called the "A" ring, and three are placed evenly in the fourth ring or "D" ring of the reactor core. The control rods in the fourth ring are the safe rod, shim rod, and regulating rod, known as standard rods. From the console, an operator may drive these rods slowly up and down. He may also "scram" the rods, allowing them to drop by means of gravity back into the core of the reactor. The control rod in the center ring is called the transient rod. This rod may be driven up and down in the same manner as the other control rods. In addition, the transient rod may be fired out of the core by means of compressed air. Before firing, a stopping anvil is appropriately positioned above the transient rod. Upon firing, the transient rod lifts from the core and hits a shock-absorbing anvil. The reactor is now in pulse mode, that is, ready for a brief high-power excursion. In pulse mode, all control rods will scram after a brief period of time set by the operator, usually 500 milliseconds. When the reactor is in steady-state mode, the rod stays against the anvil and is used like a standard rod. The standard and transient control rods are shown in Figure 5.

NEUTRON SOURCE

A neutron startup source is necessary to ensure the constant availability of neutrons in the core, in order to begin a power increase. The neutron source is composed of a mixture of americium and beryllium, doubly encased in stainless steel. Neutrons are produced by this source in the following manner: Americium, a man-made element, spontaneously decays into neptunium and alpha particles. Alpha particles react with the light element beryllium to produce carbon and high-energy neutrons, known as fast neutrons. These neutrons (also called source neutrons) are needed in the core for the control of fission as the control rods are withdrawn to increase power. Without a population of source neutrons in the core, fission could occur only spontaneously, and spontaneous fission cannot be predicted or controlled.

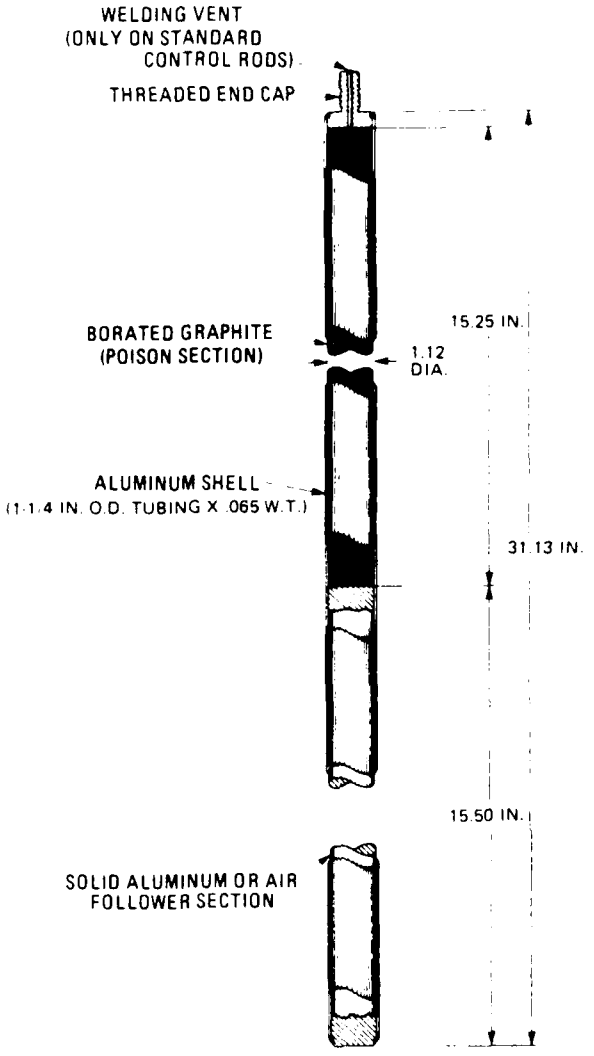

Figure 5. Standard and transient control rod

MODERATION

The AFRRI reactor has an inherent safety feature that will terminate (with or without control rods) a large and rapid rise of power (or an excursion, as it is known in reactor terms). This safety feature is based on the fact that to continue to produce enough neutrons to sustain power, neutrons must "slow down" to very low energy from the high energy at which they are born. As power is produced, heat (from fissioning) is transferred into the zirconium hydride, making it hot. When heated, the zirconium hydride does not allow the neutrons to cool to thermal energy, which in turn does not allow fissioning to occur. Without fissioning, the reactor power is terminated, because it is the heat from fission that produces thermal power. This inherent mechanism, built into the TRIGA fuel, makes an explosion or "meltdown" physically impossible.

INSTRUMENTATION

Instrumentation is placed in and around the core in order to measure and communicate information that is helpful in maintaining control over the operations of the reactor. The population levels of neutrons in and above the core are measured by detectors called ion chambers, which contain boron and are sensitive to neutrons. Also, the gamma level is measured during a reactor pulse by ion chambers that are sensitive to gamma. In addition, the temperatures of the reactor core and the pool must be monitored and controlled. To do this, thermocouples placed within the two instrumented fuel elements measure the fuel temperature, and two thermistors placed in the reactor pool measure the water temperature. One thermistor is positioned directly above the core, and one is positioned a few feet below the surface of the water, near the side of the pool.

COOLING SYSTEMS

The reactor core sits in a "swimming" pool. The pool acts as a radiation shield, protecting operation personnel from radiation. Water is an effective medium for shielding from neutron radiation, because neutrons generally travel only a foot or two in water. Gamma radiation is also greatly attenuated by water, with 16 feet of water being more than sufficient for an effective radiation shield.

In addition to protecting personnel from radiation, water in the pool serves as a means of cooling the reactor core. During operation of the reactor, heat energy is passed from the core to the surrounding water, and the water is then passed through a cooling system. From there, heat is transferred through heat exchangers to a secondary water system, and is then dissipated in the cooling towers. The water system for the reactor also provides cleaning and filtration of the water in the pool. There, filters eliminate particulate matter to maintain optical clarity in the pool. In addition, a demineralizer removes mineral ions to prevent the activation (or irradiation) of ions, which occurs naturally in water.

LEAD SHIELD DOORS

Two lead shield doors are located at the bottom of the reactor pool. The doors are aluminum shells 19 inches thick, 5 feet high, and 6 feet wide. They are filled with lead shot and transformer oil. The doors must be opened to allow movement of the core from one side of the pool to the other. They may be closed to provide shielding for scientific personnel working in the exposure rooms on the opposite side of the doors from the core. The doors rotate around aluminum poles. The poles are parallel to each other in the open position, and their edges overlap in the closed position. The edges of the doors are stepped (designed to overlap) to prevent the streaming of radiation from between the doors.

AD-A170 642 AFRRI (ARMED FORCES RADIOBIOLOGY RESEARCH INSTITUTE) 2/2
REPORTS APRIL - JUNE 1986(U) ARMED FORCES RADIOBIOLOGY
RESEARCH INST BETHESDA MD 1986

UNCLASSIFIED F/G 6/18 NL

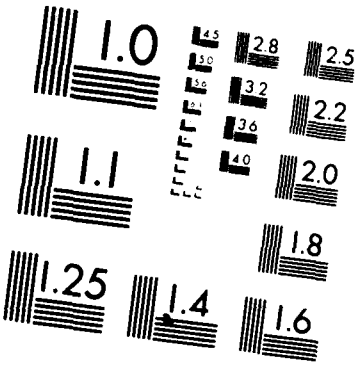

EXPOSURE FACILITIES

The Reactor has several exposure facilities for the irradiation of specimens. The AFRRI reactor has two exposure rooms, an extractor tube system, a core experiment tube, a portable beam tube system, and a pneumatic transfer system. Each of these facilities possesses unique features and provides variety in the reactor research capabilities at AFRRI. They are described in the following paragraphs.

EXPOSURE ROOM 1

Exposure Room 1 is located north of the pool, and is the most frequently used facility. The room possesses several arrays (or varieties) in shielding, which make it especially useful to investigators. The exposure room is 23 feet square and 9 feet high, with a semicylindrical section of the aluminum pool wall projecting through the south wall of the room. The reactor core can be moved to within less than 1 inch of the aluminum tank wall, separated from the tank wall by water. A cadmium-gadolinium shield is positioned on the tank projection, to absorb the leakage of thermal neutrons from the core into the exposure room. Lead curtains are suspended from the ceiling to prevent the scattering of gamma rays into Exposure Room 1 when the core is operating on the opposite side of the pool near Exposure Room 2. The walls and ceiling of Exposure Room 1 are made of concrete, covered with wood and painted with gadolinium paint. Because fast neutrons can activate concrete and thus present a hazard to personnel, the concrete is covered by wood. The wood slows down the fast neutrons emitted from the core, thus drastically reducing the chances of activating the concrete. After being slowed down or "thermalized" by the wood, the neutrons may bounce back toward the interior of the room, but are then absorbed by the gadolinium paint before they can escape into the room. The tank wall as seen from ER 1 is shown in Figure 6.

EXPOSURE ROOM 2

Exposure Room 2 is similar to Exposure Room 1 in construction. The room is slightly smaller, but the ceiling and walls follow the same design as those of Exposure Room 1: concrete walls covered with wood painted with gadolinium paint. The pool wall projects from the north wall of Exposure Room 2 just as in Exposure Room 1, but it is not shielded with cadmium. As a result, a high concentration of thermal neutrons enters the exposure room. This differs from the neutron concentration in Exposure Room 1, in which the neutron population is composed primarily of fast neutrons. Experiments needing a high thermal neutron component are exposed in this room.

INSTRUMENTATION

Instrumentation is placed in and around the core in order to measure and communicate information that is helpful in maintaining control over the operations of the reactor. The population levels of neutrons in and above the core are measured by detectors called ion chambers, which contain boron and are sensitive to neutrons. Also, the gamma level is measured during a reactor pulse by ion chambers that are sensitive to gamma. In addition, the temperatures of the reactor core and the pool must be monitored and controlled. To do this, thermocouples placed within the two instrumented fuel elements measure the fuel temperature, and two thermistors placed in the reactor pool measure the water temperature. One thermistor is positioned directly above the core, and one is positioned a few feet below the surface of the water, near the side of the pool.

COOLING SYSTEMS

The reactor core sits in a "swimming" pool. The pool acts as a radiation shield, protecting operation personnel from radiation. Water is an effective medium for shielding from neutron radiation, because neutrons generally travel only a foot or two in water. Gamma radiation is also greatly attenuated by water, with 16 feet of water being more than sufficient for an effective radiation shield.

In addition to protecting personnel from radiation, water in the pool serves as a means of cooling the reactor core. During operation of the reactor, heat energy is passed from the core to the surrounding water, and the water is then passed through a cooling system. From there, heat is transferred through heat exchangers to a secondary water system, and is then dissipated in the cooling towers. The water system for the reactor also provides cleaning and filtration of the water in the pool. There, filters eliminate particulate matter to maintain optical clarity in the pool. In addition, a demineralizer removes mineral ions to prevent the activation (or irradiation) of ions, which occurs naturally in water.

LEAD SHIELD DOORS

Two lead shield doors are located at the bottom of the reactor pool. The doors are aluminum shells 19 inches thick, 5 feet high, and 6 feet wide. They are filled with lead shot and transformer oil. The doors must be opened to allow movement of the core from one side of the pool to the other. They may be closed to provide shielding for scientific personnel working in the exposure rooms on the opposite side of the doors from the core. The doors rotate around aluminum poles. The poles are parallel to each other in the open position, and their edges overlap in the closed position. The edges of the doors are stepped (designed to overlap) to prevent the streaming of radiation from between the doors.

Figure 6. ER-1 tank wall with Pb shield

SHIELDING

Within the two exposure rooms, exposure to radiation can be tailored or modified by means of shielding. Shielding materials, which are often part of experimental setups (or arrays) consist of lead bricks, or bismuth bricks, or combinations of both. Currently a lead shield and a lead cave are often used together. Lead serves as a shield from gamma radiation. Placed in the path of radiation, it will enhance the relative neutron field on the other side. The lead shield is placed in front of the reactor core to shield samples from gamma rays that are emitted from the core. The lead cave is placed behind the lead shield in order to shield samples from gamma radiation that scatters from the exposure room walls. This shield-and-cave setup is shown in Figure 7. The result is a miniature lead chamber containing an enhanced neutron field. Samples inside this chamber may be placed in rotators, which aid the even bilateral exposure of specimens. The standard rotator for small specimens is shown in Figure 8. In both the lead shield and the lead cave, the thickness of the lead may be altered, to produce further variety in radiation fields.

Bismuth serves the same purposes as lead: to shield from gamma rays and to provide an enhanced neutron field. But bismuth is more useful than lead because, although both absorb neutrons, bismuth does not emit gamma rays and lead does. Because bismuth emits alpha particles upon the absorption of neutrons, the bricks are painted to shield from alpha radiation.

In addition to placing shielding materials within the exposure rooms, the amount and character of radiation reaching the samples in the exposure rooms may be modified by moving the reactor core. Moving the core away from an exposure facility places more water between the core and that exposure room. This results in a smaller number of neutrons reaching the exposure room, and those that do are generally of a lower energy. Therefore, the radiation field in that facility contains a higher percentage of gamma radiation.

EXTRACTOR TUBE SYSTEM

Exposure Room 1 is equipped with an extractor tube system, which permits the quick insertion and withdrawal of sa...ples. When in position, the extractor tube extends from directly in front of the core, through the west wall, and into the prep area, outside of the exposure room. The section of the tube in the wall follows an "S" curve, which prevents the radiation from streaming from the exposure room into the prep area. Samples are placed inside a plastic carrier and positioned within the tube by means of a motorized pulley system, controlled from the prep area. The quick retrieval of samples from the exposure room results in greater precision in evaluating the amount of radiation received by the samples, particularly for low-level exposures. This eliminates time delays in moving the reactor core, closing the lead shield doors, and opening the exposure room doors. Experimental retrieval takes place in seconds rather than the tens of minutes required for full procedures of room entry. The extraction also reduces the exposures to personnel that result from exposure room entries.

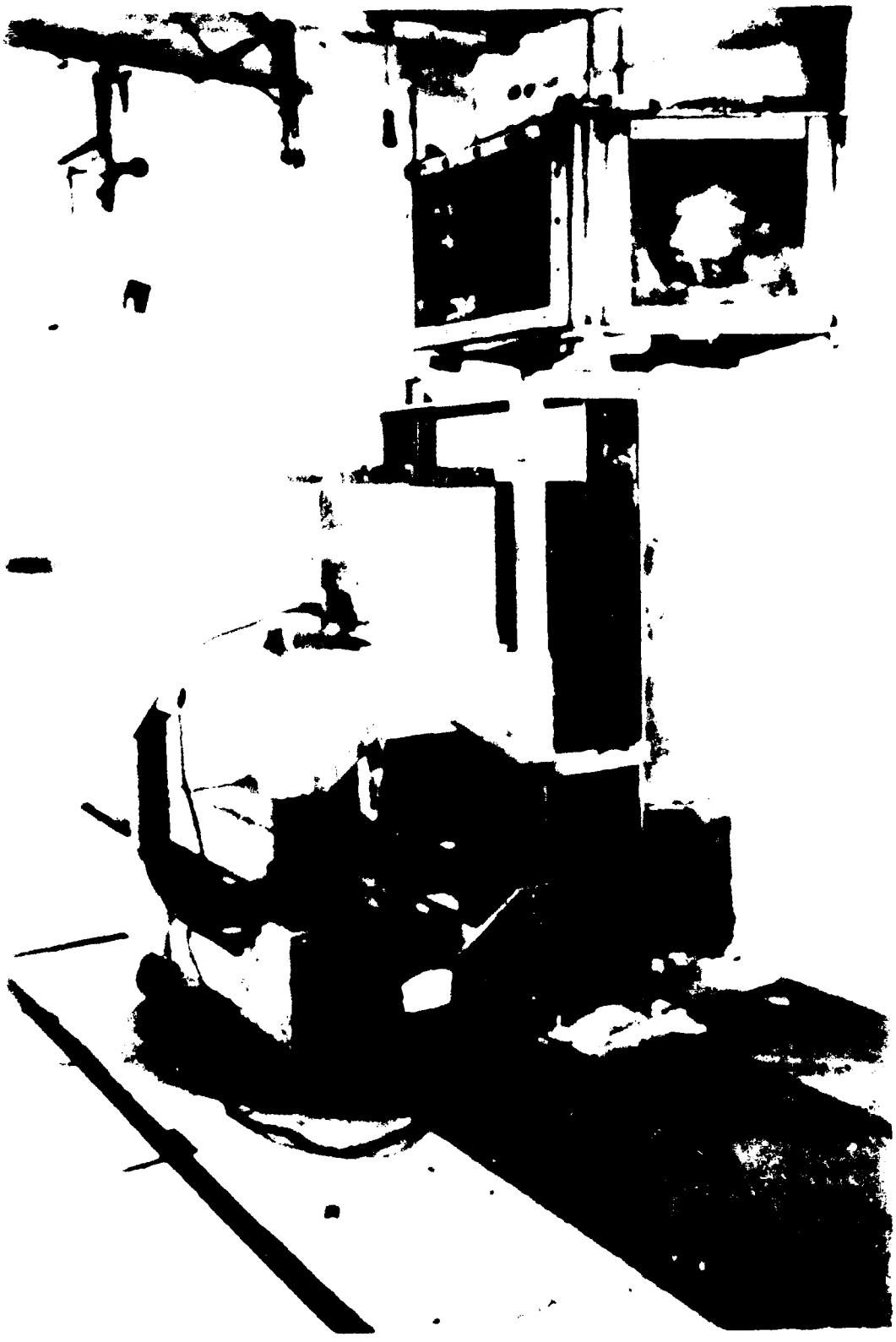

Figure 7. Setup of shield and lead cave

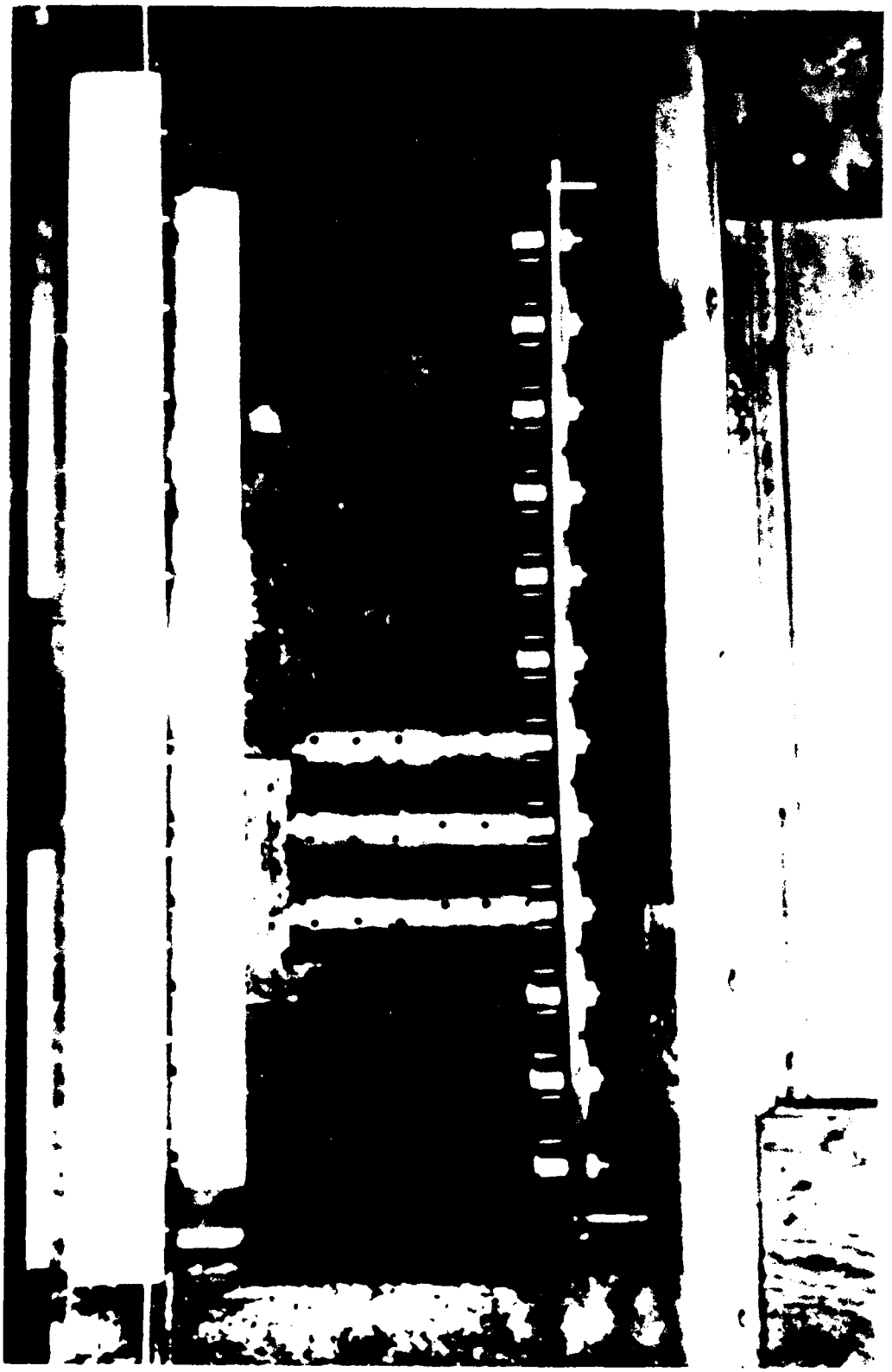

Figure 8. Standard rotator for small specimens

CORE EXPERIMENT TUBE

Samples may be irradiated in the exposure rooms, or they may be irradiated in the core itself, by means of the Core Experiment Tube. The Core Experiment Tube is a hollow aluminum tube with an "S" bend to prevent streaming of radiation. In this procedure, a fuel element is withdrawn from the core and placed in storage, and a Core Experiment Tube is placed in that fuel element location. The samples to be irradiated are placed in small polyethylene containers, called "rabbits," which are then loaded into the tube and placed directly into the core. The rabbits may be withdrawn with a modified fishing pole. The Core Experiment Tube is used primarily to produce isotopes, which are used by researchers as biological tags or tracers. Radioactive potassium is the isotope most commonly produced. Materials may be activated in the Core Experiment Tube, and the patterns of radiation emitted following activation may be used to analyze those materials. This process has several applications.

PORTABLE BEAM TUBE SYSTEM

The portable beam tube system consists of aluminum tubes suspended in the reactor containment pool. A beam of radiation is produced by this system, thus allowing the irradiation of selected areas of specimens. A variety of filters and lenses may be incorporated into experiments to vary the degree, character, and precision of the radiation.

PNEUMATIC TRANSFER SYSTEM

The AFRRI reactor also possesses a pneumatic transfer system. The system is not in use at the present time, but it may be reinstalled quickly if the need arises to produce extremely high activities of radioisotopes.

CERENKOV RADIATION

Cerenkov radiation is a bright blue color that appears around the reactor core. It accompanies a reactor pulse and also steady-state operations above 1 kilowatt. As fission occurs, charged beta particles are emitted, in addition to all other fission products. With enough energy, these beta particles travel at a speed greater than the speed of light in the given medium (water). As these particles slow down, excess energy is given off as photons of light, which are observed as a bright blue glow.

END

DTIC

9-86